Review
Nanosized hydroxyapatite and other calcium phosphates: Chemistry of formation and application as drug and gene delivery agents

Vuk Uskoković,[1] Dragan P. Uskoković[2]

[1]Division of Biomaterials and Bioengineering, Department of Preventive and Restorative Dental Sciences, University of California, San Francisco, California 94143
[2]Institute of Technical Sciences, Serbian Academy of Sciences and Arts, 11000 Belgrade, Serbia

Received 12 July 2010; revised 26 August 2010; accepted 31 August 2010
Published online 8 November 2010 in Wiley Online Library (wileyonlinelibrary.com). DOI: 10.1002/jbm.b.31746

Abstract: The first part of this review looks at the fundamental properties of hydroxyapatite (HAP), the basic mineral constituent of mammalian hard tissues, including the physicochemical features that govern its formation by precipitation. A special emphasis is placed on the analysis of qualities of different methods of synthesis and of the phase transformations intrinsic to the formation of HAP following precipitation from aqueous solutions. This serves as an introduction to the second part and the main subject of this review, which relates to the discourse regarding the prospects of fabrication of ultrafine, nanosized particles based on calcium phosphate carriers with various therapeutic and/or diagnostic agents coated on and/or encapsulated within the particles. It is said that the particles could be either surface-functionalized with amphiphiles, peptides, proteins, or nucleic acids or injected with therapeutic agents, magnetic ions, or fluorescent molecules. Depending on the additive, they could be subsequently used for a variety of applications, including the controlled delivery and release of therapeutic agents (extracellularly or intracellularly), magnetic resonance imaging and hyperthermia therapy, cell separation, blood detoxification, peptide or oligonucleotide chromatography and ultrasensitive detection of biomolecules, and *in vivo* and *in vitro* gene transfection. Calcium phosphate nanoparticles as carriers of therapeutic agents that would enable a controlled drug release to treat a given bone infection and at the same be resorbed in the body so as to regenerate hard tissue lost to disease are emphasized hereby as one of the potentially attractive smart materials for the modern medicine. J Biomed Mater Res Part B: Appl Biomater 96B: 152–191, 2011.

Key Words: bone, calcium phosphate, drug delivery, hydroxyapatite, precipitation, soft chemistry, theranostics

INTRODUCTION:HYDROXYAPATITE AS THE MAIN CONSTITUENT OF BONE

To most people, hydroxyapatite (HAP) is known as the mineral component of bone.[1–3] Therein, stiff HAP crystals are responsible for imparting an appropriate compressive strength, whereby collagen fibers, able to dissipate energy effectively, provide superior elastic properties, thus ameliorating the brittleness of the sole HAP.[4] However, the exceptional strength and toughness of bone come not only from the synergetic combination of material properties of its mineral and organic components, respectively, but also from its hierarchical, superstructural organization.[5]

Bone is an organ that not only provides a basic mechanical support to the body by generating and transferring forces that are involved in locomotion but also has various other functions.[6] For example, by storing minerals within, mostly calcium and phosphate, it presents the main mineral reservoir for the body. Absorption and release of salts is the mechanism by which bones buffer the blood and prevent excessive pH changes. Bones, such as skull or ribs, also serve to physically protect vital internal organs including brain, heart, and lungs. Some bones also act as fabrics for producing red and white blood cells. Bone has formed in coevolution with the surrounding tissues of organisms and the environment. In eukaryotic cells, calcium ions play a plethora of functions, including that of a messenger in various signal transduction pathways. Calcium-activated ATPase, Na^+/Ca^{2+} exchangers, calcium channels, and intracellular calcium binding proteins maintain a fine Ca^{2+} homeostasis in cells such as odontoblasts. On one hand, a controlled imbalance of internal calcium levels is a precursor for the bone-building activity, which, unlike in the case of amelogenesis and dentinogenesis, always proceeds through external accretion. On the other hand, increased amounts of intracellular Ca^{2+} may result in uncontrolled secretion and internal precipitation. Namely, Ca^{2+} is known to be a part of harmful deposits in the body, such as atherosclerotic plaque, kidney stones, and dental calculi.[7] It also has a strong tendency to bond with many proteins, particularly phosphorylated ones. In case of ATP, its aggregation may be induced thereby, resulting in the loss of biological function. On the other hand, binding of Ca^{2+} to phosphorylated proteins

Correspondence to: V. Uskoković; e-mail: vuk21@yahoo.com

involved in biomineralization, such as osteopontin in bone or dentin phosphophoryn, is a vital step in the formation of hard tissues of bone and dentin.[8]

Aside from its mineral and protein components, bone is also populated by cells, macromolecules, and blood vessels. Three types of cells involved in maintaining a healthy bone structure are as follows: (a) osteocytes involved in signal transduction of mechanical stimuli; (b) osteoblasts, which are derived from mesenchymal stem cells and secrete collagenous proteins, thereby building the bone material; and (c) osteoclasts, which are derived from hematopoietic marrow cells and secrete acids and proteases, thereby degrading the mineralized tissue. RANKL, a protein molecule bound to the osteoblast surface and serving to activate osteoclasts has been intensively investigated because of its role in facilitating an optimal communication between these two types of cells.[9] Overexpression of RANKL has been linked to a variety of degenerative bone diseases, including rheumatoid arthritis and osteoporosis.[10] Through the cooperative action of osteoblasts and osteoclasts, bone is constantly being remodeled in response to physiological requirements. Julius Wolff was the first to propose that bone remodels itself when force is exerted on it by the mechanism according to which the internal architecture of the trabecular bone first undergoes adaptive changes when placed under load, followed by secondary changes to the external cortical portion of the bone.[11] An evidence of an impressive remodeling capacity of bone has come from the observed modifications in bone shape and density in astronauts subjected to microgravity conditions for prolonged periods of time.[12] Bone is, for example, often regarded as a living mineral due to its continual growth and dissolution, formation and degradation, and renewal and remodeling, taking place during the organism's lifetime.

Many mysteries, such as the role of sacrificial bonds that break under stress, but only to be reformed at a later time, imparting durability and resilience to hard tissues, still surround the superior functioning of this basic material of Nature.[16] Many new functions of bone have also been gradually revealed over time. It has now been established that bone does not only act as a reservoir for minerals, primarily calcium and phosphate, which circulate through blood in supersaturated concentrations, but also stores growth factors, fatty acids, heavy metals, and other toxic elements, and is involved in buffering the blood by controlled release of alkaline salts. Be that as it may, bone presents a connective tissue and a failure of the ability to stay connected and properly transmit stress throughout the body has an implication of slowly bringing about dysfunction of many other, close or distant segments of skeleton and the body. In view of that finding the ways to heal the impaired bone tissue in timely manner can be regarded as one of the most important tasks that medicine can contribute to. In view of that bone research has a special meaning in the world of medicine. However, understanding bone is a challenging task for the modern scientists, especially because it requires an atypical interdisciplinary element in one's approach, explained by the fact that bone stands at the interface between many separate fields of science. The more one focuses one's attention on finer levels of organization, the more of the biological approaches cede their place to fundamental physicochemical methods of probing bone structure and properties.

Also just as usual, as scientific attention is focused to ever smaller physical details, the things do not get simplified but become ever more complex instead.[17] Hence, the structural arrangement of nanosized HAP crystals within the collagen matrix is still a subject of scrutiny. It is still not resolved whether mineralization first occurs within the 40 nm wide gap or the 27 nm wide overlap region of collagen fibers. Contrary to earlier assumptions, a recent cryo-TEM study has shown that upon mineralization of collagen the mineral first fills the overlap region and only then it proceeds to incorporate itself within the gap region.[18] Two forms of HAP crystals in dentin and bone can also be distinguished based on where they are found: extrafibrillar and intrafibrillar.[19] The former are larger nanocrystals (plate-shaped with 2–3 nm in thickness and a few tens of nanometers in length and width) existing in-between individual fibrils (that is, bundles of collagen fibers having $\sim$1.5–3.5 nm in diameter and are essentially individual elongated, triple helix molecules), whereas the latter are found to figure as links between individual fibers along their long axis. However, the role of each has not been discerned yet.[20]

Also, just as the structural water has been added to the basic structural diagrams of proteins in recent years,[21] its role for the proper mechanical performance of hard tissues has been increasingly pointed out by researchers.[22] Collagenous tissues, such as bone or dentin, which contain $\sim$70 wt % apatite, 20 wt % collagen, and 10 wt % water (with only about 3% of noncollagenous proteins, including some polysaccharides as well), are nowadays known to partly owe their mechanical properties to the structural water.[23,24] Hydrated dentin is, for example, shown to dramatically degrade in toughness following its dehydration.[25,26] Also, in case of collagen molecules wherein backbone hydrogen bonding between polypeptide chains in its triple-stranded structure does not present the major stabilizing force, unlike in the case of α-helices and β-sheets, additional enthalpic contributions are known to come from water molecules that form a scaffold around the surface of the triple helix, implying that water plays an intimate role in stabilizing this protein.[27] This observation coincides with the recently observed 10-fold drop in tensile properties of single fibrils of collagen following desorption of the bound water in vacuum, even though the strength of the molecule was the same in water and air.[28]

Hence, even though the fascinating properties of bone are products of precise and intricate arrangement of its building blocks on many different levels—from nanometer to millimeter scales (Figure 1)—the complexity of each one of these building blocks is equally complex as to deserve paying sole research attention thereto. In fact, the complexity of this material has ever since puzzled scientists involved in bone research; hence, the name of this compound, apatite, derives from Greek απαταο, which means to

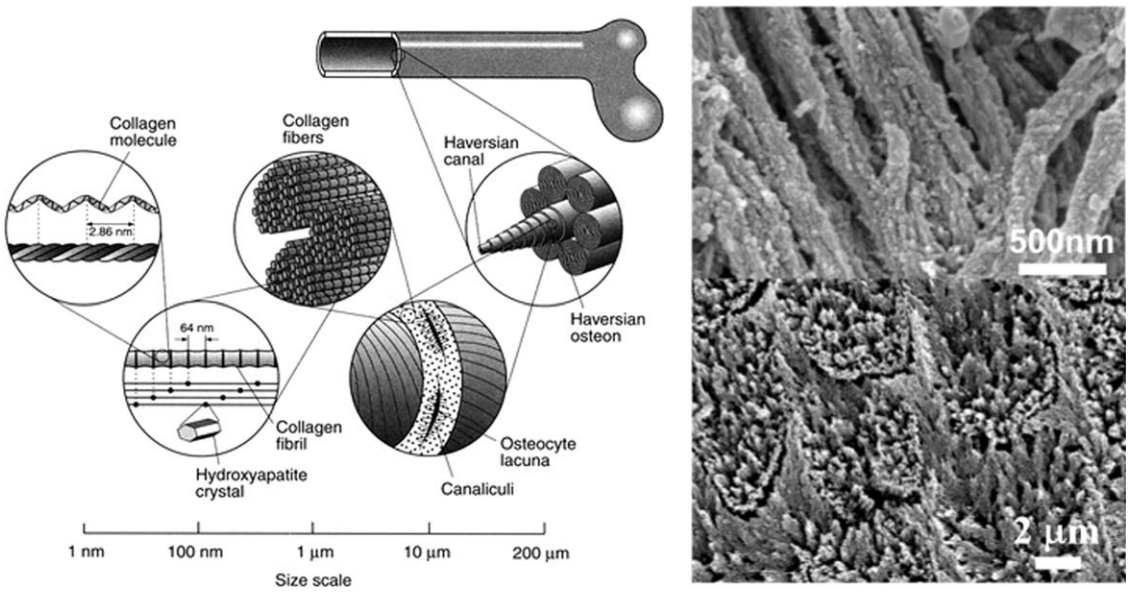

FIGURE 1. Bone (left) is a complex, hierarchically structured biological material in which the building components are precisely arranged at scales spanning half a dozen of orders of magnitude. The image on the left shows sketches of the structural elements of cortical/compact bone (which comprises the harder, outer layer of the cross-section of bone, surrounding the softer trabecular/spongy/cancellous bone) at different scales. The image on the upper right side shows the nanostructure of mineralized collagen fibers in bone, whereby the image below displays the fine structure of dental enamel, the hardest substance in the body. Within the former structure, HAP particles are incorporated within the organic matrix, whereas the latter structure is composed of an almost pure mineral with elongated HAP nanofibers connected into bundles and forming equally uniaxially directed enamel rods. Reproduced with permission from Fawzy and Farghaly, J Dentistry, 2009, 37, 963–969, reproduced from Ref. 27, with permission from JAI Press, and reproduced with permission from Cui and Ge J, J Tissue Eng Regen Med 2007, 1, 185–191, John Wiley & Sons.

deceive. The respective mineral was, however, named so because it had easily been mistaken for other, more precious minerals[29]; yet, a drop of lime juice was sufficient to dissolve it. Unlike some other similarly complex materials, such as doped manganites, which exhibit an enormous set of electric and magnetic behaviors depending on the structural arrangement of the constitutive ions[30,31]; in case of HAP, the main emphasis is on the breadth of possible mechanical properties depending on different phase arrangements and the structure and morphology of the compound. Another remarkable feature of this material is a considerably low crystal growth rate even under relatively high super saturations. The reason for this is thought to lie in the complex growth mechanism that involves precipitation of amorphous, ~1 nm sized solid units called Posner's clusters in the first stage of the process, and their aggregation and ionic rearrangement followed by an increased compactness and crystallinity in the second stage.[32] Owing to the fact that this mechanism resembles the one of the growth of protein and viral crystals that involves chirality selection and orientation arrangements, the low crystal growth rate of HAP is often compared with that of these biological compounds.[33] Low crystallinity of particles precipitated under physiological conditions and stoichiometric sensitivity to mildest changes in synthesis conditions are additional characteristics of the formation of HAP, which will be discussed more in the following section. All of these fundamental peculiarities are currently subject of intensive scrutiny.

The main content of this review is divided to two parts: fundamentals and application. In the first part, the reader will get acquainted with the fundamental properties of HAP and the chemistry of its formation, whereas in the second part, the advanced applications of this compound will be numbered and discoursed on.

FUNDAMENTALS

Chemical identity and basic properties

HAP is a mineral from the family of apatites, the general formula of which is $M_5(ZO_4)_3X$, where M is a rare-earth metal, such as Ca^{2+}, Cd^{2+}, Sr^{2+}, Ba^{2+}, Pb^{2+}, Zn^{2+}, or Mg^{2+}, ZO_4 could be PO_4^{3-}, CO_3^{2-} or SO_4^{2-}, and X is OH^-, F^-, Cl^-, or CO_3^{2-}. Whereas $Ca_5(PO_4)_3OH$ is the formula for HAP, $Ca_{10}(PO_4)_6(OH)_2$ is the formula of the unit cell thereof, and its pK_{sp} (K_{sp} = solubility product) equals 58.65 at 37°C. HAP is, therefore, the most stable calcium orthophosphate (CAP) phase in the pH range of 4.2–12.4. The unit cell of stoichiometric HAP can also be represented with the following formula: $M1_4M2_6(PO_4)_6(OH)_2$, where M1 and M2 are two different crystallographic positions for 10 calcium atoms. Four Ca atoms in the unit cell of HAP thus occupy M1 position where they are surrounded by nine oxygen atoms, which belong to PO_4 tetrahedra. The other six Ca atoms occupy M2 site where they are coordinated by six O atoms of the PO_4 tetrahedra and one of the two OH^- groups.[34,35] In biological conditions, HAP is subject to an extensive substitution of ions, so that human bone is, for example, best described as $(Ca,Z)_{10}(PO_4,Y)_6(OH,X)_2$, where Z = Na^+, Mg^{2+}, K^+, Sr^{2+}, and so forth, Y = CO_3^{2-}, HPO_4^{2-}, and X = Cl^-, F^-.

TABLE I. The Main CAP Phases Obtainable Upon Precipitation from the Solution

Phase	Chemical Formula	Space Group	pK_{sp} at 37°C	Ca/P Molar Ratio
Monocalcium phosphate anhydrous (MCPA)	$Ca(H_2PO_4)_2$	Triclinic $P\bar{1}$	1.14	0.5
Monocalcium phosphate monohydrate (MCPM)	$Ca(H_2PO_4)_2{\cdot}H_2O$	Triclinic $P\bar{1}$	1.14	0.5
Dicalcium Phosphate (DCPA, Monetite)	$CaHPO_4$	Triclinic $P\bar{1}$	7.0	1
Dicalcium Phosphate Dihydrate (DCPD, Brushite)	$CaHPO_4{\cdot}2H_2O$	Monoclinic I_a	6.6	1
α-Tricalcium Phosphate (α-TCP)	$Ca_3(PO_4)_2$	Monoclinic $P2_1/a$	25.5	1.5
β-Tricalcium Phosphate (β-TCP, Whitlockite)	$Ca_3(PO_4)_2$	Rhombohedral R3cH	29.5	1.5
Tetracalcium Phosphate (TTCP)	$Ca_4(PO_4)_2O$	Monoclinic $P2_1$	37.5	2
Octacalcium Phosphate (OCP)	$Ca_8H_2(PO_4)_6{\cdot}5H_2O$	Triclinic $P\bar{1}$	97.4	1.33
Hydroxyapatite (HAP)	$Ca_{10}(PO_4)_6(OH)_2$	Pseudohexagonal $P6_3/m$	117.3	1.67

Irrespective of whether it is found in enamel, dentin, cementum, or bone, biogenic apatite is always impure and nonstoichiometric. The major impurity is CO_3^{2-} (3–8 wt %), whereby minor impurities include Na^+ (0.5–1 wt %), Mg^{2+} (0.4–1.2 wt %), K^+ (0.03–0.08 wt %), Cl^- (0.01–0.3 wt %), and F^- (0.01–0.06 wt %). Some of these substitutions, such as $OH^- \rightarrow Cl^-$, $PO_4^{3-} \rightarrow CO_3^{2-}$ or $Ca^{2+} \rightarrow Mg^{2+}$, Sr^{2+}, are known to weaken the apatite structure and make it more soluble, whereas others, such as $OH^- \rightarrow F^-$, are known to additionally strengthen it and also lessen its solubility.[36] In fact, most of these impurities, except fluoride, contribute to increased solubility of the resulting apatite stoichiometry, which explains why fluorine is added to toothpaste formulations,[37] although health risks concerning its unfavorable effects on the gut flora and indications that it may even act as a neurotoxin[38] are currently under research. Also, extensive amounts of fluoride in the apatite structure have been shown to lead to increased porosity and weakening of the material.[39]

CO_3^{2-} is the most common dopant in biological apatite,[40] and carbonated HAP is shown to have an improved bioactivity compared with pure HAP, which has been attributed to the greater solubility of the carbonated phase.[41] Incorporation of CO_3^{2-} ions within the HAP crystal structure has also been shown to have a retarding effect on the crystal growth.[42] The complexity of this substitution is, in fact, so high that it extends beyond the area of biomineralization and touches the most fundamental problems of crystallography and crystal growth phenomena.[43] When apatite is synthesized by precipitation, at atmospheric conditions, B-type of carbonated HAP normally forms where CO_3^{2-} ions substitute for PO_4^{3-}. Typically, when HAP is prepared by means of an annealing treatment, A-type forms where CO_3^{2-} ions substitute for OH^-, owing to the high mobility of OH^- groups.[44] However, this is not necessarily the case because A-type substitution was also observed in HAP prepared by precipitation at room temperature.[45] Biological apatite also normally presents a mixture of A and B types.[46,47] In both cases, the fact that the divalent carbonate substitutes trivalent phosphates or monovalent hydroxyls implies the necessity to compensate for the imbalanced charges by modifying the stoichiometry of the compound or favoring incorporation of other impurities into the crystal lattice. On the basis of charge neutrality, the chemical formula of carbonated HAP is $Ca_{10-x/2}[(PO_4)_{6-x}(CO_3)_x][(OH)_{2-2y}(CO_3)_y]$, where x and y are numbers of CO_3^{2-} ions substituting for PO_4^{3-} and OH^-, respectively.[48]

The most frequently encountered structure of HAP belongs to a hexagonal system with $P6_3/m$ space group. The less common symmetry of HAP lattice is described by $P2_1/b$ space group within the monoclinic crystal system.[49] The unit cell dimensions of pure hexagonal HAP are: $a = b = 0.937$ nm, $c = 0.6881$ nm. However, each one of the substitutions has an effect on the lattice parameters, so that biological HAP deviates from the perfect crystal arrangement of ions depending on the additives and the positions that they occupy in the lattice. For example, A-type substitution upon carbonation of HAP implies larger CO_3^{2-} ions replacing smaller OH^- ions and thus expanding the a axis and contracting the c axis, whereas B-type substitution has an opposite effect.[50,51] These changes in crystal lattice parameters often induce changes in crystallinity, thermal stability, morphology, solubility, and other physicochemical and biological properties of the material.[52]

HAP is a ceramic material, and most of the primary chemical bonds found in ceramic materials are a mixture of ionic and covalent types, which explains for complex interplay of latent properties that HAP and ceramic materials in general are prone to exhibit. As expected, CAP can adopt numerous crystal structures depending on stoichiometry and conditions of formation. Some of the main CAP phases are listed in Table I, whereby the crystal structure of HAP is illustrated in Figure 2.

Typical synthetic pathways

Numerous methods have been applied for the synthesis of fine particles of HAP, including reactions in solid state,[53–56] abrupt or continuous precipitation from solution,[57–60] hydrothermal processing,[61,62] electrospraying,[63] electrospinning,[64] flux cooling method,[65] spray pyrolysis,[66] ultrasound[67] and mechanochemical processing,[68,69] microwave irradiation-assisted precipitation,[70,71] microemulsion- and surfactant-assisted precipitation,[72–76] sol–gel syntheses based on hydrolysis of metal organic precursors,[77,78] and chemical vapor[79] and plasma deposition.[80] However, from the point of view of control over apatite structure and morphology, these methods could be roughly divided to low and high temperature ones. The latter typically involve

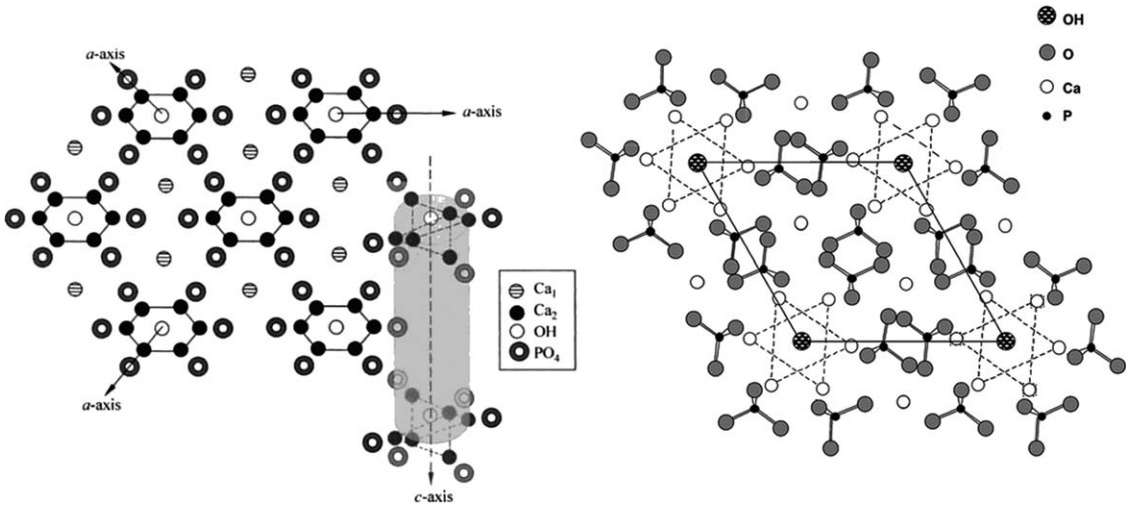

FIGURE 2. Crystal structure of HAP showing its *c*-axis perpendicular to 3 *a*-axes lying at 120° angles to each other (left), with projection on the 001 plane of HAP structure (right).

mechanochemical homogenization of precursor compounds, such as $Ca_3(PO_4)_2$ and $Ca(OH)_2$, and their subsequent annealing at ~1000°C. The advantage of this method lies in the ability to precisely set the stoichiometry of the final product, whereas long reaction times and high annealing temperatures are some of the main downsides. In general, if the molar ratio of Ca/P is not set to 1.667 during preparation, extraneous phases normally appear: α- or β-TCP at lower values and typically CaO at higher values, which is especially the case upon annealing (with α-TCP forming at higher temperatures, such as around 1200°C, and β-TCP forming at lower temperatures, such as up to 900°C). In addition to the high levels of energy consumption, another major downside of high-temperature, solid state methods lies in the difficulty to produce uniform nanosized particles by their means. The latter are, on the other hand, known to promote a favorable biological response, including higher osteoinductivity and osteoconductivity, leading to a quicker integration of the implanted HAP-based material.[81] Low-temperature methods that involve precipitation from solution have a disadvantage in the frequent presence or transient and metastable phases in the final product. As we shall see in what follows, it is exactly this multitude of possible phase combinations, sensitive to subtle changes in synthesis conditions,[82] that may be linked to the aforementioned Greek origins of the word apatite.

HAP is a sparingly soluble salt in neutral and alkaline aqueous solutions, and forms crystals with high edge free energies. As surface/interfacial energy of a crystal is indicative of the difficulty of its forming, sparingly soluble salts as a rule have higher interfacial free energy values that soluble ones. Also, as the interfacial tension can be expressed as proportional to the size of the critical step/nucleus upon dissolution/crystallization, high values of the latter can be deduced and correlated with the experimentally observed slow dissolution/crystallization of HAP.[83] As a direct result, synthesized HAP typically exhibits not only a wide distribution of particle sizes (partly caused by the aggregation mechanism of growth, which will be discussed in the next subsection, and partly by slow crystallization, which makes it difficult to avoid the overlap between nucleation and diffusional crystal growth phases), but also highly irregular particle shapes. In view of that, finding conditions for a controllable synthesis of HAP nanoparticles with tunable sizes and shapes presents a worthwhile research challenge. Various additives have been applied in precipitation syntheses for the sake of attaining this aim, including cetyltrimethyl ammonium bromide,[84] poly(acrylic acid),[85] poly-(allylamine hydrochloride),[86] and others.

Biological apatite is, moreover, known for its high content of defects, caused in part by a relatively large percentage of impurities, all of which affect the lattice parameters, crystal morphology, crystallinity, solubility, and the thermal stability of the material. HAP crystal surface is thus rarely smooth, and the reason is related to its biological significance. The exceptional roughness of biological HAP, comprising surface irregularities in the order of size of single unit cells, hypothetically corresponds to the tendencies to increase protein binding in the process of biomineralization.[87] Previous studies have shown that rough surface improves biocompatibility of the material and has a positive effect on inflammatory reactions, whereas the viability of monocytes seeded on flat surfaces tends to be far lesser.[88] Also, cells are constantly creating and decomposing HAP in bone, and rougher surfaces provide conditions for an easier anchoring of cells thereto. An *ab initio* model has showed that amino acid side chains carrying either acidic (i.e., aspartic and glutamic acids) or basic (i.e., lysine or arginine) residues are prone to interact with HAP crystal surfaces, which is in agreement with numerous spectroscopic and other modeling data that report both carboxylic and amino residues typically found in close proximity to the HAP surface.[89] In fact, the reason why phage display panning techniques on HAP surfaces have not yielded significant results so far lies exactly in the tendency of numerous peptide combinations to bind to it, which diminishes the high selectivity on which this approach inherently depends.[90]

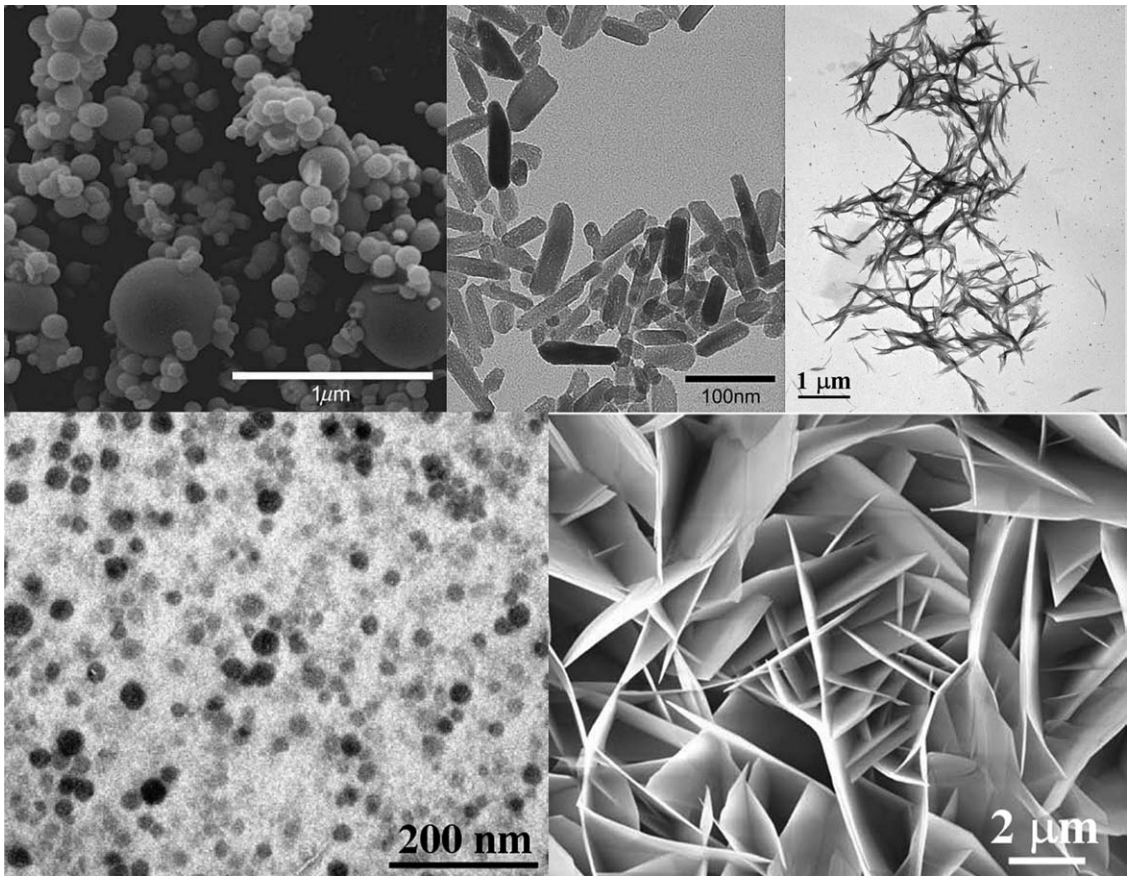

FIGURE 3. Owing to its structural flexibility, HAP can be prepared in a variety of morphologies, ranging from spheres to filaments to rods. However, HAP particles are on most occasions found in the forms of plate- or needle-shaped particles (bottom left), whereas their spherical nanosized morphologies are in most cases the sign of their amorphous nature (bottom right). Reproduced and adapted with permission from Motskin et al., Biomaterials, 2009, 30, 3307–3317, Butterworth-Heinemann in Association with the Biological Engineering Society and Fan et al., Biomaterials, 2009, 30, 478–483, Butterworth-Heinemann in Association with the Biological Engineering Society.

The typical models of protein–mineral interaction refer to specific binding of additives to crystal faces, which are then prevented from growing. Such is the case for the current model of amelogenesis wherein nanospherical particles of amelogenin are assumed to bind onto (hk0) faces of the growing HAP crystals and thus foster their uniaxial growth along [001] axis.[91] However, one of the opposing actual explanatory trends lies in invoking the surface-controlled channeling or the diffusion-controlled transportation activity of additives for the sake of building apatite crystals using either amorphous units or individual ions and complexes as building blocks. Such an idea is supported by the successful synthesis of a few ceramic materials, previously obtainable only through high-temperature annealing treatments, by precipitation at room temperature in the presence of short peptides derived from phage display libraries.[92,93]

Precipitation of HAP is, in fact, often quite morphologically sensitive (Figure 3) to the presence of additives.[94–99] Electrostatic forces that govern the interaction between growing inorganic particles and given additives and tunable by controlling the ζ-potential of colloidal particles are thus regularly shown as crucial for setting the optimal conditions for the growth of nanocrystals in desirable sizes and morphologies. For example, elongated HAP particles were obtained in the presence of poly(L-lysine), whereas in the presence of more charged poly(L-glutamic acid), small nanocrystals resulted under otherwise same conditions of precipitation.[100] This was explained by assuming that the more charged the heterogeneous nucleation surface, the more cations will be attracted thereto and the more nuclei will be formed. Consequently, the particles will be smaller and there would be no biaxial growth, unlike in the case of the less charged macromolecular surface. On the other hand, hydration effects could not be reduced to a simplistic rule of a thumb, and in reality it is difficult to predict the effects of addition of salt and pH change as they are always synergistically bound with the effects of other species present in the actual reaction system. A recent computer model[101] has thus shown ions with low charge density adsorbed preferentially on the surface of a hydrophobic particle, leading to micelle-like clusters of particles, whereas ions with high charge density tended to be depleted from the particle surface, leading to formation of similar clusters of dispersed hydrophobic particles. Only in the intermediate case, conditions for the dispersion of individual particles and avoidance of the formation of clusters were found. Generally

speaking, the effect of additives on composition, structure, and properties of HAP particles is so intensive that we can over and over again recall the words of Stephen Mann of Bristol University: "Such is the lure of the organic matrix that you can attend some scientific conferences, notably those on bone mineralization, and hardly ever come across a serious mention of calcium phosphate".[102]

Methods for preparation of fine CAP particles usually follow a soft chemical route,[105,106] which involves precipitation from solutions or suspensions of precursor salts, ideally with no subsequent high-temperature annealing treatment. Entrapment of additional composite components is carried out by precipitation of CAP in the presence of dissolved cargo molecules. Surface functionalization, on the other hand, normally requires a time-delayed introduction of the surface-anchoring molecules owing to a sufficient aging that the initial precipitate has to undergo in solution before the formation of HAP phase. Conjugation of proteins, peptides, polymers, cell-penetrating moieties, reporter groups, and other functional ligands to the carrier surface is in the case of CAP particles expected to proceed noncovalently, that is, via adsorption governed by hydrophobic or van der Waals forces.

Amphiphilic mixtures in form of reverse micelles, other microemulsion phases or simple steric dispersants could be implemented with the purpose of preventing agglomeration of particles and stabilizing their suspensions.[107–109] Spray drying enables drying of the precipitated powders either without inducing an undesired agglomeration of the particles or with forming attractive and uniform agglomerates of smaller particles.[110] Bis(2-ethylhexyl)sulfosuccinate (AOT) has thus recently been used for the purpose of assembling HAP particles into enamel-like bundles.[111] Successive modification of surface charges of the particles and of an adsorbent during the cycles of washing and rinsing can also be carried out to avoid agglomeration and yield pure and stable dispersions of CAP nanoparticles. Agitation by means of ultrasound is often used for the same purpose, although it can markedly affect not only the particle size distribution but also their morphologies. Hence, in a particular study, ultrasound applied during the ripening of a precipitate comprising hollow CAP nanospheres led to their transformation into fibrous particles.[112] As for the particle composition, 80% HAP and 20% TCP is usually pointed out as an ideal phase composition ratio from the point of view of the optimal bioresorbility of the compound.[113] However, by varying HAP/TCP ratio in the final compound, the optimal degradation rate thereof, defined by the intended application in the body, can be set. Porosity, usually controlled using a porogenous agent, such as poly(methyl methacrylate),[114] presents another structural property of the particles that can be used to control the release rate of encapsulated compounds.[115] The particle size presents another important parameter that defines the bioresorption rate of HAP materials. As expected, smaller, nanosized particles are associated with significantly higher resorption rates compared with the bigger, microsized ones.[116] In addition to composition and size, the particle shape is also known to influence the uptake efficiency of the encapsulated drug.[117] The morphology of CAP particles may be thus used as a parameter in optimizing a favorable bioresorbability thereof. It is usually claimed that the particles produced in forms of powders or suspensions should ideally be nonagglomerated, spherical, and uniform in size and morphology, which is to ensure the reliability and reproducibility of their application in the body. With respect to that the surface of HAP particles could be modified with various additives, such as: hexanoic and decanoic acids that hydrogen bond to the surface P—OH groups; alkanoic acids with longer alkyl chains so as to render the surface hydrophobic; oleic acid typically applied for the stabilization of magnetic fluids; sodium dodecyl sulphate or other surfactants; or through covalent bonding, the example of which may be esterification of surface P—OH groups with dodecyl alcohol, alkyl phosphates, pyrophosphoric acid, hexamethyldisilazane, or various silanes, which could be used as precursors for silica coating.[118,119] Surface modifications affect the surface charge, hydrophilicity, colloidal stability of the particles and their interaction propensities, thereby affecting their biological response as well.

For the purpose of obtaining small, nanosized particles, abrupt precipitation procedures, yielding a high density of crystallization nuclei, are to be performed. Avoiding the overlap of nucleation and crystal growth phases is normally considered as the key to achieving monodispersity of synthesized particles. Low nucleation rates and fast crystal growth rates are, in contrast, the fundamental recipe for producing elongated HAP crystals. For example, when a slow and controlled decomposition of urea was used to promote changes in pH and provide conditions for precipitation, the HAP crystals formed were of plate-shaped and needle-shaped character.[120] Highly strained single-crystal apatite fibers with 20–60 μm in length and 100–300 nm in diameter were also obtained in a precipitation reaction using urea as the alkaline agent.[121] pH and precipitation temperature as well as the molar ratio of precursor ions are control parameters often used to optimize and fine-tune the structural, the morphological, and, thereupon, the biodegradation properties of the carrier particles. As it is known that the formation of HAP follows a multistep route permeated with complex solid–solid transformation pathways, dictated by the empirical Ostwald–Lussac's rule of kinetics of phase transformations,[122] aging time is another experimental parameter applied to optimize the synthesis conditions (namely, insufficient aging can lead to amorphous components remaining in the system, whereas an overly extensive aging can lead to Ostwald ripening and broadening of the particle size distribution that ripening naturally entails). What follows is exactly a discussion of the critical aspects of this complex chemical mechanism.

Mechanism of formation of HAP by precipitation

Even if explored all alone, without any involvement of additives, precipitation of HAP, especially at low supersaturations, still presents an enigma. This process is not only sensitive to the mildest influences within the experimental

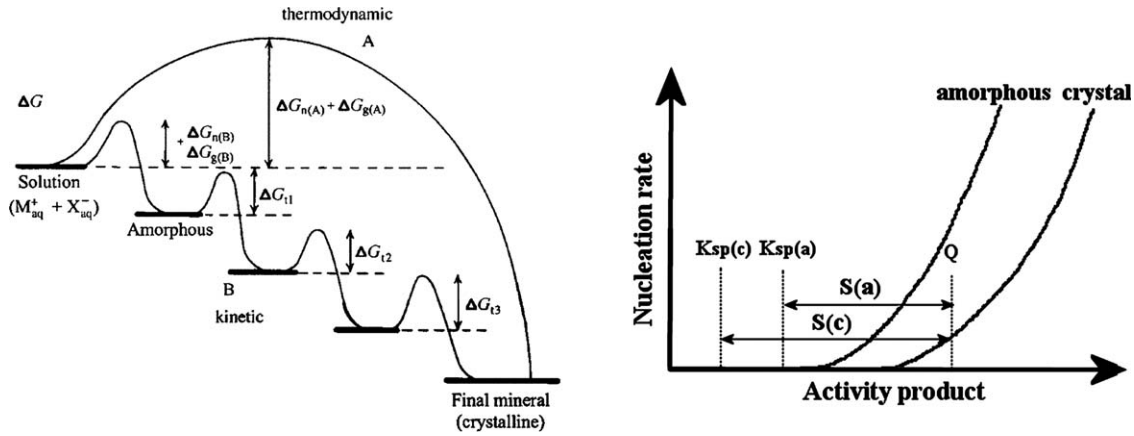

FIGURE 4. An inability of the system to transverse multiple energy barriers posed on its way to the final, most energetically favorable state implies its transition through a number of transient stages. As the Ostwald–Lussac rule suggests the less stable polymorph will pose the lowest energy barrier in front of itself, so that the precipitated ions will adopt it as one of the temporary states on their way to settle into a more stable phase. The image on the left is reprinted with permission from Xu et al., J Mater Chem, 2007, 17, 415–449, Royal Society of Chemistry. The diagram on the right demonstrates how even though supersaturation may be higher for a crystalline phase ($S(c)$) than for the amorphous ($S(a)$), the nucleation rate of the amorphous phase is higher at any given value of the product of ionic activities (Q), which is a consequence of a lower S being offset by a reduced interfacial energy.

conditions, such as the amount and nature of impurities or the texture and chemical identity of the reaction vessel (which sometimes drastically affects the level of critical supersaturation) but also the chemical pathways leading to the formation of HAP as the final phase are subject to change depending on mildest modifications of the initial experimental conditions. Because of this reason, researchers in the biomineralization field are still in dispute over the exact chemical mechanism of formation of HAP in biological and *in vitro* conditions alike. Ostwald–Lussac's rule predicts the highest nucleation rate for the least stable phase for which the supersaturation limit is exceeded under given conditions, implying that amorphous CAP will under most circumstances be the first phase to precipitate, followed by the solid state transformation to OCP first and only then to HAP. $Ca(OH)_2$ or TCP may be secondary phases depending on the exact stiochiometric ratio between the precursor Ca^{2+} and $H_xPO_4^{x-3}$ ions in the solution. However, the exact chemical pathways, the transformation mechanism (dissolution/recrystallization or bulk rearrangement of ions within the prime crystal lattice), the transient compounds, and time frames for the nucleation and growth of each one of the phases are still subject to uncertainty.

In any case, the nature of formation of HAP as predicted by Ostwald–Lussac's rule presents an argument against the sole diffusional growth of these crystals. Although for a long time the latter has been the major paradigm in explaining the formation of biological crystals, what we are witnessing today is a paradigm shift wherein the growth of crystals via amorphous precursors is slowly becoming the major explanatory model in the field.[123–125] A large amount of evidence has been collected recently in favor of this new paradigm, which proposes the role of macromolecules in linking and organizing precursor amorphous or crystalline units within the growing crystals.[126] As of today, many variations on this theme flood the literature. According to one of the models, amorphous CAP acts as a mortar in cementing the bricks that are nanosized HAP units transported by biological molecules and is also able to subsequently crystallize, contributing to the integrity of the final structure.[127] Another model proposes these building blocks to be bubbles of a phase that stands at the boundary between liquid and amorphous solid. These small liquid/amorphous-like entities are supposed to form even without a polymeric process-directing agent, although in such case they are short-lived and difficult to detect. In addition, a strict application of Ostwald–Lussac's rule implies the formation of a structured liquid phase before the formation of an amorphous solid (usually considered as the first one to form, subsequently transforming to more stable solid phases). D'Arcy Thompson in his book *On Growth and Form* had thus argued: In accordance with a rule first recognized by Ostwald, when a substance begins to separate from a solution, so making its first appearance as a new phase, it always makes its appearance first as a liquid.[128] Most of the polymer phase is returned back to the solution, although on rare occasions it may get trapped between the crystalline layers, serving as an evidence of said nature of formation.[129,130] Invoking this mechanism, even monocrystalline systems, such as the basic crystalline units of enamel, microsized apatite fibers, are accepted to be, may form through aggregation of subunits. The recent TEM studies have confirmed the existence of transient amorphous CAP phases in the developing enamel.[131] It has also been documented that long and defect-free filaments with the aspect ratios of up to 10^4 can be obtained by the aggregation mechanism,[132] overthrowing the idea that so grown apatite fibers would be prone to fracture due to many defects. In fact, in the context of a highly anisotropic organization of apatite crystals within enamel, such a slightly imperfect crystalline nature could be even proven as favorable.

As a consequence of Ostwald–Lussac's rule (Figure 4) and the relatively large number of phase compositions, the

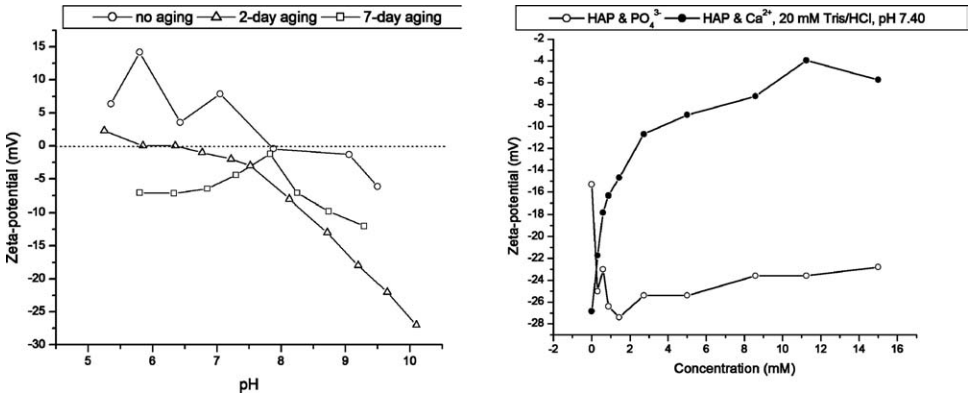

FIGURE 5. (a) ζ-potential versus pH curves for as-prepared, 2-day-aged and 7-day aged CAP prepared by precipitation from a solution comprising 25 m*M* $CaCl_2$ and 15 m*M* KH_2PO_4 at pH 10.5. (b) ζ-potential of suspended HAP nanoparticles vs. [Ca_2+] (-o-) and [$H_2PO_4-/HPO_{42}-$] (-●-) at pH 7.40 ± 0.02. The graph shows that both of these ionic species adsorb on the HAP particle surface. The plateau observed in both cases signifies the adsorption of ions reaching a saturated level.

stages of which the precipitate has to pass through before reaching HAP crystal symmetry, the formation of the latter compound by precipitation can be expected to proceed at a relatively slow pace. The complexity and the crucial impact of the slow formation rate are best illustrated by the fact that the whole process of formation of elongated HAP crystals in dental enamel, having aspect ratios of up to 10^4, takes more time to complete than is needed for the entire embryo to be created *in utero*.[133] In view of such a slow rate of crystallization, there is a question whether this process could ever occur as a slow stream of crystallization, and not as a back-and-forth stream of crystallization/dissolution/crystallization, in which mistakes are made, but recognized and subsequently corrected, as is otherwise typical for biological syntheses.[134,135] Namely, it is not the perfect reproduction but a high selectivity for the product properties that typifies biosynthetic phenomena. A similar stochastic nature can be, in fact, seen as ingrained in practically every aspect of creativity exhibited in the biological world, from human thinking and reproduction to the evolution of life.[136] This may also shed light on why the simultaneous activity of two types of cells—osteoblasts that build the bone material and osteoclasts that degrade the mineralized tissue—is required to maintain the functional structure of bone.

As far as the major parameters that could be controlled so as to optimize the formation of HAP along a desired route are concerned, the following can be numbered: pH, ionic strength, temperature, concentration and identity of additives, Ca/P molar ratios, and supersaturation.[138] pH primarily affects precipitation of HAP with its effect on the amount of free hydroxyl groups and on the balance of phosphate species. A shift to lower pH will lower the saturation level by decreasing the concentration of free OH^- groups and shifting the balance of phosphate species from PO_4^{3-} to HPO_4^{2-} to $H_2PO_4^-$ to H_3PO_4. Hence, the lower the pH, the more of the phosphate groups will be protonated, and the precipitation will be less favored. Also, pH can shift the surface charge of the interacting particles by changing the distribution of proton and hydroxyl groups hydrating the interface. Although H_3O^+ and OH^- are usually considered as charge-determining ions in case of HAP particles, ions other than these can adjust the surface charge, and in calcium-containing solutions, Ca^{2+} ions may bind to the negatively charged HAP surface at pH > IEP (isoelectric point), leaving the surface neutral rather than negative. The opposite effect can take place in phosphate-rich solutions when binding of $H_xPO_4^{x-3}$ species at pH < IEP may result in a negatively charged HAP particle surface rather than the positive. These insights were, however, gained not by means of electrophoretic analyses but through the Brönsted isotherm[139] and are not necessarily in agreement with the electrophoretic studies.[140] In view of the propensity of HAP to undergo dissolution/recrystallization processes, it is questionable how stable the structure and composition of the interface layer of HAP particles is as they undergo a pH change. It is known that the drastic effect of F^- in the suspension medium on the ζ-potential can be explained only by assuming its incorporation in the crystal lattice of the apatite.[141] Hence, an intensive exchange of ions between the solution and HAP particles is expected to take place, frequently shifting the ζ-potential in hardly predictable ways. This may explain why the surface composition of suspended or precipitated HAP particles is different compared with their bulk composition.

A hydrated layer containing relatively mobile ionic species is assumed to be present on the surface of precipitated CAP particles in the solution. The composition of this layer would be subject to change depending on pH and ionic content of the medium. Experiments carried out in our laboratory have, furthermore, shown that the ripening time of CAP precipitate has a marked effect on the surface charge of the particles. As can be seen from Figure 5a, ζ-potential of the particles in the pH range of 5–8 shifts from positive to negative values with increasing the aging time in solution from 10 min to 7 days. The high surface ion mobility is also thought to be responsible for the relatively high electrical conductivity exhibited by HAP. In addition to the high surface area of the mineral particles in bone, the ion-exchange propensity of HAP may be another factor crucial in

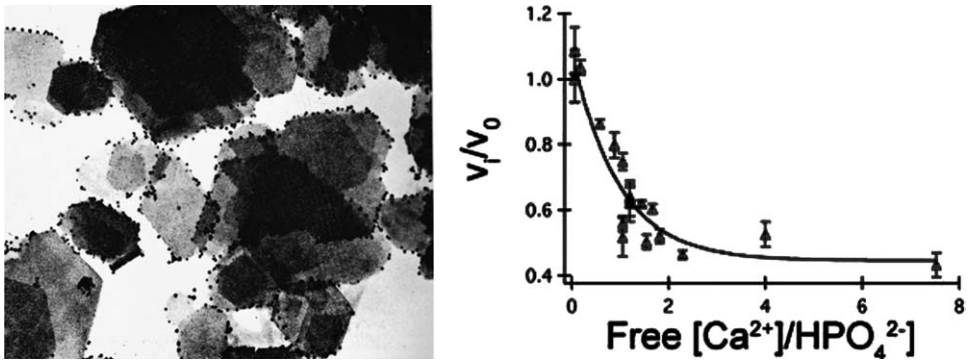

FIGURE 6. Both microsized kaolin crystals and nanosized gold particles on the left image are negatively charged as a whole. However, because edges of kaolin crystals are positively charged, gold nanoparticles effectively adsorb onto them. HAP crystals show a similar modulation of charges over their surface, which enables them to interact with an array of species relying on electrostatic attraction. Reprinted and adapted with permission from Cai et al., Chem Mater, 2007, 19, 3081–3083, American Chemical Society. The image on the right shows increasing HAP crystal growth rates when the activity/abundance of $H_xPO_4^{x-3}$ ions in the solution dominates over the activity/abundance of Ca2+ ions. Reproduced from Ref. 163, with permission from Springer.

providing the cellular environment with an access to the constituent ions for the sake of facile bone remodeling or consumption of ions for other purposes (as bone also acts as a frequently accessed mineral reservoir). One of the consequences of the maturation of bone may thus be correlated with the loss of these ion-exchange properties.[142] On the other hand, despite the high mobility of surface ions, HAP is typified by its sparsely soluble nature and slow crystal growth even at very high supersaturations.[143,144] This implies facile reorganization and restructuring of ionic layers (i.e., the solid surface layer of the particle and the double-layer of ions surrounding it) that contribute to surface charges following changes in the ionic environment. Indeed, ζ-potential of HAP particles has been observed to change with the immersion time for certain compositions, suggesting an intensive exchange of ions across the interface layer and its restructuring following changes in the solvent medium.[145,146] It is natural to expect that the structure of the mobile surface layer would depend on the physical and chemical conditions under which the particles were prepared, and this effect can be invoked to explain a large discrepancy between the IEPs and surface potential values for HAP particles reported in the literature. Consequently, it has been evidenced that methods for preparation and any changes in stoichiometry (Ca/P ratio) significantly affect IEP of HAP.[147] Pure HAP powders precipitated in acidic conditions were, for example, shown to possess 1–3 pH units lower IEPs compared with those precipitated from alkaline solutions.[148]

HAP particles in sols are also excessively prone to selective leaching of ions, which leaves different ζ-potential versus pH curves of the same powder in different solvent media as a consequence.[149] Such mild solubility effects are known to be responsible for the scatter in IEPs and points of zero charge values reported in the literature. Thus, whereas some studies report negatively charged particles in the entire pH range in which HAP is the stable phase,[150] others report IEP values at anywhere between 5 and 7.5, below which the particles should become positively charged.[151,152] There are, however, reports[153] on IEP of HAP suspensions detected at pHs as high as 10. In addition, HAP has two types of crystal planes, which carry different net charges: positive on *a* planes and negative on *c* planes, and there as speculations that the *a* planes tend to adsorb acidic proteins, whereas the *c* planes tend to attract the basic ones.[154] Elongation of HAP particles along the *c*-axis would thus lead to a shift toward more positively charged particles with a higher specificity of adsorption onto negatively charged acidic proteins.[155] As biological entities are predominantly dispersed on the negative side, it comes as no surprise that positively charged HAP promotes good adhesion of cells thereto, whereas poor cellular adhesion and growth was observed on negatively charged HAP surfaces.[156] Extracted biological HAP crystals were thus also shown to comprise a series of discrete and alternating domains of variously charged (in both magnitude and sign) surfaces (Figure 6a), independently of topography, indicating their intrinsic potential for periodic binding of matrix proteins under physiological conditions.[157]

In addition to ions in the double layer surrounding the particle, HAP particles in suspension undergo practically all the mechanisms that contribute to the charged surface (that is, adsorption, ionization and selective dissolution), which additionally increases the complexity of this physical effect. In case of hydrous metal oxide sols, in general, the surface hydroxyl groups (M—OH) become deprotonated at high pH values, transforming from —OH to $—O^-$ and thus contributing to the negative charge of the particle surface, whereas they become protonated, transforming from —OH to $-OH_2^+$ at low pH values. As Ca^{2+} ions on the CAP particle surface are bound to OH^- groups owing to hydration effects, protonation/deprotonation thereof can influence the particle charge. HAP particles also cannot be considered as immune to selective dissolution, which is known to contribute to imbalanced neutrality of ionic crystalline particles as wholes in many ionic crystals. For example, in the case of AgI particles, $pK_{sp} = 16$; however, the zero point charge does not exist at pAg 8, but is displaced to pAg 5.5 (i.e., pI 10.5)

because smaller and more mobile Ag^+ ions are held within the AgI crystal lattice less strongly than heavier and less mobile I^- ions.[158] A similar discrepancy in the mobility between Ca^{2+} and $H_xPO_4^{x-3}$ ions can be inferred for the case of HAP crystal symmetry. Namely, Ca^{2+} ions are more flexibly arranged within the lattice, which is therefore more prone to display Ca^{2+} vacancies, whereas PO_4^{3-} groups are practically those that define the hexagonal structure of the crystal. The atomic arrangement of all calcium orthophosphates is built up around the network of PO_4^{3-} groups that provide stability to the structure.[159] This may also explain why the crystallization of a few CAP phases has been shown[160] to be much more sensitive to the activity of phosphate species than to that of Ca^{2+} [Figure 6(b)], even though both ions adsorb well to the surface of HAP particles [Figure 5(b)]. This is presumably due to weaker hydration attraction of solvated $H_xPO_4^{x-3}$ groups to the surrounding protons than of solvated Ca^{2+} ions to the adjacent OH^- groups. As a result, a higher activation barrier is attributed to Ca^{2+} in the solution than to $H_xPO_4^{x-3}$, which is also in agreement with the generally observed more pronounced solubility effect for anions of the Hofmeister series than for cations,[161] corroborating their more significant effect on the morphology of precipitated nanoparticles as well.[162]

Ionic strength plays a role in screening ion–ion interactions (as well as the ones between charged colloidal particles) in the solution. Namely, surface charge density is equal to $\sigma = \varepsilon\kappa\psi_o$, where ε is the dielectric constant of the medium (inversely proportional to the ionic strength), $1/\kappa$ is the length of the diffuse double layer (composed of Stern layer of adsorbed counter-ions and a diffuse layer composed of both counter-ions and coions, yielding as a sum the Debye length at which the electrical neutrality is again established), and ψ_o is the surface potential. The addition of an inert electrolyte compresses the diffuse layer of charged ions and coions around each of the dispersed and charged particles. Namely, a higher concentration of coions and counter-ions implies screening of the particle surface charge at a closer distance to the particle. In other words, $1/\kappa$ decreases that entails either an increase in σ or a decrease in ψ_o or both. For example, in case of AgI particles whose potential depends on the concentration of Ag^+ and I^- in the solution, addition of electrolyte and the corresponding drop in κ leads to adsorption of potential-determining Ag or I ions, which increases σ but keeps ψ_o constant. However, for an ionogenic surface, σ stays constant, but ψ_o drops. Simply saying, increasing ionic strength causes the layer of counter-ions around the charged particle to shrink and thus increases the propensity of the dispersed particles to agglomerate, which is known as salting out effect, and is known to be involved in the pathological calcifications in the body.[164]

Now, it is well known that Nature disperses colloids almost exclusively on the negative side. Most cells and biological surfaces are thus negatively charged. The same can be said for HAP particles in physiological conditions. The effect of the ionic strength on (de)stabilization of biological colloids, including HAP, should thus be in theory primarily sensitive to the valence of the cation. Critical coagulation concentration (ccc) of the cation may be calculated using the following empirical formula: ccc $= 0.8/v^6$, where v is the valence of the cation. One can then see that for monovalent Na^+ ccc $= 0.8M$, for divalent Ca^{2+} ccc $= 12.5$ mM, and for trivalent Al^{3+} ccc $= 1$ mM. However, although CAP more efficiently nucleates on negatively charged surfaces, it can nucleate on positively charged ones as well for as long as the proper chemical identity is selected.[165] On the other hand, the sign and intensity of the charge of the nucleation surface are known to play a determining role in defining the crystal symmetry of the resulting precipitate.

Ca/P molar ratios affect the formation of HAP firstly as the result of unequal activation barriers for cations and anions [Figure 6(b)]. Although most crystal growth models neglect this effect by treating all the inclusive ions identically, whenever the crystal growth rate depends on the rate-limiting ion, this effect has to be taken into account in addition to other thermodynamic and kinetic factors.[166] For example, because of extensive readsorption of $H_xPO_4^{x-3}$ ions onto the particle surface, Ca/P molar ratios in the equilibrium solution were often measured to be as high as 25 despite the composition of the precipitate corresponding to almost stoichiometric HAP.[167] The ratio between Ca^{2+} and $H_xPO_4^{x-3}$ ions in the solution is also important because it may trigger precipitation of a specific phase combination and induce a particular phase transformation pathway in the solid state. Different Ca/P ratios can thus initiate different kinetic pathways for the reaction, which brings us to the discussion of the mechanism of precipitation of HAP.

The main parameter used to describe the latter is supersaturation ratio, S, defined as

$$S = Q/K_{sp}$$

Q is the product of ionic activities of precursor ions in the solution for the given stoichiometry, and for half a unit cell of HAP equals

$$Q = \{Ca^{2+}\}^5\{PO_4^{3-}\}^3\{OH^-\}$$

K_{sp} is the product of ionic activities for the given compound at the saturation level. In view of the continuous transfer of matter across the solid/liquid interface in both directions, K_{sp} could be also defined as the product of activities of dissolved ions of a solid substance in equilibrium between the dissolved ions precipitating and the precipitated ions dissolving. Ostwald–Lussac's rule dictates that the most soluble phase (i.e., the least stable) for which $S > 1$ will be the first to precipitate, which will be successively followed by precipitation of less soluble phases. The reason for this is that the thermodynamic barrier posed between the state occupied by dissolved ionic species and the solid phase will be the lowest for the thermodynamically most unstable phase. An important contributor to this effect is the surface/interfacial energy, that is, the work required to increase the surface area of a substance by one area unit, which is the hurdle that must be overcome when forming a solid phase.

Amorphous phase is less ordered and will have a lower interfacial energy (and that particularly if it is hydrated—as such, it is actually most similar in chemistry to the surrounding aqueous environment) than any crystalline phase, which means that it tends to be the first to precipitate prior to subsequently transforming into a more stable, crystalline modification. In case of the precipitation of calcium phosphates, this means that HAP would be the last phase to form. The initial precipitation of the amorphous CAP is normally followed by nucleation of OCP at a certain stage. However, note that only phases with $S > 1$ are involved in this successive precipitation. Those for which $S < 1$ are assumed not to be precipitated at any stage of this process, and their appearance may only be transitory during phase transitions that involve rearrangements of ions in the solid state. This kinetic rule was empirically observed, although it can be nowadays supported by theoretical arguments. In one such calculation,[168] it was shown that in simulated body fluid (SBF), whose S normalized per growth unit ($n = 9$ for HAP) equals 19.5 with respect to HAP, the nucleation rate of OCP is higher than the one for HAP, implying that OCP would be the preceding crystalline phase to form. DCP, however, cannot form under these conditions because the solution itself is undersaturated with respect to it. Only if $[Ca^{2+}]$ and $[H_xPO_4^{x-3}]$ in the fluid increase so that the solution becomes supersaturated with respect to DCP, the nucleation rate for this phase would become higher compared with the one for OCP and HAP. Also, as pH of SBF increases, the difference between the nucleation rates for the formation of HAP and OCP decreases, and at ~pH 10 they become equal. In fact, as phases such as DCPD or OCP are thermodynamically less stable than HAP, they would never form in reality if it were not for their ability to grow at a comparatively high rate. HAP is a relatively hard crystal, ranking 5 on the Mohs scale but despite that as previously noted, it has an unusually low interfacial energy, which explains for the facility with which it nucleates in form of small particles in both biological and *in vitro* conditions. If HAP had a high interfacial energy, the long persistence of these tiny crystals in both the biological and geological environments would not be possible. However, these other, thermodynamically less stable CAP phases have even lower surface energies, which is the reason why they nucleate even faster than HAP, and thus, often present intermediates leading to the eventual formation of HAP.

OCP crystals almost always come in plate-shaped (100) morphologies. Namely, (100) OCP faces are more hydrated than others and thus do not provide that favorable conditions for the attachment of PO_4^{3-} and Ca^{2+} ions as other phases. Consequently, the crystals grow slower along [100] axis, which results in (100) faces being the dominant in the final crystal morphologies. Also, (100) faces have the lowest interfacial energy, so that the crystal growth proceeds in such a way to maximize their exposition on the crystal surface. This rule, which is in accordance with the Wulff construction,[169] does not necessarily apply for biomineralized HAP for which, because of the growth regulated by organic adsorbents and matrices, the crystals often predominantly expose less thermodynamically stable faces. For example, the outer surface of the tooth enamel is composed of the smallest habit face, (001), which is more resistant to dissolution under acidic conditions than (100)[170]. Still, as (100) faces are the principal ones on both OCP and HAP crystals, and since there are two of them on an OCP crystal and six of them on a HAP crystal, OCP should indeed have a plate-shaped or leafy morphology, whereas HAP should most optimally possess a hexagonal acicular morphology. However, when OCP acts as a precursor (an intermediate phase) for the formation of HAP, the final HAP particles retain the plate-shaped or acicular and fibrous morphologies in which (100) faces are dominant. Sometimes thus they retain forms of rosettes and fascicles with protruding blades or fibers. Intermediate phases are thus expected to play a crucial role in defining the morphology, interfacial properties, and the growth mechanism of the HAP phase.

The first phase that should form upon precipitation of CAP is thus an amorphous phase with the stoichiometric formula of $Ca_9(HPO_4)_x(PO_4)_{6-x}(OH)_x$ ($x < 0.5$). In contrast, notice that the stoichiometric formula of HAP is usually written as $Ca_{10-x}(HPO_4)_x(PO_4)_{6-x}(OH)_{2-x}$ ($0 < x < 1$). The particles initially formed would actually be agglomerates of amorphous CAP units. Only in the following stage, the transformation of this phase into HAP and any other phase with $S > 1$ under the given conditions would take place. Under most of the conditions that resemble the physiological ones (pH ≈ 7.4 and $T = 37°C$), the identity of the precipitate changes over aging time (although OCP is accepted to be the transient phase in physiological conditions and at pH < 9, the mechanism is not clearly defined at higher pHs), eventually resulting in a stable and most often biphase product (HAP/TCP). Solubility isotherms for DCPD and OCP at room temperature and for Ca/P molar ratio of 1.16 (resembling the Ca/P ratio within the initially precipitated amorphous phase) intersect at pH 6.7 (above this value, OCP is a more stable phase, and the trend is reversed at lower pHs), which implies that according to Ostwald–Lussac's rule,[171] the transformation of the amorphous phase to HAP should follow OCP→DCPD→HAP route at pH < 6.7 and DCPD→OCP→HAP route at pH > 6.7. Interestingly, magnetic field has been shown to accelerate the phase transformations along steps defined by the Ostwald–Lussac rule upon precipitation of CAP, also modifying ζ-potential of the particles.[172] The same effect was observed in the case of calcite[173,174] and many other inorganic and organic diamagnetics, including proteins,[175] where owing to the diamagnetic anisotropy of the crystalline order or the peptide bond an external magnetic field has an effect on precipitation and assembly thereof.

If the trend of pH change during this process is followed, it would be observed that the stage of formation of the amorphous phase is followed by a mild decrease in pH caused by the higher alkalinity of Ca^{2+} compared with the acidity of $H_xPO_4^{x-3}$. The subsequent formation of HAP is, however, entailed by a more significant drop in pH due to OH^- ions getting incorporated in the crystal lattice. The time span between mixing the reactants and the point when

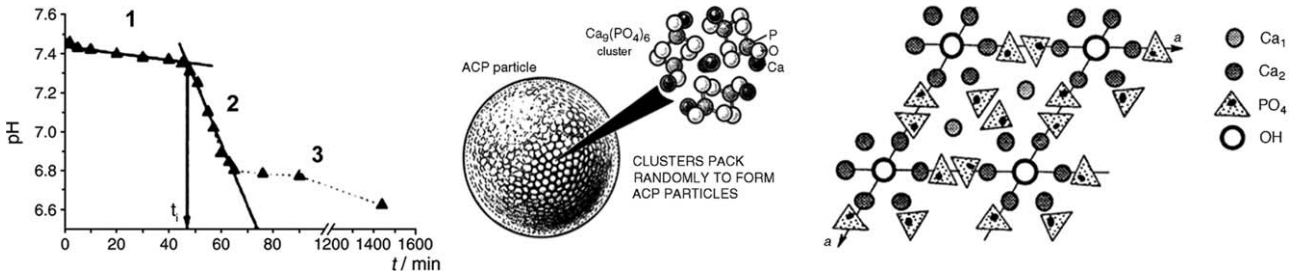

FIGURE 7. Three stages in the trend of pH drop following precipitation of CAP and formation of HAP (left), the presumed random packing of amorphous clusters into nanosized amorphous CAP (middle), and their rearrangement into symmetry that corresponds to HAP (right). Reproduced with permission from Sikiric, Adv Colloid Interface Sci, 2006, 128–130, 135–158, Elsevier and Posner et al., Prog Cryst Growth Charact Mater, 1980, 3, 49–64, Elsevier.

a more drastic pH drop is detected is considered as the induction time (a.k.a. nucleation lag time), τ, which is inversely proportional to S. Hence, the induction time is taken not as the time between the point of mixing the components and the formation of the first amorphous CAP particles, but as the time that passes before HAP starts forming, which is marked by the onset of the more significant pH drop (Figure 7). The third stage is typified by a pH drop rate with a similar slope as in the first phase, which is the sign of stabilization of the phase transformation. The slope eventually approaches zero, meaning that the stable phase has formed. All in all, the overall pH drop trend is the one of sigmoidal shape. As expected, the induction period decreases with increasing the initial reagent concentrations, temperature and pH. However, pH change cannot be used to precisely estimate the rate of nucleation and crystal growth, primarily because of the inevitable presence of the buffering phosphate species. Even without their buffering activity, it is known that the nucleation rate increases with time (as $1 - \cos x$ function), from $t/\tau \approx 0.5$ to $t/\tau \approx 6$ when the constant nucleation rate is reached. This explains why the part of the pH versus t curve where the onset of the pH drop is observed typically follows the trend of increasing its slope with time, all until the mother phase gets depleted of the growing units and the curve approaches the third stage of the process, that is, the one of mere rearrangement of the crystalline phase.

Hence, the process of the formation of HAP in a precipitation reaction from a pure solution can be divided to following stages[178]: (i) homogeneous nucleation; (ii) aggregation of primary amorphous CAP particles into typically spherical units; (iii) aggregation of spheres into chain-like structures; (iv) growth of these structures; (v) secondary precipitation and phase transformation. The initially precipitated particles of the amorphous phase were observed to be round-shaped with 20–30 nm in size (although they can reach 120 nm in size),[179] but composed of smaller particles of 4 nm in size on average. It was also observed that an increase in the ripening time implied aggregation of spherical singlets and formation of needle-shaped CAP particles of about 20 nm in length.[180] This aggregation model for precipitation of HAP (Figure 8) is in agreement with numerous literature reports. Matijevic has pointed out that most microsized uniform colloidal particles form not through following the classical LaMer's model that refers to successive stages of nucleation and crystal growth but by involving an aggregation of primarily precipitated units at a certain stage of the process.[181–183] Microstructural investigations of fine particles obtained by precipitation thus in most cases reveal structures composed of aggregated subunits,[184] and this mechanism of growth has been evidenced for numerous inorganic and organic systems alike.[185–187] A recent high-resolution *in situ* observation of formation of fine particles has shown an intensive coalescence of nanoparticles during their growth.[188] The structural nature of the primary units and their transformation pathways are, however, still the subject of disagreement among different research groups. The difficulty in assessing the structure of primarily precipitated units stems from the fact that owing to its transient nature, the amorphous CAP normally remains undetected unless it becomes stabilized by additives, such as rare-earth metal ions or peptides.

However, the exact pathway of phase transformations following precipitation and leading to HAP as a final product is subject to change depending on the experimental conditions, including ionic concentrations, molar ratios of precursor ions, pH, T, the presence of additives, and so forth. Thus, for example, under given conditions that involved [Ca] $> 0.5M$ and pH 10–11, it was shown that OCP is the first phase that forms, transforming subsequently to amorphous CAP (which was observed to be the fastest step), which then transforms to DCP, which eventually transforms to HAP.[191] The process was sensitive to temperature, as 24 h was required to attain HAP at 25°C, whereas the same process was over in only 5 min when taken place at 60°C. When precipitation was carried out at 95°C and at pH 10.6, the formation of HAP was so quick that all other phases were virtually undetectable. This may have been due to a sufficiently high heat content of the system, which enables rapid transcending of the stages dominated by intermediate phases. In support of this observation, (a) DSC/TGA analysis led to detection of only the adsorbed water loss peak; (b) X-ray diffraction (XRD) showed unmodified phase identity and no change in the lattice parameters (which would result from the loss of OH^- ions from the crystal lattice and the formation of vacancies during annealing) after heating up to

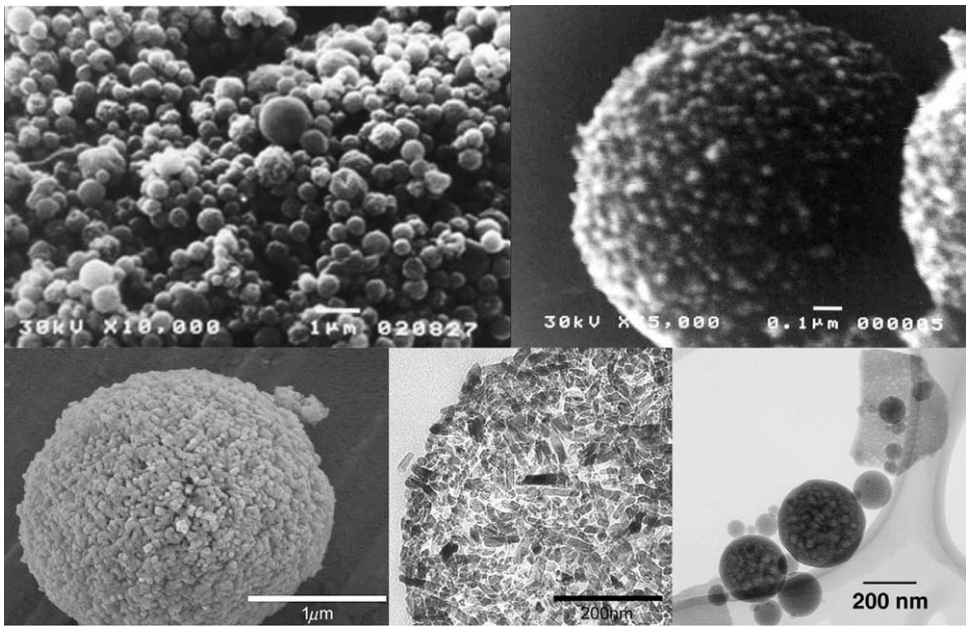

FIGURE 8. Uniform spherical HAP particles obtained using ultrasonic spray-pyrolytic processing (upper left), forming through aggregation of smaller spherical subunits (upper right). Reproduced with permission from Jokanovic et al., J Ceram Process Res, 2004, 5, 157–162, Hanyang University Press. Spray drying is another method that routinely leads to formation of microsized HAP particles through aggregation of nanosized subunits, and some of the morphologies are shown in images in the bottom row. Reproduced from Chow and Sun L, J Res Natl Inst Stand Techol, 2004, 109, 543–551, U.S. National Institute of Standards and Technology.

1100°C; and (c) IR spectroscopy showed only bands at 3572 and 631 cm^{-1} coming from stretching and vibrational modes of OH^- ions and those at 1087, 1032, 962, 601, 571, and 474 cm^{-1} ascribed to PO_4^{3-} vibration modes, whereas the HPO_4^{2-}-derived band at 875 cm^{-1}, CO_3^{2-} absorption at 1410 cm^{-1} and weak shoulders at 990, 970, and 945 cm^{-1} indicative of α- and β-TCP were absent.[192] In another one of the studies,[193] any $T < 95$°C required ripening periods extending up to 20 h to obtain pure HAP. The size and crystallinity of HAP particles increased with increasing the precipitation temperature. Intuitively, this could be explained by assuming that the number of nuclei formed is proportional to *S*, which would be lower at a higher temperature. Smaller number of nuclei, on the other hand, implies the formation of larger particles. However, simple solubility product calculations can show that an increase in temperature corresponds to higher, not lower *S*, and the magnitude of change in *S* per °C is higher in the vicinity of the physiological conditions than in alkaline conditions with pH > 10.[194] In fact, according to the principle of Le Châtelier, an increase in temperature entails a rise in solubility in case of endothermic dissolution processes and a drop in solubility in case of exothermic ones. As the precipitation of CAP can be considered an endothermic process,[195] an increase in temperature will yield lower solubility and, therefore, higher *S*. However, the fact that precipitation of HAP involves numerous transitions between phase intermediaries, some of which are exothermic and some of which are endothermic, predicting the temperature effect on the phase transformation pathways is difficult. The fact that these theoretical predictions (i.e., higher *S* and smaller particle size at higher temperatures) often deviates from experimental observations implies that the thermodynamic complexity of these phase transformation pathways may have a decisive effect on the morphology and size distribution of the precipitated CAP particles. The reason for failure of one such standard model may also be due to the effect of higher diffusion rates at higher heat contents of the solution offsetting the dependence of *S* on the temperature of the system. Namely, higher diffusion rates contribute to the ability of ions to find more energetically favorable positions in the crystal lattice, resulting in a better crystallinity.

The composition of the initial amorphous phase is known to depend on pH, and is approximately $Ca_3(PO_4)_2$ (Ca/P molar ratio = 1.5) at high pH values, whereas the Ca/P ratio approaches 1 at lower pHs.[196] It is assumed that as the amorphous phase matures at an almost constant pH, its Ca/P molar ratio increases to values that correspond to HAP stoichiometry, which implies that the transformation process will take place faster at higher pHs. The rate of conversion of the amorphous CAP to HAP has been shown to increase with pH in the range of 7–10 and then to decrease at higher pH.[197] Typically, measuring $[Ca^{2+}]$ and $[H_xPO_4^{x-3}]$ in the supernatant results in observing a drop in $[Ca^{2+}]$ that follows a sigmoidal trend, similar to the one of the aforementioned pH versus *t* dependence, whereas $[H_xPO_4^{x-3}]$ increases yielding also a sigmoidal curve. The reason is that from the point of precipitation of amorphous CAP, the phase transformation proceeds with the shift in the Ca/P molar ratio of the precipitate from 1–1.5 to 1.667, implying a release of PO_4^{3-} ions into the solution over the course of ripening. This also implies that a decrease in the induction time can

be related to a decrease in $[HPO_4^{2-}]$ and an increase in $[CaPO_4^-]$ in the solution, pointing to the former as a retarding and the latter as a promoting parameter of crystallization. It is, however, still not clear if this phase transformation takes place through an internal structural rearrangement of the metastable phase or by dissolution/reprecipitation. Ever since the dark line observed in the center of enamel crystals[198] was shown to be OCP phase, it has been speculated that it should be a remnant of the OCP phase composition of either the initially precipitated or the most dominant transitory phase.[199,200] Claims that the precipitated apatite is normally a solid solution rather than a double salt of OCP and HAP may speak in favor of partial or complete transition between these CAP phases in the solid state. Brown et al. have thus proposed that the hydrolysis of a unit cell thick layer of OCP transforms the latter to a two unit cell thick layer of HAP, which may thus be the mechanism for OCP → HAP transformation.[201] If that were so, the phase transformations would be both solution-mediated and controlled by the diffusion of ions within the lattice. A contrary argument is that since the amorphous phase is a random network of bonds rather than a periodic structure, there could be no direct structural matching between the crystalline phases, implying that the phase transformation has to proceed via dissolution. If that were true, the process would be diffusion- or surface-reaction-controlled and consequently highly dependent on temperature and pH, which has indeed been experimentally confirmed. It was also shown that washing the precipitate at the stage where it is still amorphous increases the final Ca/P ratio because of removing the acidic layers of $H_xPO_4^{x-3}$ ions surrounding the growing particles (as already mentioned, it appears that $H_xPO_4^{x-3}$ ions are more effectively absorbed onto HAP particles than Ca^{2+}, and can be therefore used for manipulating their ζ-potential[202,203] and thus controlling the efficiency of adsorption of biomolecules and cells thereto[204]), thereby validating the effect of exchange of ions between the solution and the precipitate on the final identity of the latter.[205] This can also be confirmed by the fact that during the ripening period, the precipitate could be isolated as a powder and analyzed for its structure without being subject to phase transitions in the solid state. If the presence of the liquid phase is required for the proper ripening, the transition has to at least partially follow a dissolution/recrystallization mechanism. That these phase transitions are solution-mediated can also be supported by another set of experiments in which it was observed that the amorphous-to-crystalline conversion starts sooner in the presence of more intensive stirring, as well as that the amorphous precipitate is prevented from undergoing the transition to crystalline CAP phases by placing it in ethanol or acetone instead of water.[206]

On the other hand, under low saturation conditions when the crystal formation occurs primarily through diffusion of ions onto already existing surfaces, the mechanism of nucleation can be substantially different in comparison with the one existing at high S when amorphous apatite is known to present the intermediate. In biological conditions, S is maintained at low levels for the purpose of letting the crystallization proceed as controlled by macromolecules and not by the thermodynamic propensities of the system. In view of that the possibility that HAP forms directly upon a preexisting template cannot be discarded. Epitaxial effects were many times proven as essential in self-assembly procedures, and many biomineralization mechanisms (e.g., crystallization of thin flakes of nacre in the mollusk shells) inherently depend on the interfacial structural matching between an organic substrate and an inorganic phase. The driving force for the epitaxial growth is the tendency of the growing phase to approach the state of a minimal interfacial energy, which occurs when the two lattices precisely match each other. It is a general rule that a certain lattice mismatch in the overgrown phase (as compared with the ideal lattice parameters) occurs irrespective of the nature of the substrate (organic or inorganic), so that a certain flexibility in the overgrown phase is required for the epitaxial growth to be favored. HAP certainly presents one such phase as it can form even at Ca/P molar ratios as low as 1.33 (although Ca/P of biological HAP is normally in the range of 1.5–1.67) owing to a high structural flexibility and tolerance to defects, primarily in terms of calcium vacancies in the crystal lattice of HAP. HAP at such a low Ca/P molar ratio would require a removal of two calcium atoms from the stoichiometric formula and protonation of two PO_4^{3-} groups (i.e., $Ca_8(HPO_4)_2(PO_4)_4$ with completely empty halide and hydroxyl columns and the hexagonal structure preserved, which is required to maintain the charge neutrality).[207] Biomineralization processes are, in fact, based on using only a few inorganic minerals, but endowed with exceptional structural flexibilities, such as calcite, silica or HAP, so that they could be shaped into materials with a wide variety of different properties.[208] However, there is one problem tied with the hypothesized immediate formation of HAP during its precipitation in biological environments, and it is a large local drop in pH following its formation. Namely, for each unit cell of HAP formed, eight protons are released into the solution:

$$10Ca^{2+} + 6HPO_4^{2-} + 2H_2O \rightarrow Ca_{10}(PO_4)_6(OH)_2 + 8H^+$$

This number may, however, be lower depending on the amount of carbonate (or other ions present in the solution) incorporated in the lattice and whether hydrogen or dihydrogen phosphates, as dominant in the physiological pH range of biomineralization, are consumed in the process as precursor phosphate ions. Also, phosphate and carbonate species as well as proteins in the extracellular matrix (ECM) in which the mineralization proceeds may act as adequate buffers to mitigate the release of protons following the formation of HAP if the process proceeds at a slow pace. Nevertheless, HAP is the second most basic CAP phase (TTCP being the only more basic phase thereof), and the intensive pH drop following its direct formation still may be harmful for the surrounding tissues. Brown et al. have thus claimed that TTCP, a rarely mentioned CAP phase, may present an intermediate in the formation of biological HAP.[209]

However, they have also observed that its immediate transformation to HAP would produce a significant increase in pH due to release of OH^- groups. Namely, the TTCP→HAP transition via hydrolysis of TTCP is entailed by a rise in pH:

$$3Ca_4(PO_4)_2O \rightarrow Ca_{10}(PO_4)_6(OH)_2 + 2Ca^{2+} + 4OH^-$$

The formation of TTCP as one of the intermediary phases, however, implies that pH does not necessarily need to drop during the formation of HAP. For example, if TTCP happens to be mixed with some of the more acidic CAP phases, such as DCPD, DCPA, or MCPM, the transformation reaction may proceed without drastic changes in pH of the medium and, therefore, without imposing chemical stress on the adjacent tissues. The latter mechanism could be supported by the fact that solubility curves for TTCP and DCPA closely match at around pH 7.6. From this observation, it can be concluded that the complexity of phase transformations during the formation of HAP is enormously high and still largely open to exploration, scrutiny, and dispute.

During the TTCP→HAP transformation, pH can climb up to almost 12 before eventually descending down to close to neutral or even acidic values. The magnitude of this increase was shown to depend on whether stoichiometric or calcium-deficient HAP forms, with the pH increase being more pronounced in the former case. The trend is, as expected, dependent on the temperature, owing to large activation energies intrinsic to these reactions. It is interesting that the concentrations of Ca^{2+} and $H_xPO_4^{x-3}$ ions in the solution are also prone to exhibit humps following complex transformations for which it is still not clear whether they take place in the solid state or entail dissolution/recrystallization pathways.[210] Incorporation of CO_3^{2-} into HAP crystal lattice is another factor contributing to the decrease in pH, and that especially when the reaction is carried out under atmospheric conditions. This clearly brings us to the task of discerning the influence of dissolved gases on the precipitation processes. It is known that precipitation of numerous ceramics crucially depends on the presence of oxygen and the oxidation reactions brought about in its presence.[211] In view of that it is also worth recalling that atomic aggregates do normally present crystallization nuclei (and 1.2 nm is usually considered as the critical size after which an unstable embryo becomes able to transcend the free energy barrier and continue to grow by diffusion and/or ripening), this is not necessarily the case. This role is sometimes fulfilled by individual molecules in the excited or ionized state, such as in the case of formation of water droplets from supersaturated vapor. Likewise, the nucleation process during precipitation of ferrites from an alkaline solution is supposed to be centered around the Fe(II) → Fe(III) oxidation process.[212,213] Gas bubbles are proposed as acting as electrostatic carriers of the incompletely understood long-range attraction forces between hydrophobic surfaces,[214,215] and their full range of influence, similarly to that of ions in Hofmeister series in terms of their effect on protein aggregation and assembly, is still unknown.[216,217] The fact that small differences in the gaseous content can trigger significant ones in the experimental outcomes is quite intriguing, and yet often omitted from serious chemical analyses.[218] The effect of the nucleation surface, which is often disguised in terms of the reaction vessel walls, is another frequently neglected factor that, however, sometimes crucially defines the morphological propensities of the particles. In that sense, there is the example of $BaSO_4/BaCrO_4$ nanofilamentous superstructures formed after their self-assembly either on glass walls or TEM grids, but when the identical procedure was attempted in plastic bottles, the crystallization experiments failed.[219] Many similar examples wherein changes in the vessel geometry or batch size significantly altered the experimental outcomes may be found in the literature.[220] Minor changes in the rate at which the reactants are mixed or introduced to the mixture can often have a drastic effect on the identity of the precipitate. Namely, upon abrupt mixing, even though S may in theory correspond to a metastable supersaturated state, locally produced high reactant concentrations may lead to irreversible formation of nuclei and a premature precipitation under uncontrolled local conditions (wherein pH and ionic activities may significantly differ from measured or calculated bulk values[221]). It is known that texture and porosity of the external substance are important as they can heavily influence the HAP nucleation efficiency.[222] This probably explains why Tadashi Kokubo, the inventor of the method for evaluating the bioactivity of a compound by immersing it in SBF and awaiting the formation of HAP, suggested discarding any plastic bottles with visible scratches and never reusing them for storing SBF.[223] Namely, SBF is a metastable solution with S with respect to HAP normalized per growth unit equivalent to 19.5, and to avoid premature crashing of one such solution storing it in a vessel with smooth wall surface and without any particulate remnants of formerly formed precipitates therein stands forth as of vital importance for reliable bioactivity analyses. A metastable solution, which could be in theory stable throughout geological times, may often turn into an immediately crashing solution if the slightest amount of impurities is introduced to it, as in accordance with the more energetically favorable heterogeneous nucleation compared with the homogeneous. In fact, it is claimed that CAP is sensitive to impurities of less than 10^{-6}% (0.01 ppm); that impurity molecules present condensation centers for the formation of amorphous CAP; and that they as such present the basis for the primary particle formation during crystallization of HAP.[224] The kinetics of enamel dissolution has also been found to be strongly influenced by the presence of impurities released to the solution during the reaction.[225] In view of this, depending on minor effects of impurities or changes in the experimental conditions, an unexpected pH versus t trend can be triggered, signifying deviations from the standard precipitation pathways. Solutions that are particularly prone to exhibit this sensitivity are those that lie toward the middle of the metastability zone, between the levels of saturation ($S = 1$) and critical supersaturation ($S > 19.5$).

One of the ways to assess the metastability of CAP solutions and the extent of the nucleation promoting/inhibiting

effect of additives is to measure the aforementioned nucleation induction time of the solutions at different saturations and different concentrations of additives. As a direct measurement of the nucleation rate is difficult, one of the most common ways to assess the kinetics of nucleation is to measure the induction time at different supersaturations.

Expressions for the inverse of the induction time for nucleation, τ, and for the nucleation density, N, are given by classical nucleation theory as:

$$1/\tau = \Omega \exp(\Delta G^*/kT) = A \exp(-\beta v^2 \gamma^3/(kT)^3(\ln S)^2)$$

$$N = B \exp(-\beta v^2 \gamma^3/(kT)^3(\ln S)^2)$$

ΔG^* is the activation energy for nucleation, Ω is a preexponential factor, γ is the interfacial tension for the formation of the critical nucleus (typically comprising 10–100 atoms), S is the supersaturation ratio of the solution, β is a shape factor, ν is the molecular volume, k is the Boltzmann constant, T is temperature, and A and B are constants. Induction time is the consequence of the activation energy required for nucleation, ΔG^*, which depends on the interfacial tension for formation of the critical nucleus, γ, and S. From the equations above, we could see that the induction time is reduced and the nucleation density is increased by lowering the interfacial tension, γ, of a CAP solution. For example, promotion of heterogeneous nucleation of CAP in the presence of another solid surface indicates that this other phase reduces the CAP solution interfacial tension compared with homogeneous nucleation of CAP in the absence of the additive. The equations above also predict that nucleation is promoted by increasing S. They also indicate that systems with higher nucleation densities, leading to smaller particles, should also have shorter induction times. The amount and nature of precipitated CAP also varies with the concentration of the additive. Higher amounts of a peptide additive may result in higher degrees of binding of Ca^{2+} and $H_xPO_4^{x-3}$ ions, causing depletion of species from the solution, lowering S and reducing the driving force for nucleation. Certain additives may also have opposite effects on nucleation depending on their concentration. It was thus pointed out that the concentration of amelogenin, the main protein of the developing enamel matrix, has a directly proportional effect on the amount of CAP precipitated and is inversely proportional to the induction time at low concentrations.[226] There is, however, evidence that this trend becomes reversed at high concentrations, when amelogenin starts acting as a nucleation inhibitor.[227]

Furthermore, in case of the classical heterogeneous nucleation, the nucleation rate is equal to:

$$J = A \exp(-\Delta G/kT) = A \exp(-16\pi \upsilon^2 \gamma^3 f(\theta)/3k^3T^3(\ln S)^2)$$

Molecular volumes defined by the crystal structure, υ, for HAP, OCP and DCP equal 263.24, 310.59, and 126.53 A^3, respectively; γ was estimated as $\sim$40 mJ/m^2 at the interface between a growing HAP phase and a metastable supersaturated solution[228]; $f(\theta)$ is the contact angle function for a nucleus on a substrate; $(16\pi/3)$ is the geometric factor, corresponding to spherical nucleus, and is different for other nucleus shapes (e.g., 32 for cubic).

So we see that as $\exp(-1/\ln S^2) = S^2$, both the nucleation density and the nucleation rate are proportional to S^2, whereas the crystal growth rate, J, is proportional to S^x. It can be represented as equal to kS^x, where k is the rate constant and x is the reaction order. Different reaction orders correspond to different mechanisms of crystal growth with four main scenarios: (a) mass transport and diffusion-limited growth at very high levels of S ($x = 1$); (b) polynucleation of surface growth islands at high S ($x > 2$); (c) layer-by-layer growth at moderate S ($x = 1$); and (d) screw dislocation growth at low S ($x = 2$). Except for the case of $x > 2$, all these mechanisms are valid for both growth and dissolution. For diffusion-limited growth, typically taking place at high S, $x = 1$. This implies that in a relatively high S range, an increase in S would lead to the nucleation rate increasing more than the crystal growth rate does. This explains why the smaller the particles one tends to obtain the conditions of higher S one should produce. More nuclei are then produced, and consequently the final particles will be smaller in size. In contrast, to obtain a monocrystal, a single nucleation event has to be produced in the solution, followed by the crystal growth; consequently, conditions with a low S need to be set.

Crystallization of HAP at low S, with or without the presence of an organic phase, is shown to be a second-order reaction, corresponding to a surface-diffusion-controlled spiral growth mechanism.[229] The fact that stirring of the reaction mixture does not typically produce any effect on the crystal growth rate excludes the possibility that the rate-determining step under low S could be the bulk diffusion of ions. At very low concentrations, additive molecules cannot influence the volume transport processes and their effect, therefore, must be due to their participation in the surface reactions in the adsorption layer. However, sometimes at low concentrations and that particularly when polynucleation mechanism of growth takes place, additives may promote nucleation by increasing its rate. On those occasions, additive molecules may be adsorbed specifically on certain sites of the crystal surface (in general, their binding will be strongest at kinks, moderate at steps, and weakest on crystal terraces), so that bridges are formed, wherein the additive molecules may transport the growth units more efficiently to the crystal surface. This mechanism bears resemblance to the one describing the formation of silicon nanowires in the vapor–liquid–solid (VLS) process, during which nanodroplets of gold deposited on top of silicon wafers attract silicon atoms from the vapor, and after becoming supersaturated with respect to silicon begin to precipitate it, building well-aligned nanowires oriented perpendicular to the underlying surface.[230,231] That the same additive may promote nucleation at low surface coverage and inhibit it at higher concentrations has been explained by hypothesizing lowering of the surface energy following absorption whenever the nucleation-promoting effect takes place. However, as pointed out by Zhang and Nancollas,

because the surface underneath covered by additive molecules can no longer participate in the formation of surface nuclei, this explanation for rate promotion is merely phenomenological.[232] On the other hand, at higher concentrations, the adsorbent layers are expected to hinder the delivery of growing units from the solution onto the growing sites on the crystal surface.[233]

Finally, it is worth keeping in mind that the conceptual framework for analyzing CAP phase transitions based on supersaturation is an approach that possesses fundamental limitations. Related to free energy of the dissolution reaction ($\Delta G_s = -RTlnK_{sp}$), K_{sp} is a thermodynamic property. ΔG of the precipitation reaction is equal to: $\Delta G = -RTlnS$, which implies that the larger the S, the greater the driving force for precipitation. This implies that solution speciation in general is a thermodynamic consideration. Consequently, whenever kinetic effects take place, solubility product fails to provide a good basis for describing the precipitation process. The effects of the interaction of ions and small particles with organic molecules present such cases. As the result, the effects of ion association and complexation in the solution may significantly lower the free ion concentrations compared with the calculated values.

In addition, calculating ionic activities that figure in equations for S and K_{sp} is always an approximation owing to the following effects. Firstly, all the additional species (ions, aliphatic additives and macromolecules, etc.) can influence the solubility of the given compound, even though they may not participate in the reactions. Common ion effect is the consequence of Le Châtelier's principle, and according to it, a salt will be less soluble if one of its constituent ions is already present in the solution. Uncommon ions tend to increase solubility by increasing ionic strength of the solution, which is usually referred to as the salt effect or the diverse ion effect (Figure 3). Complexation can also modify the amount of free ions in the solution (i.e., their activities). This is particularly the case for biological fluids where complexation reactions involving many organic species in the solution may make ionic concentrations markedly deviate from the resulting ionic activities. Also, in case of purely inorganic systems, the substantial complex formation introduces additional limitations in the application of the concept of solubility product.

The assumption that all the oppositely charged ions in solution are thoroughly hydrated and separate is not valid. The effects of ion association and complexation in the solution may significantly lower the free ion concentrations compared to the calculated values. Also, the equilibrium described by K_{sp} refers not to all chemical compositions of the solid phase, but to a specific phase. Hence, calcite, aragonite, and vaterite are all described with the same chemical formula ($CaCO_3$) and yet have different K_{sp}. Even so, it is only one phase that in most cases enters the equilibrium. Then, K_{sp} is defined for large monocrystals for which surface area effects are negligible. However, solubility increases with decreasing the particle size and once particles become smaller than 1 μm in diameter, this effect has to be accounted for. Specific structuring of water molecules around solutes and colloidal species also affects the thermodynamics of phase transitions in solution. For example, the release or trapping of water following the formation of a solid has been shown to modify the energy landscape of initial and final free energy states of most precipitation reactions.[234] On the other hand, just as each self-assembly event implies a coassembly of the immediate environment surrounding the assembling system,[235] each crystallization event can be seen as a process of a simultaneous rearrangement and restructuring of the interfacial water molecules. From one such point of view, the kinetic attributes of the latter process can be considered as a crucial factor in determining the crystal formation rate.

Note also that in reality every phase transition follows a nonclassical model. Although the classical nucleation model predicts that the nucleation rate should continuously increase with S, the nonclassical model is built on the assumption that there are two antagonistic effects taking place. Namely, the higher the S, the larger will be the thermodynamic driving force for nucleation, inducing the latter to proceed at a higher rate (although this rate normally decreases as nucleation proceeds due to depletion of growing units from the mother phase). But on the other hand, moving the system state away from equilibrium modifies the transfer of matter between the growing embryos and the mother phase, and since this transfer has to be ensured for the nucleation to proceed, this shift can significantly delay nucleation in some cases. In case of the glass formation, for example, an ultrafast cooling promotes the latter effect, leaving the system in the metastable state with an extremely slow transformation to the stable, crystalline form. If one made an attempt to condense water vapor at the temperature of liquid nitrogen, at first it would seem that such a transition would proceed momentarily. But it is not so.[236] Namely, at such a low temperature, the equilibrium pressure of water vapor (p_o) is so low that one collision between its molecules (which is the first step to the formation of an embryo that then has to advance forming a stable nucleus or to simply dissipate) occurs every 10^{16} years. To induce nucleation, one would have to increase supersaturation ratio (p/p_o) to $\sim 10^{12}$ by compressing the system and increasing its concentration. In contrast, the condensation of water vapor at atmospheric conditions occurs in the supersaturation range $p/p_o = 5–8$. As we see, this antagonistic effect implied by the fact that the mother phase has to ensure a reasonable supply of matter to the embryo for nucleation to proceed becomes most critical in far-from-equilibrium conditions, although complex kinetic conditions within a system may sometimes predispose it to exhibit such far-from-equilibrium characteristics even though its state lies close to equilibrium. The fact that the nucleation rate is subject to variations, both before and after the critical point is reached, and depends on the system in question, contributes to difficult predictions of nucleation and crystal growth rates in any real systems.

Characterization of structural properties

As complementary to various microscopic techniques used to visualize morphology and structure of CAP particles at

micro and nanoscales, spectroscopic techniques, such as XRD, are routinely applied to study the phase composition of CAP precipitates. Rietveld analysis can be used to detect the shift of diffraction peaks along the 2θ axis compared with the stoichiometric values. This shift is proportional to the lattice distortion (i.e., a change in the unit cell constant) and, can be correlated with calcium deficiency. Also, the intensity ratio between different peaks can be used to study the crystallographic orientation for a given morphology. For example, if (100), (200), and (300) reflections are more intense than those of a standard HAP, it signifies that the particles (fibers in this case) grew along the *c*-axis, that is, with the preferred orientation along the {h00} planes. Even the morphological difference between needles and bars of HAP could be thus clearly read on the corresponding XRD patterns.[237] The specificity of orientation of crystals on a given substrate, particularly interesting for HAP growth experiments that aspire to result in enamel-like structures ($f = 0.86$), can also be estimated from an XRD analysis by calculating the Lotgering orientation factor, $f = (P - P_o)/(1 - P_o)$, where $P = I(00l)/I(hkl)$ of the sample and $P_o = I(00l)/I(hkl)$ of the standard.[238] The crystallite size can be calculated from the broadening of (002), (222), and (300) diffraction peaks using the Debye–Scherrer equation, assuming that HAP crystals are prism-shaped with the height equal to the crystallite size along (002) plane (*c* plane) and the length corresponding to the crystallite size along (300) plane (*a* plane).[239] The main diffraction peaks for DCPA, α- and β-TCP, DCDP, CAP, and OCP are listed in Table II, whereas those for stoichiometric HAP are shown in Table III.

Infrared (IR) and Raman spectroscopies are often used to qualitatively detect and discern CAP phases, although with much less precision than XRD (Figure 9). IR and Raman spectroscopies are, on the other hand, particularly useful for studying the structure of inorganic/organic composites, owing to a facile detection of bonds within organic molecules as well as a high sensitivity of the position of the bands depending on the local environment surrounding the given vibration. However, unlike IR spectroscopy where a large absorbance of water poses obstacles in probing precipitates in their aqueous environments, Raman spectroscopy does not suffer from this problem. As in XRD analyses, the bandwidth can be used as an indicator of crystallinity and the amount of defects of the material in the sense that wider peaks indicate lower short-range order. As vibrational frequencies of stretching vibrations are correlated to bond length and bond strength, frequency shifts of IR/Raman bands can be used to estimate changes in the local environment surrounding the active species.[241] As a rule, hydrogen bonding decreases the frequency of stretching vibrations, as it lowers the restoring force, but increases the frequency of bending vibrations.

The main Raman band for HAP is $\nu_1(PO_4)$ at 960 cm^{-1}, deriving from a totally symmetric, nondegenerated stretching mode of the free tetrahedral phosphate ion. The other three phosphate peaks are found at 400–500 (ν_2), 550–650 (ν_4), and 995–1120 cm^{-1} (ν_3). The latter band is particularly

TABLE II. Most Important Peaks in the X-Ray Patterns of DCPA, α and β-TCP, DCPD, CAP, and OCP

DCPA[a]			α-TCP[b]β-TCP[h]			β-TCP[c]			DCPD[d]			CAP[e]			OCP[f]P		
d (Å)	I/I_1 %	Miller Indices	*d* (Å)	I/I_1 %	Miller Indices	*d* (Å)	I/I_1 %	Miller Indices	*d* (Å)	I/I_1 %	Miller Indices	*d* (Å)	I/I_1 %	Miller Indices	*d* (Å)	I/I_1 %	Miller Indices
6.74	13	(010), ($1\bar{1}0$)	7.31	25	(111)	6.49	15	(006)	7.57	100	(020)	3.46	25	(002)	18.68	300	(100)
3.48	13	($1\bar{2}1$)	4.00	20	(150)	5.21	20	(110)	4.24	100	(021)	278	100	(211), (112)	9.36	45	(200)
3.37	70	020	3.91	40	(202)	4.06	15	(204)	3.05	75	(111), (041)	2.68	40	(300)	9.05	40	
3.35	75	(110), ($2\bar{2}0$)	3.88	40	(241)	3.45	25	(1.1.10)	2.93	50	($22\bar{1}$)	2.23	16	(310)	5.52	25	
3.33	17	($21\bar{0}$)	3.69	40	(132)	3.21	55	(214)	2.62	50	(220), ($15\bar{1}$)	1.93	16	(232), (401)	3.66	30	
3.13	20	($11\bar{1}$)	3.66	17	(151), (222)	3.01	15	(300)	2.60	30	($20\bar{2}$)	1.84	16	(213)	3.44	60	
2.96	100	($1\bar{1}2$), ($1\bar{1}\bar{2}$)	3.01	20	(510)	2.88	100	(2.1.10), (217)	2.17	20	(151)				3.42	50	
2.94	35	($10\bar{2}$)	2.95	20	(113)	2.76	20	(218)	2.15	17	($24\bar{2}$)				3.21	25	
2.75	20	($2\bar{3}0$)	2.92	35	(402), (023)	2.61	65	(220)	1.82	20	(241)				2.87	30	
2.72	35	(200), (102)	2.91	100	(441), (170)	1.93	20	(4.1.10), (327)							2.83	100	(260)
2.25	15	(030)	2.86	30	(511)	1.90	15	(328)							2.82	95	(320), (241)
2.50	15	($23\bar{1}$), ($02\bar{2}$)	2.62	50	(043), (352)	1.73	25	(2.2.20)							2.78	45	
2.20	13	(003)	2.59	30	(080)										2.75	35	
															2.71	25	
															2.67	50	(700)
															2.64	35	

TABLE III. List of the Peaks Observed in the X-Ray Powder Diffraction Pattern of HAP and the Respective Data for Stoichiometric HAP

A.S.T.M. Card No, 9-432			
2θ (°)	I/I_1 %	*d* (Å)	Miller Index of the Corresponding Reflection
16.84	5	5.250	(101)
18.78	3	4.720	(110)
21.60	9	4.070	(200)
22.97	9	3.880	(111)
	1	3.510	(201)
25.90	40	3.440	(002)
28.22	11	3.170	(102)
29.14	17	3.080	(210)
31.86	100	2.814	(211)
32.20	60	2.778	(112)
32.90	60	2.720	(300)
3422	25	2.631	(202)
35.51	5	2.528	(301)
39.26	7	2.296	(212)
39.86	20	2.262	(310)
	1	2.228	(221)
42.10	9	2.148	(311)
	3	2.134	(302)
43.80	7	2.065	(113)
	1	2.040	(400)
45.32	5	2.000	(203)
46.69	30	1.943	(222)
48.16	15	1.390	(312)
48.59	5	1.871	(320)
49.51	40	1.841	(213)
50.53	20	1.806	(321)
51.33	11	1.780	(410)
52.24	15	1.754	(402), (303)
53.27	20	1.722	(004), (411)
54.45	3	1.684	(104)
55.87	9	1.644	(322), (223)
57.15	7	1.611	(313)
58.17	3	1.587	(501), (204)
60.01	5	1.542	(420)
60.45	5	1.530	(331)
61.66	9	1.503	(214), (421)
63.07	11	1.474	(502)
	3	1.465	(510)

interesting because it presents the key for discerning HAP from OCP, the two CAP phases that show a tremendous resemblance in their IR and Raman spectra.[242,243] Namely, unlike HAP, OCP exhibits a peak at ~1015 cm^{-1} positioned between $\nu_1(PO_4)$ and the main doublet of ν_3 bands with peaks at 1045 and 1075 cm^{-1}. The main CO_3^{2-} peak is at ~1080 cm^{-1} or ~1110 cm^{-1}, depending on whether the fully or partially carbonated HAP is of B-type or A-type, respectively.[244] This peak can, however, overlap with the main triply degenerated asymmetric stretching mode vibration[245] of the P—O bond, ν_3, at 1087 cm^{-1}. The other two components of this vibration are said to appear at 1046 and 1032 cm^{-1}, whereas the weak peak at 472 cm^{-1} with the shoulder at 462 cm^{-1} belongs to the doubly degenerated bending mode of PO_4 group, ν_2, and the peaks at 601, 575, and 561 cm^{-1} are assigned to a triply degenerated bending mode, ν_4, of the O—P—O bond. In addition, IR spectroscopy could be used to detect CO_3^{2-} ions in the apatite structure. The CO_3^{2-} bands appear at 755 cm^{-1} for the ν_4 stretching mode, 872 cm^{-1} with the shoulder at 880 cm^{-1} for the ν_2 stretching mode, and at 1418, 1456, 1506, and 1558 cm^{-1} for the ν_3 stretching mode. The bands at 872, 1418, and 1456 cm^{-1} indicate the B-type of carbonated HAP, whereas the those at 880 and 1558 cm^{-1} are typical of the A-type.[246,247] The intensity ratio between 880 and 872 cm^{-1} bands (I_{880}/I_{872}) can be used to determine the ratio between CO_3^{2-} substitutions of OH^- (A-type) and PO_4^{3-} (B-type) groups in carbonated HAP.[248] On the other hand, alterations in the HAP lattice parameters could be used to detect the presence of carbonate and other additives from XRD. XRD is thus ideally used to detect phase purity, whereas X-ray fluorescence proves convenient for detecting Ca/P molar ratio and content of other additives or impurities. Incorporation of CO_3^{2-} ions in the crystal lattice of HAP leads to reduction of symmetry, a decrease in the crystallite size and increased degree of distortion, thereby inducing an increase of the band width and a shift of the $\nu_1(PO_4)$ band to lower wavenumbers. If $\nu_1(PO_4)$ peak at 960 cm^{-1} is shifted to ~965 cm^{-1}, it signifies the presence of noncarbonated, pure HAP, whereas a large shoulder at 950 cm^{-1} signifies amorphous CAP. Hence, broadening of this spectral line can be calculated to estimate the proportion of carbonated apatite in a HAP sample. For β-TCP, the symmetric stretching band is split to a peak at 950 and a peak at 970 cm^{-1}. This splitting that reflects the difference in the intratetrahedral P—O bond lengths for the different nonequivalent PO_4^{3-} ions of β-TCP structure is much smaller for HAP and FAP. Lattice modes for HAP are present at <350 cm^{-1}, and $\nu_1(OH)$ is present at 3575 cm^{-1}.

APPLICATION

Owing to their being the elementary constituent of hard tissues, CAP materials have been so far mostly used for biomedical purposes, that is, for the substitution of damaged hard tissues. The application of HAP, however, extends beyond the scope of biomedicine. For example, HAP has been applied as an adsorbent in chromatography for separation of proteins and DNA.[250,251] In nanosized form, it has been applied as a stimulus-responsive stabilizer in Pickering emulsions,[252] following the observation that colloidal CAP in milk is involved in stabilizing casein micelles.[253] It has also been used as a nutritional supplement and a raising agent in the food industry. In the field of fertilizers, HAP has been used as the essential ingredient of dialysis pouch systems for maintaining concentration of phosphates in the plant root environment.[254] In the context of water purification processes, both synthetic and biological HAPs have been applied for the removal of heavy ions.[255] However, although CAP materials have been used for a variety of purposes, the main area of their application is still medicine, and this is why this part of our discussion will focus on this particular field.

The promises of nanomedicine

It has been shown that an increasing ability of humans to control physical phenomena at ever finer scales implies the

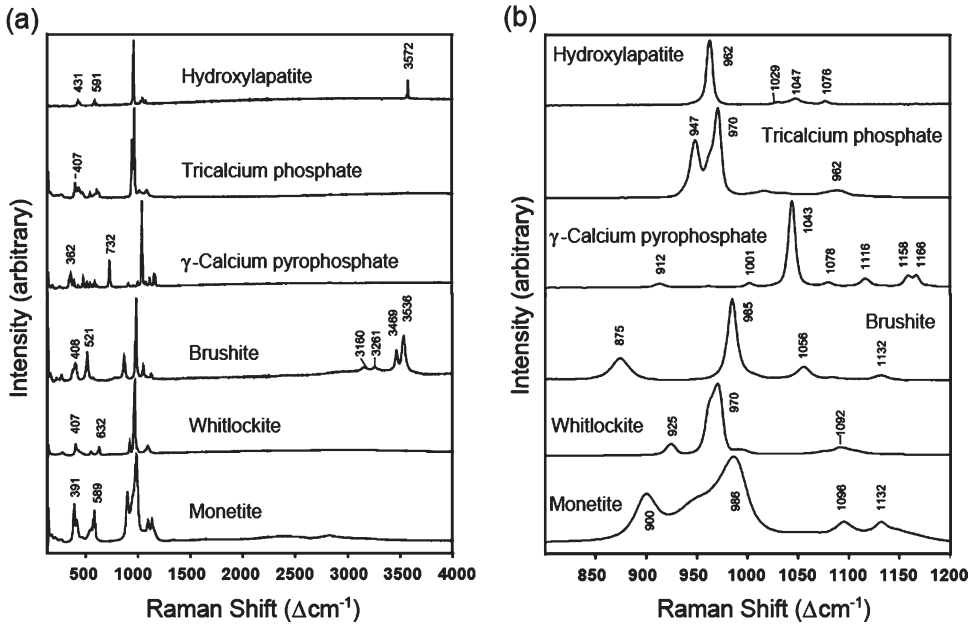

FIGURE 9. Typical Raman spectra for the main CAP phases. All visible peaks are caused by P[bond]O stretching and bending modes of vibration. The 800–1200 cm^{-1} wavenumber area magnified on the right shows only stretching P—O modes. As a consequence of different crystal symmetries of the different CAP phases, the P—O vibrations in each one of them are surrounded by a specific atomic environment, which causes a specific shift of the corresponding bands along *y*-axis. This shift can be used to identify the given phases. Reproduced with permission from Wopenka and Pasteris, Mater Sci Eng C 2005, 25, 131–143, Elsevier Sequoia.

trend of continual miniaturization of electronic devices and the eventual descent of human technologies into the nanorange.[256] Consequently, nanoscale tools and devices are expected to increasingly find usage in numerous aspects of the modern society. The modern medicine is thus only one among the fields that is currently undergoing a transition towards ever finer and more sensitive methodologies in terms of finely targeted and superiorly efficient delivery of pharmaceutical agents that minimizes the side effects of medical treatments.[257]

Many eyes are thus focused on the promises of nanomedicine (Figure 10), which can be roughly defined as the application of physical chemistry of nanoscale phenomena for biomedical purposes.[258] Although only a few nanoparticle-based drugs have so far been approved by the FDA, it is estimated that the impingement of nanomedicines on the modern society will only increase in the coming years.[259] Also, with approaching the patent expiration times, the biotech industries are intensively seeking new competitive business strategies, and nanomedicine is often mentioned as one of the key focuses. In view of their offering solutions to fundamental pharmaceutical problems ranging from poor solubility of drugs to the lack of target specificity, nanotechnologies are viewed as a potential revolution in the world of medicine.

A particular emphasis in biomedical research is, therefore, placed on nanosized drug delivery carriers for either local or systemic use. Many biopharmaceuticals have limited long-term structural stability when formulated at high concentrations, which limits their shelf-life. In addition, many are susceptible to biodegradation when delivered, which in addition to their frequently extensive hydrophobicity, reduces their bioavailability. For localized treatments, the delivery vehicle is meant to be retained at the delivery site, ensuring the local and rate-controlled administration of the therapeutic. For therapeutics delivered systemically, through the vasculature, the nanoparticulate carrier is expected to: (a) prolong the circulation time in plasma; (b) enable carrying of hydrophobic drugs to their destination in the body, thus preventing their clumping in the blood and increasing their bioavailability; and (c) through a proper mechanism (such as surface functionalization or guiding via an external field), it may direct the therapeutic to a desired tissue.

The majority of nanomedicines on the market are still merely pharmaceuticals that are formulated into nanosized structures to manipulate the pharmacodynamics, biodistribution, and overall effectiveness of the drug.[260] The main purpose of decreasing the particle size of poorly water-soluble drugs down to nanoscale is an accelerated absorption and a higher efficacy produced thereby. This results from the fact that the solubility and dissolution rate of a drug can be increased by reducing the particle size to increase the interfacial surface area, in accordance with the Noyes–Whitney equation.[261] However, using nanoparticles as smart drug carriers for both a controlled drug release and ultrasensitive diagnostics would present the next step. Irrespective of the delivery method (local or systemic), the nanomaterial would in this case act as a depot and a carrier for therapeutic agents, providing a convenient solubilizing and protective environment. Both the shelf-life of the therapeutic before administration and the delivery efficacy upon administration are thus expected to be increased. The efficacy of

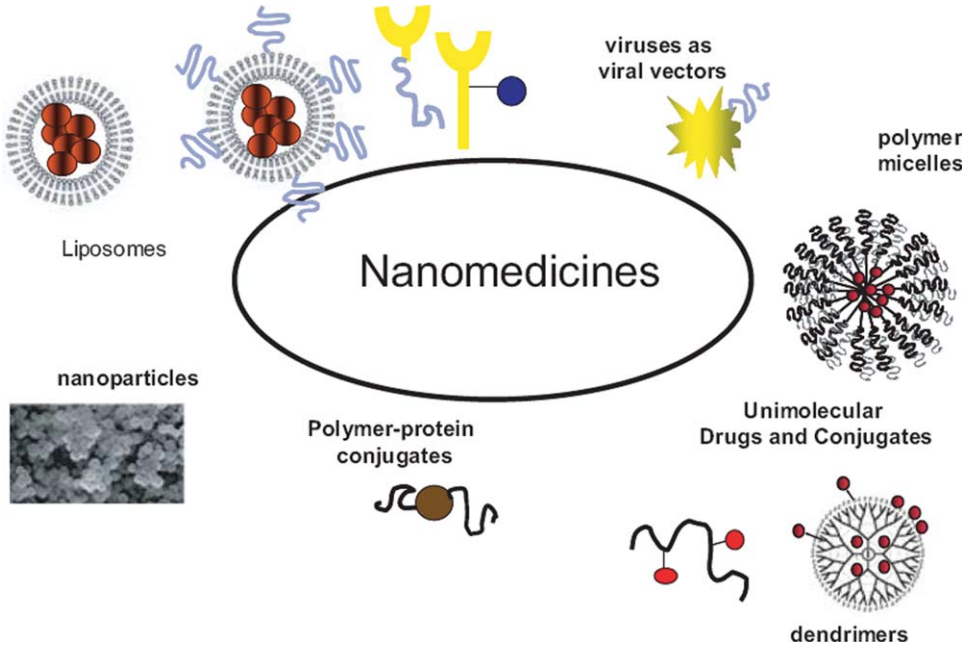

FIGURE 10. A few of the major contemporary candidates for drug and gene delivery carriers. Reproduced with permission from Wopenka and Pasteris, Mater Sci Eng C, 2005, 25, 131–143, Elsevier Sequoia. [Color figure can be viewed in the online issue, which is available at wileyonlinelibrary.com.]

delivery of many other drugs, including human growth hormone, leuprolide, insulin, and highly water insoluble drugs, such as paclitaxel (small hydrophobic drug used for the treatment of cancer), levonorgestrel (used for female birth control), and morphine was increased upon their incorporation within specific drug delivery vehicles, whereby pharmaceutical compounds having been delivered so far by nanocarriers include mostly small molecules, peptides, and DNA.[262]

Many different systems are nowadays investigated for their usage as drug delivery carriers, including micelles, vesicles, polymers, microspheres, hydrogels, and solid implantable devices, such as microchip-based drug delivery systems consisting of microfluidics combined with sensors.[263] However, as we shall see, inorganic nanoparticles offer many advantages in comparison with other concurrent systems. In addition, owing to their high surface-to-volume ratios, nanoparticles offer enhanced reaction sites compared with their bulk counterparts. As smaller, they also more easily penetrate the extracellular space and are more efficiently absorbed by the cells, thereby increasing the efficiency of the therapeutic action.

Why calcium phosphates?

CAP particles with tunable phase composition and thus the resorption rate offer an advantage of increasing the efficiency and local character of the drug delivery as well as a controlled release over time. A reduced dosage and frequency of administration, and consequently fewer side effects, would result thereby. By means of fine CAP particles that are stable before injection and then comparatively slowly resorbed in the body, the active compound is protected until the particles are injected and delivered to the targeted site, after which a controlled release, tunable to anywhere between a few days to a few weeks, may be set to take place.

CAP particles are also able to permeate the cell membrane and dissolve in the cell, which makes them an attractive candidate for gene delivery agents too.[264–266] The encapsulation of DNA into CAP nanoparticles protects the nucleic acid from cytoplasmatic environment and enables its efficient delivery into the cell nucleus. Nonviral gene delivery systems have been, in fact, intensively investigated as possible alternatives to viral vectors for the transfection purposes. Although nonviral gene delivery vectors typically possess lower transfection efficiencies compared to viral ones, their excellent safety profiles are appealing for gene therapy.[267] Several nanomaterial-based vectors have been developed using functionalized multiwall and single-wall carbon nanotubes, metallic, bimetallic, TiO_2 and silica nanoparticles, magnesium phosphate, manganous phosphate, and various dendrimers.[268] However, unlike many of these options, including poly-L-lactic acid (PLLA) and a few other polymeric particles proposed as drug/gene delivery carriers (PLLA, e.g., is typified by a very slow dissolution rate in the body, which disables a prompt release of an encapsulated active ingredient, whereas in the later stages of dissolution it undergoes a self-catalytic degradation reaction owing to an increased release of acidic products harmful for the surrounding tissues[269]), the degradation of CAP does not produce any toxic chemicals apart from the release of Ca^{2+} (which may in the worst case scenario initiate protein aggregation), and these particles are also scalable in size and imply low manufacturing costs. In that sense, nanosized

CAP particles present one of the most viable options for gene delivery systems, and for that reason they have been extensively used as an *in vitro* gene delivery agent for over 30 years and are currently being investigated for *in vivo* purposes as well.[270,271]

Structural and chemical features of CAP particles may provide all the essential requirements for their efficient usage as genetic transfection agents, including: the binding affinity of DNA molecules onto HAP crystals[272]; the composite particle stability in extracellular space; an efficient cellular uptake and resorbability of the particles followed by a gradual release of the DNA and its escape from the endosomal network into the cytoplasmatic intracellular space, and eventual cytosolic transport and nuclear localization for transcription.[273]

- Compared with other drug delivery carriers, CAPs possess the following advantages:
- Favorable biodegradability and biocompatibility properties in general.
- Soluble and less toxic than silica, quantum dots, carbon nanotubes, or magnetic particles.[274]

More stable/robust than liposomes, which predisposes them for a more controlled and reliable drug delivery. Contrary to liposomes and other micelle-based carriers, which are subject to dissipation below specific critical concentrations (which presents a clear obstacle upon injecting them into the bloodstream), CAP-based systems and particularly those with Ca/P molar ratio close to the one of HAP, are negligibly soluble in blood, which is by itself supersaturated with respect to HAP.

Higher biocompatibility and pH-dependent dissolution compared to polymers.[275] Namely, the dissolution of CAP is accelerated at low pH media, which are typically found in endolysosomes and in the vicinity of tumors, providing an advantage in the delivery of drugs into malign zones or cell organelles. Also, unlike most metallic and oxide nanoparticles, including Au, Ag, Co, Cr, Cd, Se, Te, TiO_2, CuO, and ZnO, which have all been shown to induce damage to DNA, produce oxidative lesions, increase mutation frequency and decrease cell viability, nanosized CAP belongs to the class of the safest nanomaterials evaluated so far (together with SiO_2 and most likely Fe_2O_3 and C_{60}).[276]

Low production costs and excellent storage abilities (not easily subjected to microbial degradation).

Preparation of nanosized CAP is not a complicated task, provided we recall that with the exception of enamel, CAP in the biological domain almost exclusively exists in form of nanoparticles. This is explained by the free energies of nucleation and of crystal growth being approximately the same for a wide range of conditions, implying that the formation of elongated HAP crystals is not a strictly favorable process unless it occurs through aggregation of smaller, nanosized units.[277] A multihierarchical model of naturally highly defective HAP crystals has thus been proposed,[278] the lowest element of which corresponds to the so-called Posner's clusters of $\sim$1 nm in size. In that sense, CAP nanoparticles require less effort and are less time-consuming to prepare compared to quantum dots and dendrimers, respectively.

- Unlike other alternatives, both Ca^{2+} and PO_4^{3-} are naturally found in the body in form of amorphous and crystalline solids in hard tissues as well as in blood (in concentrations of 1–5 m*M*). Ideally, CAP particles would safely be distributed throughout the body, with the dissolved material being regulated by the action of kidneys, avoiding their precipitation as pathological deposits.
- Unlike most other ceramics, nanosized CAP can be prepared *in situ*, under ambient conditions, in a wide array of morphologies, from spheres[279] to platelets[280] to rods[281] to fibers.[282] In one particular set of experiments, combinations of two different temperatures (25, 40, 60, and 80°C), four pH values (8, 9, 10, and 11), and three drying methods (atmospheric, vacuum and freeze drying) yielded a variety of HAP particle morphologies, ranging from spheres to rods to wires and needles to bamboo-leaf-like ones.[283] The particle morphologies could be optimized for the most favorable dissolution and adhesive properties in the body. For example, whereas nanospheres would exhibit less friction while moving through plasma, platelets, and needle-shaped particles would have a higher propensity to adhere,[284,285] which may be desirable in situations where clearance from the mucosal tissues by the mucosal layer disfavors an effective uptake of the drug.
- CAPs can also be prepared with a variety of phase compositions (Table I), thereby enabling fine tuning of the dissolution properties *in vivo* at the structural level as well. For example, the higher the content of TCP on the account of the content of HAP in biphasic CAP, the higher the dissolution and resorption rates of the material.[286,287] The optimal drug release rates could thus be tuned by changing the HAP/TCP molar ratio within the particles aside from modifying their size and/or morphology. Calcination time and temperature can also be used to control the particle size and composition, and have consequently been shown to affect the drug delivery performance of HAP nanoparticles.[288] In general, in case of biphasic CAP, tiny differences in chemical composition may lead to significant differences in material properties.[289] Control over a single synthesis parameter can thus be used to prepare CAP materials with a wide range of intrinsic properties.[290]

The main potential downside of injecting CAP nanoparticles in the body, which needs yet to be assessed before reaching clinical application stages, certainly comes from the possible atherosclerotic complications associated with their undesirable deposition along the arterial walls. Namely, it is known that cholesterol and its derivatives, altogether with various CAP phases, primarily HAP, comprise the largest percentage of atherosclerotic plaque[291] (Figure 11). Structural matching between crystal lattices of cholesterol and HAP and their consequent epitaxial coprecipitation are largely assumed to be responsible for their entwined presence in these pathological cardiovascular deposits.[292] First, crystals of both HAP and cholesterol monohydrate typically develop (001) faces. Furthermore, OH^- ions of HAP lie in planes parallel to (001) face and are thus facilely engaged in hydrogen bonding across the exposed (001)

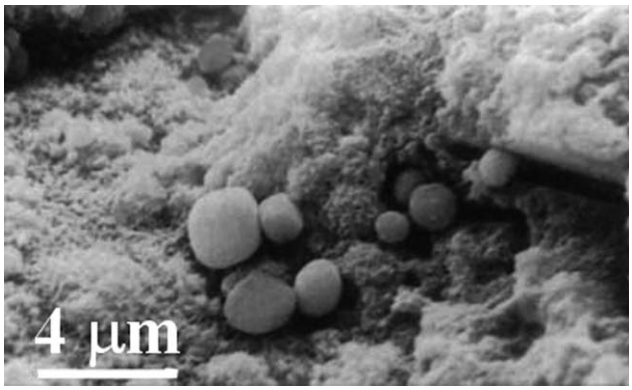

FIGURE 11. Spherical CAP particles found in segments of atherosclerotic deposits. Reproduced with permission from Dorozhkin and Epple, Angew Chem Int Ed, 2002, 41, 3130–3146, Wiley-VCH.

crystal planes, especially since a fit of the (001) planes of the two crystal structures shows a close superposition of the hydrogen bonding groups.[293] A crystalline layer of either of the two structures can thus serve as a quasi-epitaxial nucleation surface for the growth of the other.

To be truly innovative and advanced, drug delivery carriers should be made multifunctional, that is, allow for more than one function upon their injection in the body. Theranostic systems that possess the capacity for a simultaneous controlled drug delivery and imaging/diagnostics thus hold great prospect in this sense. Smart delivery rates and amounts depending on the diagnostic response are meant to be integrated within these particulate systems. As recently observed by Sumer et al., successful development of theranostic nanomedicine requires significant advances in materials science and nanocomposite materials; ideal nanomedicine platforms should be small in size, provide high drug-loading densities, be efficient in targeting to the diseased tissues with minimal nonspecific uptake, provide responsive release mechanisms to improve drug bioavailability and also imaging ultrasensitivity to prevalidate and monitor therapy.[295] By combining several useful properties within a single particle, multifunctional pharmaceutical nanocarriers may significantly enhance the efficacy of many therapeutic and diagnostic protocols, and it is them that could be considered as the most exciting synthetic ideal in the field of controlled drug delivery, as of today.

Prospective applications

The first and still the foremost application of nanosized HAP is as components of scaffolds for the reparation of impaired hard tissues.[296,297] In surgical procedures, allografts and autografts as parts of hard tissues taken from donors or the patient itself make up for 95% of materials used as bone grafts, whereas only 5% are synthetic materials.[298] Whereby in case of autografts, two separate surgical procedures are required followed by an increased risk of infection and failure, a risk of implant rejection and disease transmission, including the need for an extensive sterilization procedure during which the properties of the substitute material are often degraded, are present in the case of allografts. Hence, there is a great impetus on the research of novel and reliable synthetic materials for substitution of hard tissues. Although metals including Fe, Co, and Ti are often used to fill bone defects and provide the internal fixation, fatigue, corrosion, tissue infection, and poor implant-tissue interface result on many occasions.[299,300] On the other hand, there are problems that prevent the wide usage of ceramic-based materials for reparation of hard tissues. For example, HAP is all by itself an exceptionally brittle material, similarly to most ceramics. Hence, it does not provide a sufficient mechanical support for the surrounding bone/skeleton. HAP is the most osteogenic CAP phase, which can be attributed to its being the major mineral phase of bone, dentin and enamel; however, its rate of resorption is quite low. The rate of resorption smaller than the rate at which new bone forms is a discrepancy that impedes proper healing of the bone defect. It has to be set to precisely match the rate of expected bone regeneration to maximize the efficacy of the healing process.[301] Henceforth, much research has been done on exploring the mixtures of HAP and TCP, known as biphasic calcium phosphates, for the most optimal restoration of hard tissues.[302,303] Namely, TCP and, as of recently $CaSO_4$,[304] present more rapidly resorbable osteogenic phases than HAP, and are used to balance the low resorption rate of the latter. A medical interest in amorphous CAP has likewise been sparkled after the discovery of its higher bioresorbability compared to HAP and other CAP phases.[305] However, the main drawbacks associated with the application of amorphous CAP in the body include its low mechanical strength and difficult injectability. On the other hand, CAP phases with Ca/P ratio of less than 1 are not suitable for biological implantation due to their overly high solubility. The design of a material that is both mechanically strong enough for bone replacement and biodegradable is an especially difficult challenge for scaffold-based strategies. One of the strategies used to design a biomaterial that is both biodegradable and mechanically strong enough to serve as a bone substitute is to couple particle dimensions in the nanorange with a soft component that contributes tensile properties to the stiff ceramic component. Polymer matrices have thus been reinforced with HAP nanocrystals to improve the mechanical properties of these polymers.[306,307] Poly-L-lactide,[308] poly(lactic-*co*-glycolic acid) (PLGA)[309,310,311] and collagen[312] all present prospective choices as polymeric phases that promote cellular adhesion, proliferation and growth. In fact, inorganic nanoparticle fillers in general have been shown to add tensile strength, stiffness, abrasion resistance, crack resistance, and stability to polymer networks. Depending on the time scale of the desired biodegradation of the polymer phase, one may simply vary its chemical nature; PLLA thus requires ~1 year to be fully resorbed, polycaprolactone has a biodegradation period of about 6 months, whereas PLGA degrades in the body in a month or so. Another step in developing advanced regenerative biomaterials comprises introducing growth factors (BMP-2 and PDGF), cells, antibiotics and additional ions into injectable composites based on CAP and various polymers or proteins.[313]

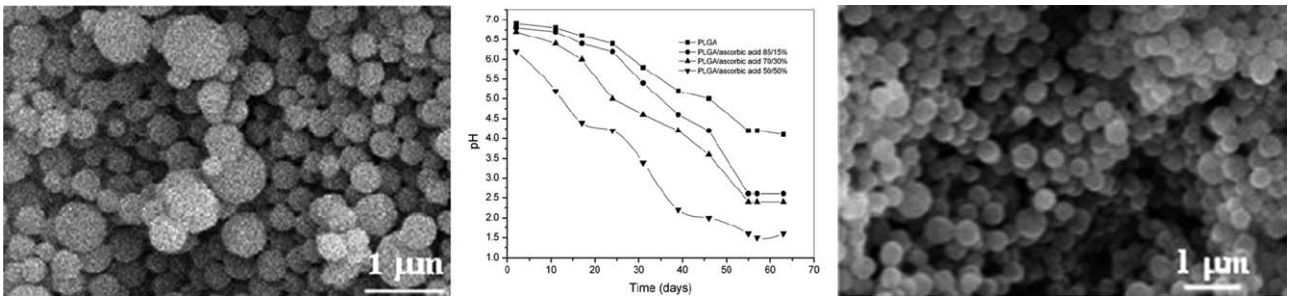

FIGURE 12. Uniform polylactide-*co*-glycolide spheres injected with ascorbic (left) and folic acid (right). The composition and size of the particles could be modified so as to optimize the release rate of the encapsulated model compound (middle). The same approach could be applied for the fabrication of drug-carrying CAP/HAP nanoparticles with controlled drug release rates. Reproduced with permission from Stevanovic and Uskokovic, Curr Nanosci, 2009, 5, 1–14, Bentham Science Publishers.

However, the main application that this review will focus on will be the usage of HAP/CAP nanoparticles as theranostic drug delivery and gene therapy carriers. In view of that the primary interest may be given to CAP nanoparticles with encapsulated antibiotics. Examples of such compounds may be gatifloxacine[314] (a fluoroquinolone that has bactericidal property for both anaerobic and aerobic bacteria) and ciproflaxacin,[315] both of which are used for treating osteomyelitis. In this case, the inflammation of bone tissue destroys vascular channels, leaving a portion of dead and infected bone (sequestrum) detached from the adjoining healthy bone. Owing to the impaired vascularity, antibiotics may not be delivered adequately to the lesion by the intravenous route. It is usually recommended that the administration of antibiotics lasts 4–6 weeks in the treatment of chronic osteomyelitis; however, through a drug delivery with sustained and controlled release rate the necessity of repetitive, daily injections of adequate doses of the drug would be eliminated. The thing of main concern here is the ability to design a material that would enable a high enough initial burst of the drug release, which would surpass the minimal inhibitory concentration for the given infective agent, such as a bacterial colony. If, on the other hand, the amount of the released drug is continuously lower than this critical level, it may result in developing antibiotic resistant organisms, rather than keeping their population under control, through such a controlled release of the antibiotic.

By means of antibiotic-impregnated CAP nanoparticles, a local delivery of antibiotics would also be coupled to remineralization of the lost portion of bone. Such an approach would overcome difficulties that implantable antibiotic delivery systems currently face; namely, the need for the removal of the implant at the end of the treatment. CAP/HAP particles carrying gentamicin and vancomycin were thus shown not only to exhibit an antibiotic effect on the healed tissue but to stimulate the growth of the new bone owing to the bioactivity of the carrier and its similarity to the natural composition of bone.[316] CAP particles are in this case also expected to be more effective than polymers (e.g., polycaprolactone)[317] in view of the latter not being able to provide support for bone tissue reconstruction at the targeted space. Another antibiotic effective in treating osteomyelitis, recently injected within PLLA nanospheres coated with CAP,[318] is tigecycline, which possesses activity against both gram-positive and gram-negative pathogens, binding to the 30S ribosomal subunit and inhibiting protein synthesis.[319] Cefuroxine was also impregnated within porous HAP/TCP and successfully used to treat osteomyelitis, with the implants inducing the highest concentration of the antibiotic in bone and serum 21 days after the implantation.[320] Amoxicillin, one of the most common antibiotics prescribed to children has also recently been injected into PLGA microspheres coated with HAP,[321] whereby the same research group also managed to encapsulate indomethacin, a hydrophobic drug, within HAP-coated liposomes based on 1,2-dimyristoyl-sn-glycero-3-phosphate and 1,2-dimyristoyl-sn-glycero-3-phospliocholine.[322] Doxycycline, an antibiotic used to treat periodontitis, has also been encapsulated within HAP nanoparticles, exhibiting sustained and single or multiple stage release profiles depending on the Ca/P ratio.[323] Other compounds, such as vitamins[324–327] or Coenzyme Q10 (i.e., ubiquinone, a lipophilic antioxidant),[328] have been prepared using this method (Figure 12). Using carboxyethylphosphoric acid as an additive, uniform hollow CAP nanospheres with controllable shell thickness have recently been prepared with a potentially improved drug uptake efficiency.[329] Nanosized hollow ellipsoidal HAP/$CaSiO_3$ composites with the improved drug loading capacity were also prepared in a multistage process involving a selective dissolution of the initially precipitated $CaCO_3$ core.[330] CAP particles could be also coupled with stem cells[331–334] or bone marrow mesenchymal stromal cells,[335] both of which are known to facilitate the regenerative therapy of connective and hard tissues. Various elements of ECM could also be incorporated with the purpose of improving the biocompatibility and bioactivity of the particles or accelerating the osteoinductive response of the surrounding hard tissues.[336] Individual amino acids and their combinations have also been anchored on the surface of HAP nanorods.[337] Hydrophilic organic coatings, such as albumin, dextran, or hydroxemethylmethacrylate could also be used to enhance biocompatibility of the particles.[338] With respect to regeneration of hard tissues, all of such systems could be applied for treating their loss occurring due to infection or even treat soft tissues such as pulp[339] or cementum-gingiva-alveolar bone interface damaged by a periodontal disease in dentistry.

As CAP and bioactive glasses are still considered as compounds that the next generation of biomaterials will be based on,[340,341] synthesis of nanosized CAP particles coated with Bioglass or blended within nanophase composites[342] would present another prospective research direction. Such a material could be used both as a filler of bone defects and an efficient drug delivery carrier owing to facile surface functionalization through the silanol groups. If the layers of bioactive glass are thin enough (a few atomic layers), it would predispose the particles for a relatively quick dissolution of the coating (bioactive glass has a significantly higher rate of resorption compared to CAP), right after the attached drug has fulfilled its role, after which the CAP core can act as a bone filling or biodegradable reminalization agent. In such a way, both the ideals of an efficient drug delivery and bioremineralization would be satisfied. Furthermore, by controlling the thickness of the coating (achievable through varying the control parameters of the synthesis), the time control over the dissolution of the bioactive glass and the consequent release of the drug could be possessed. Coating with silica glass is typically carried out via a hydrolysis of given alkoxides (i.e., tetraethyl orthosilicate (TEOS) in most cases) and localized polycondensation on the surface of the core particles.[343,344,345] LaSr-manganite particles were thus coated with silica,[346] whereas cholesterol platelets were coated using sodium silicate solution and a procedure involving a reaction with an ion-exchange resin.[347] A challenge would be to coat CAP particles with Au (metal-ceramic coatings are difficult to achieve owing to different thermal expansion coefficients between the two components among other factors), but if succeeded, such particles shelled with Au could be used for photothermal therapies and diagnostics, such as optical coherence tomography.[348] The absorption efficiency of Au is a few orders of magnitude higher than that of conventional photothermal dyes, and Au surfaces can be facilely functionalized with antibodies and other bioactive molecules. On the other hand, instead of being the core component of drug delivery nanoparticles, CAP phase can be coated around another phase. Such an approach was used to prepare CAP-coated PLLA microspheres with a sustained 30-day release profile of attached bovine serum albumin (BSA) in SBF compared with noncoated particles typified with an initial burst in the drug release.[349] An opposite approach, that is, coprecipitation of PLGA and a drug, tigecycline, in the presence of precursor HAP nanoparticles was recently implemented, resulting in HAP/PLGA/drug composite particles.[350] They turn out to be particularly appealing not only because of their biocompatible and biodegradable nature, but because HAP releases hydroxyl groups upon dissolution, whereas PLGA releases acidic products of degradation. In combination, the two components thus balance each other's potentially harmful pH changes. Notice, however, that the higher the amorphous content in CAP/HAP particles, the less intensive the corresponding increase in pH is. A convenient circumstance is that such phases with a lesser number of hydroxyl groups in the stoichiometric formula dissolve faster than HAP. As a result, the slow dissolution of HAP in biological conditions does not necessarily produce pH changes that could not be buffered by the organism. To achieve this simultaneous dissolution of the polymer and mineral components and avoid the two-step drug release profile, dispersion of nanosized CAP particles within polymeric particles as matrices may have to be ensured instead of the classical core-shell model where the drug-containing polymer would thoroughly coat the CAP core. Another favorable feature of both HAP and PLLA/PLGA[351] is their negatively charged surface under the physiological conditions, which naturally fosters the attachment of cells thereto.

For the theranostic purposes, particles need to satisfy the requirements for simultaneous imaging/diagnostics and therapeutic effect. For the imaging purposes, the particles could be doped with specific ions or compounds, which would enable their detection using an appropriate external device. Some of the methods for imaging include fluorescence imaging (in which case fluorescent probes need to be incorporated within the particles), MRI (in which case, doping the particles with magnetic ions is carried out), gammascintigraphy (in which case, doping the particles with heavy atoms such as ^{111}In, ^{99m}Tc, Mn, and Gd is required[353]), X-ray computed tomography and ultrasonography. At a finer scale, one could perform molecular imaging, which is defined as visually representing, characterizing and quantifying (sub)cellular biological processes within the organism. These processes include gene expression, protein–protein interaction, signal transduction, cellular metabolism, and both intracellular and intercellular trafficking. For optical imaging, the particles are normally doped with organic fluorophores, such as Cascade Blue (dark blue), 10-(3-sulfopropyl) acridinium betaine (SAB; light blue), fluorescein (green), rhodamine WT (orange), and Cy3 amidite (magenta), which were all recently encapsulated within CAP nanoparticles.[354] However, CAP particles could be equally doped with Eu^{3+}, Tb^{3+}, Gd^{3+}, or other lanthanides in order to be made fluorescent.[355,356] Nanocrystals actually offer the advantage of structurally integrating the fluorescent entities within the crystal lattice by doping, thereby transcending numerous drawbacks of using organic dyes, fluorescent proteins, and lanthanide chelates, such as broad spectrum profiles, low photobleaching thresholds, and poor photochemical stability.[357] The pathways of such nanoparticles were successively followed inside pancreatic cells.[358] Accumulation of DNA-loaded CAP nanoparticles which also contained red-fluorescing tetramenthylrhodamine isothiocyanate BSA inside a cell and its nucleus was observed by fluorescence microscopy.[359] Combining CAP with semiconductor quantum dots[360,361] at the particle level could also be used to enable monitoring of the route that the particles follow in the body.

It has been evidenced that the addition of ions that substitute Ca^{2+} in HAP crystal lattice can induce a more favorable capturing of the carried biocomponent, such as DNA.[362] Evaluating the effect of additives, such as Mg^{2+}, CO_3^{2-}, K^+, and Al^{3+}, most of which are known to be present in biological apatite, may thus be useful. The effects of many external ions on precipitation of HAP have previously been

established, and it is known, for example, that citrate, pyrophosphate and molybdate ions reduce the crystallinity of HAP, whereas Mg^{2+}, Al^{3+}, and Sn^{2+} at high concentrations inhibit the hydrolysis of the initially precipitated amorphous CAP phase.[363] At low concentrations, however, Mg^{2+}, Al^{3+}, and Zn^{2+} promote the formation of substituted β-TCP. MgO and SrO have been shown to suppress β- to α-TCP transition and also promote attachment, proliferation and differentiation of osteoblast cells.[364] Strontium is present in tiny concentrations in bone and is, such as Si ions, supposed to play a role in early bone formation, whereby 0.01% of the human body weight is amorphous silica. Similar to other ions, such as carbonate, sodium, and magnesium, these two also occur as lattice substitutions at the atomic level. Quite rarely, as in the case of strontium-based toothpastes, strontium precipitates in form of $Sr_3(PO_4)_2$ with $SrCl_2$ being the intermediate. In any case, the mechanism by which Si increases *in vivo* bioactivity is still unresolved. Mechanisms proposed to explain this effect can be divided to: (a) passive, including the Si-induced effect of decreased apatite grain size, a change in the protein conformation on the biomaterial surface or modifications of the surface topography and therefore the cellular response; and (b) active, referring to the release of Si ions, its cellular uptake and promotion of gene expression in the direction of an increased bioactivity.[365] In general, understanding the precise biological mechanisms with respect to implantation of HAP in the body is still required, which is why an enormous shift of interest towards looking at genetic expression pathways following the implementation of HAP and bioactive glasses is witnessed today.[366,367] There are ongoing efforts to follow the genetic expression pathways in osteoblast and fibroblast cell cultures and thus design the most optimal ionic composition of the implantable material, which would presumably lead to the so-called third generation of biomaterials.[368] In that sense, exploration of additives that may not even be present in the body and evaluating their bioactivity responses, may present a reasonable choice.

Another interesting direction is doping CAP with magnetic ions, such as Co[369,370] or Fe,[371,372] or even coprecipitation of magnetite.[373] There are indications that magnetic HAP and electrically polarized one (owing to OH groups in HAP crystal lattice) possess a more pronounced osteogenic response.[374,375] The structure and composition of HAP have been shown to be stable upon substitution with exogenous metallic ions in the lattice.[376,377] Such particles could be guided to the targeted area in the organism by means of an external magnetic field. They could be used either as contrast agents for MRI, for cell separation, or as a heat mediator in hyperthermia therapies.[378] Magnetic HAP synthesized by coprecipitation in the presence of $FeCl_2$, thereby partially substituting Ca^{2+} with Fe^{2+} in the resulting crystal lattice, was recently successfully applied in treating murine colon cancer by hyperthermia, following a subcutaneous injection of the particles.[379] Owing to their small sizes, the particles would be superparamagnetic and would thus resist agglomeration caused by magnetic dipole–dipole interactions outside of the external field.[380] Also, heavy metal atoms, such as ^{111}In, ^{99m}Tc, Gd, or Mn, loaded into the nanocarrier via a carrier-incorporated chelating moiety can lead to particles for gamma- or MR imaging applications. Hetero-epitaxial growth of magnetite on HAP resulted in 300-nm sized magnetic composite particles with saturation magnetization of 30 emu/g.[381] The particles showed an increased transfection of stem cells with the gene for glial cell line-derived neurotrophic factor in the magnetic field compared to the transfection efficiency reached in the absence of the external field. Superparamagnetic CAP composite nanospheres could also be applied for the blood detoxification. Functionalized with target-specific antitoxin receptors and let freely circulate within the bloodstream after simple intravenous injection, the particles would sequester the blood-borne toxins using their surface receptors. The blood is then circulated via a catheter through a portable high gradient magnetic separator device where the magnetic toxin complexes are retained and the detoxified blood is returned back to the bloodstream.[382] Unlike sole drugs, 98% of which cannot transverse the blood-brain barrier (BBB) nor penetrate the skin, some nanoparticles can,[383] which makes them attractive for acting as carriers for drugs that are to be delivered across the BBB and the epithelial junctions of the skin that normally impede the delivery of drugs to the desired target.[384]

In fact, because the type and efficiency of the transport of nanoparticles across the cellular membrane largely depends on their size, developing synthesis methods for the size-controlled fabrication of HAP nanoparticles is essential for fine-tuning their application as drug and gene delivery agents. The transport mechanism may also predispose the particles to exert a specific effect on the cell. Particles smaller than 20 nm typically either pass the cell membrane through the membrane channels or by following vesicular or caveloae-based endocytosis routes.[385] If the particle size fits the size of the active part of receptor molecules docked on the cell membrane, a receptor-induced transport with a possible synergetic effect on the cell may be triggered. A few studies have shown that nanoparticles of ~50 nm in size cross the cell membrane faster than those smaller than 15 nm or bigger than 200 nm on average, and that smaller is not necessarily the better when it comes to choosing the most optimal size for a given drug/gene delivery application.[386,387] In fact, different application purposes require different optimal particle sizes.[388] Whenever an external control of the particles in the body is to be established, a compromise needs to be made regarding their size, because particles that are too small would tend to difficultly oppose the direction of the bloodstream and would respond to the external field with a less intensive signal, whereas particles that are too big would be less movable owing to their tendency to get interlocked between macromolecular complexes, cells, and tissues.[389]

Surface modification by means of adding cell-binding peptides onto the surface or in the bulk of biomaterials has been used to attain control over cell-biomaterial interactions and promote a more efficient healing process upon the injection of the biomaterial in the body.[390] By the action of

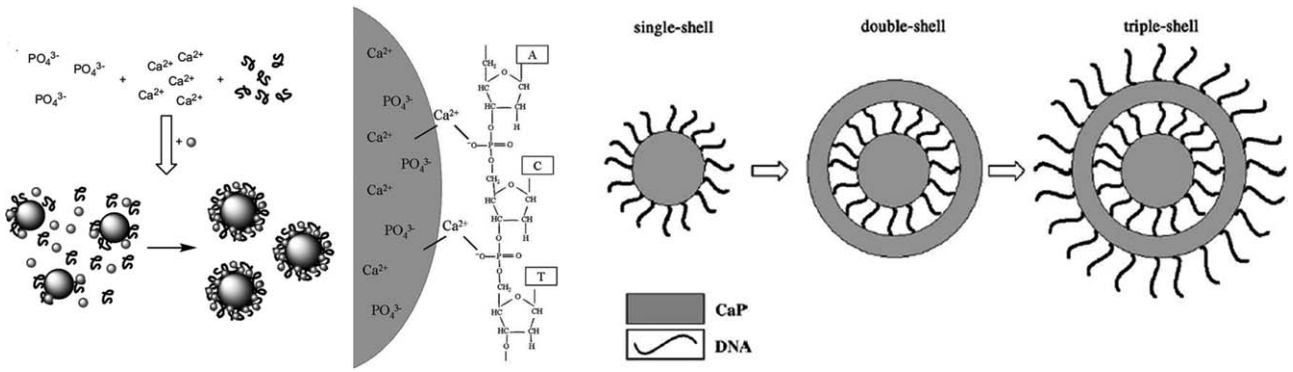

FIGURE 13. Precipitation of CAP in the presence of steric agents and other active molecules or particles (red dots), such as fluorescent probes, superparamagnetic entities or drugs, may lead to stable dispersions of medically functional CAP nanoparticles. The model for the attachment of nucleic acids onto the surface of these particles is shown in the middle, whereas different types of multilayered DNA-CAP composite particles prepared by the coprecipitation technique are shown on the right. Reproduced and adapted with permission from Sokolova et al., Biomaterials, 2006, 27, 3147–3153, Butterworth-Heinemann in Association with the Biological Engineering Society.

surface-functionalized nanoparticulate carriers, the drug can be locally focused within the diseased area, so that a controlled and extended on-site release, with lesser doses required, can be achieved, with a greater control over toxicity and bioavailability of the drug. As for the intracellular delivery, surface functionalization can be used to optimize the charge of the particles, keeping in mind that positively charged particles are endocytosed at a higher rate compared to negatively charged ones (as cell membrane is negatively charged due to the surface-exposed phospholipids).[391] Good efficiency of CAP nanoparticles carrying a photoactive dye against rabbit synoviocytes and murine macrophages was thus attributed to their positive charge achieved by means of functionalizing the particle surface with poly(ethyleneimine) (PEI).[392] The most common peptide for biomimetic surface modification is Arg-Gly-Asp (RGD), a ubiquitous peptide present on ECM proteins and shown to promote cell adhesion in multiple cell types.[393] Specific targeting ligands, usually monoclonal antibodies, may be attached to the carrier surface, thus promoting a diagnostic molecular recognition and the immunocarrier character of the particles. PEG as a protecting polymer or BSA can be attached to the surface of the particles so as to increase the circulation time of the nanocarrier in the blood.[394,395] Such a strategy was employed by Abraxis Bioscience, to increase the uptake efficiency of the anticancer drug, paclitaxel, and prevent the side effects associated with using toxic solvents. Cell-penetrating peptides attached to the carrier surface would also allow for an enhanced uptake by the cells. CAP nanoparticles could also be functionalized[396] or encapsulated[397] with chitosan, a naturally derived polysaccharide, which is known to have apoptotic effects on tumor cells *per se*.[398–400] A method for injecting doxorubicin, a cancer therapeutic chemical into degradable CAP non–agglomerating particles with 20–40 nm in size, with the result of having the same efficacy but significantly less expressed side effects, has recently been reported.[401] Methotrexate, another anticancer drug, was also successfully loaded into 250-nm sized CAP particles prepared by reverse micelle technique.[402] CAP nanoparticles conjugated with *cis*-diammine-dichloro-platinum (CDDP, cisplatin) were also prepared, exhibiting twice higher IC_{50} values when compared to the free drug in an *in vitro* cell proliferation assay using a human ovarian cancer cell line.[403] Folic acid with its high affinity for folate receptors that are often overexpressed in cancer cells presents another compound that may be added to CAP nanoparticle carriers.[404] Also, photosensitizers, such as 2-devinyl-2-(1-hexyloxyethyl)pyropheophorbide (HPPH), could be incorporated in or coated on the surface of CAP particles, which would thus render the particles capable of being applied in cancer photodynamic therapy.[405] Raman labels, such as basic fuchsin or nanoscopic domains of silver or gold to initiate surface-enhanced Raman scattering (SERS) could also be attached to the core particles, which would make their antibody-conjugated versions detectable upon binding to cells or specific biomolecules by means of Raman spectroscopy.[406] Finally, all of these functional surface additives could be simultaneously applied in the role of emulsifiers, stabilizing the nanoparticulate suspensions and preventing agglomeration of the particles.[407]

Owing to the affinity of Ca^{2+} ions on the surface of CAP particles to the helical PO_4^{3-} groups of DNA, HAP has been applied as an adsorbent in chromatography for separation of DNA.[409] As Ca^{2+} ions can interact with carboxylate residues on the protein surface, whereas PO_4^{3-} functional groups can interact with basic protein residues, HAP has also been used for the separation of proteins.[410,411] Functionalizing the surface of HAP particles with polymers, peptides, proteins, cell-penetrating moieties, DNA, or oligonucleotides can thus be facilely carried out (Figure 13). Simple coprecipitation procedures were reported for the synthesis of DNA/CAP composites, with the biocomponent either encapsulated or anchored on the surface.[412] DNA could be attached to the particle surface, thus enabling their use as cell transfection agents, that is, nonviral vectors for the gene therapy.[413] The usage of CAP particles for this application dates back to the works of Graham et al. in 1973,[414] and is nowadays routinely used for *in vitro* transfection procedures. As far as the state-of-the-art is concerned, although nonviral delivery systems show a lesser efficiency compared

with the viral ones, they are markedly safer. Producing particles that would possess transfection efficiencies comparable to those of viral carriers thus remains a challenge, particularly in view of the fact that FDA has not approved any gene therapy carriers yet.[415] However, DNA can also be injected within the particles, thus preventing its detachment in the blood stream and ensuring its secure intracellular delivery.[416] In addition, by sequential precipitation of CAP and adsorption of DNA, core-shell particles with multiple layers of therapeutic organic components separated by walls of CAP and thus released at different time points and rates could be prepared.[417] The same technique of layer-by-layer precipitation could be applied for producing other types of multilayered polymeric/peptide/CAP particles.[418] Functionally graded HAP coatings encapsulating a drug can also be synthesized to enable tunable time-dependent drug release profiles.[419] As for the gene transfection a delivery of DNA into the cell nucleus has to be ensured, antisense strategies using siRNA (gene silencing) require a simpler approach, as in this case it is sufficient to deliver siRNA into the cytoplasm.[420] To ensure a more effective size control and serum tolerability and, therefore, a more effective genetic knockdown with CAP nanoparticles as siRNA-carriers, they were used as components of hybrid micelles together with PEGylated polyanion block copolymers, such as PEG-*b*-poly(aspartic acid) and PEG-*b*-poly(methacrylic acid).[421] Also, attaching oligonucleotides to nanoparticles has been shown to increase the resistance of the DNA fragments with respect to enzymatic degradation.[422] Coating CAP particles with the protective layer of oligonucleotides in addition to conjugating other functional compounds thereto (adsorbed, covalently bound or entrapped in the crystal structure) is thus an interesting research direction to explore.

Osteoinductive and cytotoxic behavior of CAP nanoparticles has been evaluated both on cell cultures and *in vivo*,[423–426] with the purpose of providing insights into their biocompatibility (biosafety as much as biofunctionality) characteristics. However, these tests have so far been proven as sufficient only to permit the usage of CAP nanoparticles as filler components in scaffolds implementable in reparation of hard tissues. For the purpose of applying these particles as drug delivery vehicles, significantly more extensive and qualitatively more complex evaluations need to be performed, particularly in view of the fact that toxicity of a compound can be different depending on size and/or morphology of the particulate form in which it is applied, and the fact that circulating nanoparticles can get into contact with practically any tissue in the organism, producing unforeseeable effects thereon. One report thus shows how polytetrafluoroethylene particles with ~20 nm in size are harmful when inhaled, whereas 130-nm-sized particles with the same composition do not produce any toxic effects.[427] On the other hand, there are nanoparticulate compositions that are prone to agglomeration upon their intravenous administration, and are only in such form evidenced as damaging for the body.[428] Sometimes, also, it is only a specific window of particle sizes that produces a given, desired or undesired biological response, as it has, for example, recently been shown how 2 and 12 nm sized particles did not induce a specific biological response that 7-nm-sized particles did.[429] As already noticed, a possible side effect of introducing extensive amounts of CAP into the body may be induced local atherosclerosis; hence, possible methods for assessing this effect include analyzing the cross-sections of arteries or looking at the deviations from the normal body weight gain in mice following administration of the drug delivery agent. Serum analyses can be used to follow bone metabolism (via levels of Ca^{2+}, $H_2PO_4^-/HPO_4^{2-}$ and alkaline phosphatase), kidney function (via BUN-to-creatinine ratio), and nutrition (via albumin and total levels of protein). Although intracellular injection of CAP particles may pose concerns in terms of the possibly harmful increase in levels of Ca^{2+} in the cytoplasm, such concerns are significantly minimized during the extracellular drug administration. Also, following the injection of typically a few hundreds of milligrams per kg of the body weight, histological and weight analyses of the dissected vital organs as well as hematological analyses (haematocyte and hemoglobin content and thrombocyte count) are often performed to evaluate the possible pathological effects of the drug delivery procedure.

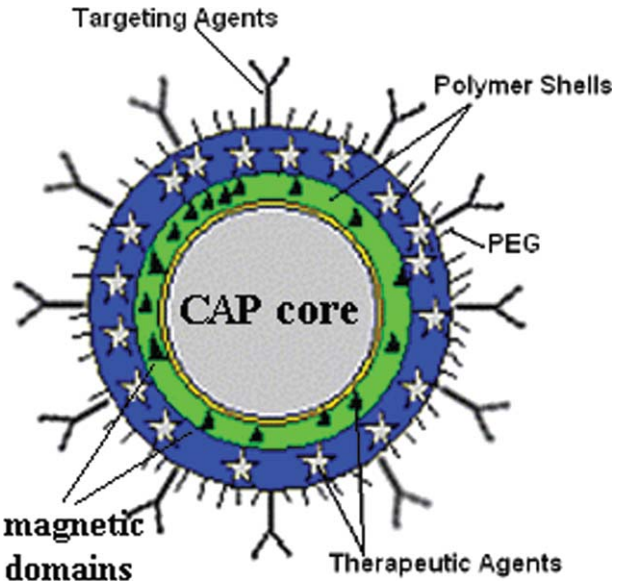

FIGURE 14. An example of a multifunctional drug delivery particle composed of CAP core surrounded by a polymeric shell in which magnetic domains are dispersed for the purpose of enabling the guidance of the particle in an external magnetic field and potentially producing localized heat under alternating magnetic field in hyperthermia or thermoblastic therapies. The external polymeric shell contains dispersed therapeutic agents, whereby its surface is covered by a targeting agent and PEG molecules so as to increase the circulation time of the carrier in the blood. [Color figure can be viewed in the online issue, which is available at wileyonlinelibrary.com.]

Finally, the ideals of multifunctionality dictate using multiple structural and surface modifications of CAP nanoparticles mentioned hereby in parallel, and exploring their synergy. One example of such a multifunctional composite particle is shown in Figure 14. Composite nanoparticles composed of magnetite nanodomains interspersed within a

polystyrene core, and coated with amine-functionalized quantum dots have recently been synthesized as a material for simultaneous fluorescent imaging and hyperthermia therapy.[430] Another type of particles based on BSA-stabilized manganese-doped magnetite nanoparticles comprising green fluorescence protein (GFP) and Arg-Gly-Asp peptide (known to bind specifically to $\alpha_v\beta_3$ integrin, which is expressed in tumor cells) bound to Cy5-dye-labeled thiolated siRNA (inhibiting the expression of GFP), for the purpose of simultaneous molecular imaging and gene silencing, was also recently produced.[431] Theranostic HAP nanocrystals doped with Eu^{3+} and Gd^{3+} were engineered to enable simultaneous contrast enhancement for three different imaging techniques (XRD, MRI, and near-infrared fluorescence imaging) as well as to act as therapeutic agents by being conjugated with the cell-membrane receptor ligand folic acid and by having their surface aminized with a dendigraft polymer, PEI.[432] Also, particles comprising 100-nm-sized silica core and Au shell with finely dispersed 10-nm-sized particles of Fe_3O_4, functionalized with anti-HER2 antibody with the purpose of specifically targeting epidermal growth factor receptors, were prepared and successfully applied, displaying an optical resonance peak, magnetic response, an intensive surface plasmon-enhanced scattering in targeted cells, and the ability to selectively destroy the penetrated cells depending on the frequency of the light source.[433] A similar approach may be performed relying on CAP as the core material. The first step in producing multifunctional composite CAP-based nanoparticles would be to establish convenient methods for fabrication of CAP nanoparticles with tunable structure and properties. Subsequently, the nanoparticles could be doped and surface functionalized with a wide array of atomic and molecular entities. To succeed in this, it is certain that inventing efficient and elegant methods of synthesis and conceiving innovative ideas on how to probe the fundamental understanding of the formation of complex composite and surface-functionalized nanoparticles relying on soft, bottom-up chemistry approaches, is essential, just as the availability of ultramodern imaging and other analytical techniques is. In other words, it is only a coordinated effort of soft, self-assembly, bottom-up synthetic techniques and top-down methods of manipulating the material structures at the fine scale that could yield desired results along this line of research.

CONCLUSIONS

After everything said, we can conclude that nanomedicine holds immense promises for the medical treatments of the future, whereby a research focused on multifunctional theranostic CAP nanoparticles capable of diagnosing the disease and being activated as a therapeutic at a chosen site, despite the fact that there is still a long way to go before the understanding of the chemical mechanisms of their formation is made complete, presents a prospective path for the development of this field that is still, as of today, in its embryonic stage. To be successful in these endeavors, the gap between life scientists and materials scientists sustained by different methods, terminologies, and subjects of scrutiny existing on each one of the separate research coasts, has to be bridged. As of today, however, the fruitful reconciliation of these two scientific areas can be seen as nothing but enormously challenging. The other side is often hardly intelligible to most scientists, which fosters them to stick to their own fields and narrow their views into ever more specialized cognitive panoramas. Organic and biochemical entities often disobey facile analytical reproducibility and require different, oftentimes more pertinacious strategies, quite unlike more robust and macroscale technologies implementable within materials science study concepts. Yet, the development of nanomedical methods and tools will crucially depend on the ability of natural scientists to stretch their curiosity to the other side and be open to communicate and form cross-disciplinary collaborations between the two. As in any other materials science design approach, a detailed understanding of the correlation between the material structure, properties and function is required for the development of CAP nanoparticles as viable drug and/or gene delivery vehicles. Hence, the basic material properties, such as particle size, morphology, specific surface area, polydispersity, and composition, including control over them have to be correlated with their corresponding performance in the biomedical settings. With its strong physicochemical roots, materials science can fundamentally supplement the biomedical approach, which is typically limited to investigating specific molecular recognition properties of biomolecules in elaborate statistical settings. With its engineering aspect, materials science can also provide a more reliable technological platform for biochemical studies. Life sciences can, on the other hand, provide the basis for the assessment of the real-life application potential of biomaterials designed in the laboratory. They can also enrich materials science with knowledge on soft matter and biochemical interactions that are critical for our ability to manipulate therewith in the design of complex multifunctional materials, such as the one that has been the topic of this review. This is all to say that to succeed in bringing CAP/HAP as advanced nanocarriers to the frontier of medicine will require a range of well coordinated interdisciplinary efforts. Bridging the gap between Materials Science and Life Science as two main contemporary research streams can be seen as a necessary precondition for satisfying this aim.

REFERENCES

1. Temenoff JS, Mikos AG. Biomaterials: the Intersection of Biology and Materials Science. Upper Saddle River, NJ: Prentice Hall; 2008.
2. Park J, Lakes RS. Biomaterials: An Introduction. Berlin: Springer; 2007.
3. Hench LL. Science, Faith and Ethics. London: Imperial College Press; 2001.
4. Balać I, Uskoković PS, Aleksić R, Uskoković D. Predictive modeling of the mechanical properties of particulate hydroxyapatite reinforced polymer composites, J Biomed Mater Res B: Appl Biomater 2002;63:793–799.
5. Fratzl P, Weinkamer R. Nature's Hierarchical Materials, Prog Mater Sci 2007;52:1263–1334.

6. Ratner BD, Hoffman AS, Schoen FJ, Lemons JE. Biomaterials Science: An Introduction to Materials in Medicine, 2nd ed. San Diego, CA: Elsevier Academic Press; 2004.
7. Onuma K. Recent research on pseudobiological hydroxyapatite crystal growth and phase transition mechanisms. Prog Cryst Growth Charact Mater 2006;52:223–245.
8. Hartgerink JD, Beniash E, Stupp SI. Self-assembly and mineralization of peptide-amphiphile nanofibers. Science 2001;294: 1684–1687.
9. Boyce BF, Xing L. Functions of RANKL/RANK/OPG in bone modeling and remodeling. Arch Biochem Biophys 2008;473:139–146.
10. Boyce BF, Xing L. Biology of RANK, RANKL, and Osteoprotegerin. Arthritis Res Ther 2007;9(Suppl 1):S1;1–7.
11. Wolff J. The Law of Bone Remodeling. Berlin: Springer; 1892.
12. Barrere F, Mahmood TA, de Groot K, van Blitterswijk CA. Advanced biomaterials for skeletal tissue regeneration: instructive and smart functions. Mater Sci Eng R 2008;59:38–71.
13. Asefa T, Yoshina-Ishii C, MacLachlan MJ, Ozin GA. New nanocomposites: putting organic function inside the channel walls of periodic mesoporous silica. J Mater Chem 2000;10:1751–1755.
14. Fantner GE, Hassenkam T, Kindt JH, Weaver JC, Birkedal H, Pechenik L, Cutroni JA, Cidade G, AG, Stucky GD, Morse DE, Hansma PK. Sacrificial bonds and hidden length dissipate energy as mineralized fibrils separate during bone fracture. Nat Mater 2005;4:612–616.
15. Cui F-Z, Ge J. New observations of the hierarchical structure of human enamel, from nanoscale to microscale. J Tissue Eng Regen Med 2007;1:185–191.
16. Fantner GE, Oroudjev E, Schitter G, Golde LS, Thurner P, Finch MM, Turner P, Gutsmann T, Morse DE, Hansma H, Hansma PK. Sacrificial bonds and hidden length: unraveling molecular mesostructures in tough materials. Biophys J 2006;90:1411–1418.
17. Uskoković V. Nanomaterials and nanotechnologies: approaching the crest of this big wave. Curr Nanosci 2008;4:119–129.
18. Nudelman F, Bomans P, Pieterse K, Brylka L, de With G, Sommerdijk N. Early Stages of Collagen Mineralization Studied by Cryo-TEM: Starting at the Overlap Region? Presented at the Materials Research Society Spring Meeting, San Francisco, CA; 2009.
19. Landis WJ. Mineral characterization in calcifying tissues: atomic, molecular and macromolecular perspectives. Connective Tissue Res 1996;34:239–246.
20. Uskoković V, Bertassoni LE. Nanotechnology in dental sciences: moving towards a finer way of doing dentistry. Materials 2010;3: 1674–1691.
21. Ball P. Water as an active constituent in cell biology. Chem Rev 2008;108:74–108.
22. Bertassoni L, Habelitz S, Kinney J, Marshall S, Marshall G. Biomechanistic perspective on the remineralization of dentin. Caries Res 2009;43:70–77.
23. Hoffler CE, Guo XE, Zysset PK, Goldstein SA. An application of nanoindentation technique to measure bone tissue lamellae properties. J Biomech Eng 2005;127:1046–1053.
24. Bembey AK, Bushby AJ, Boyde A, Ferguson VL, Oyen L. Hydration effects on the micro-mechanical properties of bone. J Mater Res 2006;21:1962–1968.
25. Kishen A, Vedantam S. Hydromechanics in dentine: role of dentinal tubules and hydrostatic pressures on mechanical stress-strain distribution. Dental Mater 2007;23:1296–1306.
26. Fawzy AS, Farghaly AM. Probing nano-scale adhesion force between AFM and acid demineralized intertubular dentin: Moist versus dry dentin. J Dentistry 2009;37:963–969.
27. Cooper A. Thermodynamics of protein folding and stability. In: Allen G, editor. Protein: A Comprehensive Treatise, Vol. 2, Stamford, CN: JAI Press; 1999. pp 217–270.
28. Shen ZL, Dodge MR, Kahn H, Ballarini R, Eppel SJ. In Vitro Mechanical Testing of Collagen Nanofibrils, Society for Biomaterials 2010 Annual Meeting and Exposition, Seattle, WA; 2010, presentation #220.
29. Dorozhkin SV. Calcium Orthophosphates. J Mater Sci 2007;42: 1061–1095.
30. Uskoković V, Drofenik M. Synthesis of lanthanum-strontium manganites by oxalate-precursor co-precipitation methods in solution and in reverse micellar microemulsion. J Magn Magn Mater 2006;303:214–220.
31. Uskoković V. Theoretical and practical aspects of colloid science and self-assembly phenomena revisited. Rev Chem Eng 2007;23: 301–372.
32. Onuma K, Ito A. Cluster growth model for hydroxyapatite. Chem Mater 1998;10:3346–3351.
33. Onuma K. Recent research on pseudobiological hydroxyapatite crystal growth and phase transition mechanisms. Prog Cryst Growth Charact Mater 2006;52:223–245.
34. White TJ, Dong ZL. Structural derivation and crystal chemistry of apatites. Acta Crystallographia B 2003;59:1–16.
35. De Leeuw NH. Local ordering of hydroxyl groups in hydroxyapatite. Chem Commun 2001;17:1646–1647.
36. LeGeros RZ. Calcium phosphate-based osteoinductive materials. Chem Soc Rev 2008;108:4742–4753.
37. Featherstone JD. Modeling the caries-inhibitory effects of dental materials. Dental Mater 1996;12:194–197.
38. Isaacson RL, Varner JA, Jensen KF. Toxin-induced blood vessel inclusions caused by the chronic administration of aluminum and sodium fluoride and their implications for dementia. Ann NY Acad Sci 1997;15:152–166.
39. Garant PR. Oral Cells and Tissues. Carol Stream, IL: Quintessence; 2003).
40. Yao F, LeGeros J, LeGeros RZ. Simultaneous incorporation of carbonate and fluoride in synthetic apatites: effect on crystallographic and physico-chemical properties. Acta Biomater 2009;5: 2169–2184.
41. Porter A, Patel N, Brooks R, Best S, Rushton N, Bonfield W. Effect of carbonate substitution on the ultrastructural characteristics of hydroxyapatite implants. J Mater Sci: Mater Med 2005;16: 899–907.
42. Kanno T, Horiuchi JI, Kobayashi M, Motogami Y, Akazawa T. Characteristics of the carbonate ions incorporated into calcium-partially-strontium-substituted and strontium apatites. J Mater Sci Lett 1999;18:1343–1345.
43. Driessens FCM, Verbeeck RMH, Kiekens LP. Mechanism of substitution in carbonated apatites. Z Anorg Allg Chem 1983;504: 195–200.
44. Somasundaran P. Encyclopedia of Surface and Colloid Science. Boca Raton, FL: CRC Press; 2004, pp 567.
45. Barralet J, Best S, Bonfield W. Carbonate substitution in precipitated hydroxyapatite: An investigation into the effects of reaction temperature and bicarbonate ion concentration. J Biomed Mater Res 1998;41:79–86.
46. Rey C, Collins B, Goehl T, Dickson IR, Glimcher MJ. The Carbonate environment in bone mineral: A resolution-enhanced Fourier transform infrared spectroscopic study. Calcif Tissue Int 1989;45: 157–164.
47. Emerson WH, Fischer ED. The infrared absorption spectra of carbonate in calcified tissue. Arch Oral Biol 1962;7:671–683.
48. Suetsugu Y, Takanashi Y, Okamura FP, Tanaka J. Structure analysis of A-type carbonate apatite by a single-crystal X-ray diffraction method. J Solid State Chem 2000;155:292–304.
49. Corno M, Rimola A, Bolis V, Ugliengo P. Hydroxyapatite as a key biomaterial: quantum-mechanical simulation of its surfaces in interaction with biomolecules. Phys Chem Chem Phys 2010;12: 6309–6329.
50. Tonegawa T, Ikoma T, Yoshioka T, Hanagata N, Tanaka J. Crystal structure refinement of A-type carbonate apatite by X-ray powder diffraction. J Mater Sci 2010;45:2419–2426.
51. Fleet ME, Lui X, King P. Accommodation of the carbonate ion in apatite: An FTIR and X-Ray structure study of crystals synthesized at 2-4 GPa. Am Mineral 2004;89:1422–1434.
52. Shi D. Introduction to Biomaterials. Singapore: World Scientific Press; 2006.
53. Brown S, Clarke I, Williams P. Synthesis and characterization of hydroxyapatite and fluoroapatite. Key Eng Mater 2002;218-2:35–38.
54. Ignjatović N, Suljovrujić E, Stojanović Z, Uskoković D. Structure and characteristics of the hot pressed hydroxyapatite/poly-L-lactide composite. Sci Sintering 2002;34:79–93.
55. Fang Y, Agrawal DK, Roy DM.Thermal Stability of Synthetic Hydroxyapatite, In: Brown PW, Constantz B, editors. Hydroxyapatite

and Related Materials. Boca Raton, FL: CRC Press; 1994, pp 269–282.
56. Ignjatović N, Suljovrujić E, Budinski J, Krakovsky I, Uskoković D. Evaluation of hot pressed hydroxyapatite/poly-L-lactide composite biomaterial characteristics. J Biomed Mater Res Part B: Appl Biomater B 2004;71:284–294.
57. Welzel T, Meyer-Zaika W, Epple M. Continuous preparation of functionalised calcium phosphate nanoparticles with adjustable crystallinity. Chem Commun 2004:1204–1205.
58. Pretto M, Costa AL, Landi E, Tampieri A, Galassi C. Dispersing behavior of hydroxyapatite powders produced by wet-chemical synthesis. J Am Ceram Soc 2003;86:1534–1539.
59. Gomez-Morales J, Torrent-Burgues J, Boix T, Fraile J, Rodriguez-Clemente R. Precipitation of stoichiometric hydroxyapatite by a continuous method. Crystal Res Technol 2001;36:15–26.
60. Tas AC, Korkusuz F, Timucin M, Akkas N. An investigation of the chemical synthesis and high-temperature sintering behaviour of calcium hydroxyapatite (HA) and tricalcium phosphate (TCP) bioceramics. J Mater Sci: Mater Med 1997;8:91–96.
61. Ashok M, Kalkura SN, Sundaram NM, Arivuoli D. Growth and characterization of hydroxyapatite crystals by hydrothermal method. J Mater Sci: Mater Med 2007;18:895–898.
62. Janaćković Dj, Janković I, Petrović R, Kostić-Gvozdenović Lj, Milonjić S, Uskoković D. Surface properties of HAP particles obtained by hydrothermal decomposition of urea and calcium-edta chelates. Key Eng Mater 2003;240-242:437–440.
63. Thian ES, Ahmad Z, Huang J, Edirisinghe MJ, Jayasinghe SN, Ireland DC, Brooks RA, Rushton N, Bonfield W, Best SM. The role of electrosprayed apatite nanocrystals in guiding osteoblast behavior. Biomaterials 2008;29:1833–1843.
64. Wu Y, Hench LL, Du J, Choy K-L, Guo J. Preparation of hydroxyapatite fibers by electrospinning technique. J Am Ceram Soc 2005;87:1988–1991.
65. Teshima K, Lee S, Sakurai M, Kameno Y, Yubuta K, Suzuki T, Shishido T, Endo M, Oishi S. Well-formed one-dimensional hydroxyapatite crystals grown by an environmentally friendly flux method. Crystal Growth Design 2009;9:2937–2940.
66. Jokanović V, Uskoković D. Calcium hydroxyapatite thin films on titanium substrates prepared by ultrasonic spray pyrolysis. Mater Trans 2005;46:228–235.
67. Fang Y, Agrawal DK, Roy DM, Roy R, Brown PW. Ultrasonically accelerated synthesis of hydroxyapatite. J Mater Res 1992;7:2294–2298.
68. I. Nikčević, Jokanović V, Mitrić M, Nedić Z, Makovec D, Uskoković D. Mechanochemical synthesis of nanostructured fluorapatite/fluorhydroxyapatite and carbonated fluorapatite/fluorhydroxyapatite. J Solid State Chem 2004;177:2565–2574.
69. Rhee S-H. Synthesis of hydroxyapatite via mechanochemical treatment. Biomaterials 2002;23:1147–1152.
70. Lak A, Mazloumi M, Mohajerani MS, Zanganeh S, Shayegh MR, Kajbafvala A, Arami H, Sadrnezhaad SK. Rapid formation of mono-dispersed hydroxyapatite nanorods with narrow-size distribution via microwave irradiation. J Am Ceram Soc 2008;91:3580–3584.
71. Liu J, Li K, Wang H, Zhu M, Yan H. Rapid formation of hydroxyapatite nanostructures by microwave irradiation. Chem Phys Lett 2004;396:429–432.
72. Zhang HG, Zhu Q. Surfactant-assisted preparation of fluoride-substituted hydroxyapatite nanorods. Mater Lett 2005;59:3054–3058.
73. Bose S, Saha SK. Synthesis and characterization of hydroxyapatite nanopowders by emulsion technique. Chem Mater 2003;15:4464–4469.
74. Liu JZ, Gou BD, Xu SJ, Wang K. Formation of calcium phosphate mineral material controlled by microemulsion. Prog Nat Sci 2002;12:615–617.
75. Sarda S, Heughebaert M, Lebugle A. Influence of the type of surfactant on the formation of calcium phosphate in organized molecular systems. Chem Mater 1999;11:2722–2727.
76. Banerjee A, Bandyopadhyay A, Bose S. Hydroxyapatite nanopowders: Synthesis, densification and cell-materials interaction. Mater Sci Eng C 2007;27:729–735.
77. Cheng K, Weng W, Han G, Du P, Shen G, Yang J, Ferreira JMF. The effect of triethanolamine on the formation of sol-gel derived fluoroapatite/hydroxyapatite solid solution. Mater Chem Phys 2003;78:767–771.
78. Chu CL, Lin PH, Dong S, Guo DY. Influences of citric acid as a chelating reagent on the characteristics of nanophase hydroxyapatite powders fabricated by a sol-gel method. J Mater Sci Lett 2002;21:1793–1795.
79. Gao Y. Synthesis and Characterization of Calcium Phosphate Coatings by metalorganic Chemical vapor Deposition, Presented at the Materials Research Society Meeting, Boston, MA; 1998.
80. Xu S, Long J, Sim L, Diong CH, Ostrikov K. RF plasma sputtering deposition of hydroxyapatite bioceramics: Synthesis, performance, and biocompatibility. Plasma Process Polym 2005;2:373–390.
81. Watari F, Yokoyama A, Gelinsky M, Pompe W. Conversion of functions by nanosizing—From osteoconductivity to bone substitutional properties in apatite. In: Interface Oral Health Science 2007, Proceedings of the 2nd International Symposium for Interface Oral Health Science, Sendai, Japan. Berlin: Springer; 2007. pp 139–148.
82. Uskoković V. Challenges for the modern science in its descend towards nano scale. Curr Nanosci 2009;5:372–389.
83. Cai Y, Tang R. Calcium phosphate nanoparticles in biomineralization and biomaterials. J Mater Chem 2008;18:3775–3787.
84. Cai Y, Liu Y, Yan W, Hu Q, Tao J, Zhang M, Shi Z, Tang R. Role of hydroxyapatite nanoparticle size in bone cell proliferation. J Mater Chem 2007;17:3780–3787.
85. Perkin KK, Turner JL, Wooley KL, Mann S. Fabrication of hybrid nanocapsules by calcium phosphate mineralization of shell cross-linked polymer micelles and nanocages. Nano Lett 2005;5:1457–1461.
86. Shchukin DG, Sukhorukov GB, Mohwald H. Biomimetic fabrication of nanoengineered hydroxyapatite/polyelectrolyte composite shell. Chem Mater 2003;15:3947–3950.
87. Kirkham J, Brookes SJ, Shore RC, Wood SR, Smith DA, Zhang J, Chen H, Robinson C. Physico-chemical properties of crystal surfaces in matrix-mineral interactions during mammalian biomineralisation. Curr Opin Colloid Interface Sci 2002;7:124–132.
88. Müller B. Tailoring biocompatibility: Benefitting patients. Mater Today 2010;13:58–58.
89. Rimola A, Corno M, Zicovich CM, -Wilson, Ugliengo P. *Ab Initio* modeling of protein/biomaterial interactions: Glycine adsorption at hydroxyapatite surfaces. J Am Chem Soc 2008;130:16181–16183.
90. Tamerler C, Sarikaya M. Molecular Biomimetics—Peptide-Based Materials for Nanotechnology and Medicine, Society for Biomaterials 2010 Annual Meeting & Exposition, Seattle, WA; 2010, Presentation #182.
91. Uskoković V, Kim M-K, Li W, Habelitz S. Enzymatic processing of amelogenin during continuous crystallization of apatite. J Mater Res 2008;32:3184–3195.
92. Ahmad G, Dickerson MB, Church BC, Cai Y, Jones SE, Naik RR, King JS, Summers CJ, Kröger N, Sandhage KH. Rapid, room-temperature formation of crystalline calcium molybdate phosphor microparticles via peptide-induced precipitation. Adv Mater 2006;18:1759–1763.
93. Dickerson MB, Naik RN, Stone MO, Cai Y, Sandhage KH. Identification of peptides that promote the rapid precipitation of germania nanoparticle networks via use of a peptide display library. Chem Commun (Camb) 2004;15:1776–1777.
94. Zhan J, Tseng Y-H, Chan JCC, Mou C-Y. Biomimetic formation of hydroxyapatite nanorods by a single-crystal-to-single-crystal transformation. Adv Funct Mater 2005;15:2005–2010.
95. Huang F, Shen Y, Xie A, Zhu J, Zhang C, Li S, Zhu J. Study on synthesis and properties of hydroxyapatite nanorods and its complex containing biopolymer. J Mater Sci 2007;42:8599–8605.
96. Zhang F, Zhou Z-H, Yang S-P, Mao L-H, Chen H-M, Yu X-B. Hydrothermal synthesis of hydroxyapatite nanorods in the presence of anionic starburst dendrimer. Mater Lett 2005;59:1422–1425.
97. Yan L, Li Y, Deng Z-X, Zhuang J, Sun X. Surfactant-assisted hydrothermal synthesis of hydroxyapatite nanorods. Int J Inorganic Mater 2001;3:633–637.
98. Wang A, Liu D, Yin H, Wu H, Wada Y, Ren M, Jiang T, Cheng X, Xu Y. Size-controlled synthesis of hydroxyapatite nanorods by

chemical precipitation in the presence of organic modifiers. Mater Sci Eng C 2007;27:865–869.
99. Walsh D, Kingston JL, Heywood BR, Mann S. Influence of monosaccharides and related molecules on the morphology of hydroxyapatite. J Crystal Growth 1993;133:1–12.
100. Stupp SI, Braun PV. Molecular manipulation of microstructures: Biomaterials, ceramics, and semiconductors. Science 1997;277: 1242–1248.
101. Zangi R, Berne BJ. Aggregation and dispersion of small hydrophobic particles in aqueous electrolyte solutions. J Phys Chem B 2006;110:22736–22741.
102. Mann S. Biomineralization: Principles and concepts in bioinorganic materials chemistry. Oxford, UK: Oxford University Press; 2001.
103. Motskin M, Wright DM, Muller K, Kyle N, Gard TG, Porter AE, Skepper JN. Hydroxyapatite nano and microparticles: Correlation of particle properties with cytotoxicity and biostability. Biomaterials 2009;30:3307–3317.
104. Fan Y, Sun Z, Moradian-Oldak J. Controlled remineralization of enamel in the presence of amelogenin and fluoride. Biomaterials 2009;30:478–483.
105. Uskoković DP. Fine Particles in Advanced Technology, International Symposium on Advanced Dielectric Materials and Electronic Devices, MS&T 2006 Conference Proceedings, Warrendale, PA. Mater Syst 1;2006:599–610.
106. Tanaka Y, Hirata Y, Yoshinaka R. Synthesis and characterization of ultrafine hydroxyapatite particles. J Ceram Process Res 2003; 4:197–201.
107. Uskoković V, Drofenik M. Synthesis of materials within reverse micelles. Surface Rev Lett 2005;12:239–277.
108. Uskoković V, Drofenik M. Reverse micelles: Inert nano-reactors or physico-chemically active guides of the capped reactions. Adv Colloid Interface Sci 2007;133:23–34.
109. Ye F, Guo H, Zhang H. Biomimetic synthesis of oriented hydroxyapatite mediated by nonionic surfactants. Nanotechnology 2008;19:245605.
110. Santos C, Rovath CF, Franke R-P, Almeida MM, Costa MEV. Spray-dried hydroxyapatite-5-Fluorouracil granules as a chemotherapeutic delivery system. Ceram Int 2009;35:509–513.
111. Chen H, Clarkson BH, Sun K, Mansfield JF. Self-assembly of synthetic hydroxyapatite nanorods into an enamel prism-like structure. J Colloid Interface Sci 2005;288:423–431.
112. Cai Y, Pan H, Xu X, Hu Q, Li L, Tang R. Ultrasonic controlled morphology transformation of hollow calcium phosphate nanospheres. a smart and biocompatible drug release system. Chem Mater 2007;19:3081–3083.
113. Ignjatović N, Ninkov P, Ajduković Z, Vasiljević-Radović D, Uskoković D. Biphasic calcium phosphate coated with poly-d,l-lactide-*co*-glycolide biomaterial as a bone substitute, J Eur Ceram Soc 2007;27:1589–1594.
114. Hornez JC, Chai F, Monchau F, Blanchemain N, Descamps M, Hilderbrand HF. Biological and physico-chemical assessment of hydroxyapatite (HA) with different porosity. Biomol Eng 2007;24: 505–509.
115. Hesaraki S, Nemati R. Caphalexin-loaded injectable macroporous calcium phosphate bone cement. J Biomed Mater Res Part B: Appl Biomater B 2009;89:342–352.
116. Ignjatović NL, Ajduković ZR, Savić VP, Uskoković DP. Size effect of calcium phosphate coated with poly-DL-lactide-*co*-glycolide on healing processes in bone reconstruction. J Biomed Mater Res Part B: Appl Biomater 2010;94:108–117.
117. Watari F, Takashi N, Yokoyama A, Uo M, Akasaka T, Sato Y, Abe A, Totsuoka Y, Tohji K. Material nanosizing effect on living organisms: non-specific, biointeractive, physical size effects. J Royal Soc Interface 2009;6:S371–S388.
118. Šupova M, Problem of hydroxyapatite dispersion in polymer matrices: A review. J Mater Sci: Mater in Med 2009;20:1201–1213.
119. Jevtić M, Radulović A, Ignjatović N, Mitrić M, Uskoković D. Controlled assembly of poly(D,L-lactide-*co*-glycolide)/hydroxyapatite core-shell nanospheres under ultrasonic irradiation. Acta Biomater 2009;5:208–218.
120. Jevtić M, Uskoković D. Influence of urea as a homogenous precipitation agent on sonochemical hydroxyapatite synthesis. Mater Sci Forum 2007;555:285–290.
121. Aizawa M, Porter AE, Best SM, Bonfield W. Ultrastructural observation of single-crystal apatite fibres. Biomaterials 2005;26:3427–3433.
122. Chung SY, Kim YM, Kim JG, Kim YJ. Multiphase transformation and ostwald's rule of stages during crystallization of a metal phosphate. Nat Phys 2009;5:68–73.
123. Beniash E, Metzler RA, Lam RSK, Gilbert PUPA. Transient amorphous calcium phosphate in forming enamel. J Struct Biol 2009: 166;133–143.
124. George A. Protein Template is Required for Nucleation and Orientation of Hydroxyapatite in Bones and Teeth, Presented at the 12th Annual Conference of the Institute of Science and Technology of Ceramics ISTEC-CNR, Faenza; 2009.
125. He G, Dahl T, Veis A, George A, Nucleation of Apatite Crystals in vitro by Self-Assembled Dentin Matrix Protein 1. Nat Mater 2003; 2:552–558.
126. Gower LB. Biomimetic model systems for investigating the amorphous precursor pathway and its role in biomineralization. Chem Rev 2008;108:4551–4627.
127. Tao J, Pan H, Zeng Y, Xu X, Tang R. Roles of amorphous calcium phosphate and biological additives in the assembly of hydroxyapatite nanoparticles. J Phys Chem B 2007;111:13410–13418.
128. Thompson DW. On Growth and Form. London, UK: Dover; 1917.
129. Chien YC, Masica DL, Gray JJ, Nguyen S, Vali H, McKee MD. Modulation of calcium oxalate dihydrate growth by selective crystal-face binding of phosphorylated osteopontin and polyaspartate peptide showing occlusion by sectoral (compositional) zoning. J Biol Chem 2009;284:23491–23501.
130. He LH, Swain MV. Understanding the mechanical behaviour of human enamel from its structural and compositional characteristics. J Mech Behav Biomed Mater 2008;1:18–29.
131. Beniash E, Metzler RA, Lam RS, Gilbert PU. Transient amorphous calcium phosphate in forming enamel. J Struct Biol 166; 2009:133–143.
132. Cao M, Wang Y, Guo C, Qi Y, Hu C. Preparation of ultrahigh-aspect-ratio hydroxyapatite nanofibers in reverse micelles under hydrothermal conditions. Langmuir 2004;20:4784–4786.
133. Smith CE. Cellular and chemical events during enamel maturation. Critical Rev Oral Biol Med 1998;9:128–161.
134. Viney C. Self-assembly as a route to fibrous materials: Concepts, opportunities and challenges. Curr Opin Solid State Mater Sci 2004;8:95–101.
135. Viney C, Bell FI. Inspiration versus duplication with biomolecular fibrous materials: learning nature's lessons without copying nature's limitations. Curr Opin Solid State Mater Sci 2004;8: 165–171.
136. Bateson G. Mind and Nature. Cresskill, NJ: Hampton Presss; 1979.
137. Xu A-W, Ma Y, Cölfen H. Biomimetic Mineralization. J Mater Chem 2007;17:415–449.
138. Orme CA, Giocondi JL. Model Systems for Formation and Dissolution of Calcium Phosphate Minerals. In: Behrens P, Bäuerlein E, editors. Handbook of Biomineralization, Vol.2. Weinheim: Wiley; 2007.
139. Harding IS, Rashid N, Hing KA. Surface charge and the effect of excess calcium ions on the hydroxyapatite surface. Biomaterials 2005;26:6818–6826.
140. Somasundaran P, Wang YHC. Surface Chemical Characteristics and Adsorption Properties of Apatite. In: Misra DN, editor. Adsorption on and Surface Chemistry of Apatite. Berlin: Springer; 1984.
141. Bengtsson A, Shchukarev A, Persson P, Sjoberg S. Phase tranformations, ion-exchange, adsorption, and dissolution processes in aquatic fluoroapatite systems. Langmuir 2009;25:2355–2362.
142. Cazalbou S, Combes C, Eichert D, Rey C. Adaptative physicochemistry of bio-related calcium phosphates. J Mater Chem 2004;14:2148–2153.
143. Campbell AA, LoRe M, Nancollas GH. The influence of carbonate and magnesium ions on the growth of hydroxyapatite, carbonated apatite and human powdered enamel. Colloids Surf 1991; 54:25–31.
144. Kanzaki N, Onuma K, Ito A, Teraoka K, Tateishi T, Tsutsumi S. Direct growth rate measurement of hydroxyapatite single crystal

by moire phase shift interferometry. J Phys Chem 1998;102: 6471–6476.
145. Rouahi M, Champion E, Gallet O, Jada A, Anselme K. Physicochemical characteristics and protein adsorption potential of hydroxyapatite particles: Influence on in vitro biocompatibility of ceramics after sintering. Colloids Surf B: Biointerfaces 2006;47: 10–19.
146. Kim H-M, Himeno T, Kokubo T, Nakamura T. Process and kinetics of bonelike apatite formation on sintered hydroxyapatite in a simulated body fluid. Biomaterials 2005;26:4366–4373.
147. Roseeva EV, Golovanova OA, Frank-Kamenetskaya OV. The influence of amino acids on the formation of nanocrystalline hydroxyapatite. Glass Phys Chem 33:283–286.
148. Barroug A, Lemaitre J, Rouxhet PG. Influence of crystallite size on the surface-properties of calcium-deficient hydroxyapatites. J Alloys Compounds 1992;188:152–156.
149. Kosmulski M. Surface Charging and Points of Zero Charge, Surfactant Science Series 145. Boca Raton, FL: CRC Press, Francis & Taylor; 2009.
150. Zhang Y, Yokogawa Y. Effect of drying conditions during synthesis on the properties of hydroxyapatite powders. J Mater Sci: Mater Med 2008;19:623–628.
151. Yao X, Tan S, Jiang D. Fabrication of hydroxyapatite ceramics with controlled pore characteristics by slip casting. J Mater Sci: Mater Med 2005;16:161–165.
152. Ma J, Liang CH, Kong LB, Wang C. Colloidal characterization and electrophoretic deposition of hydroxyapatite on titanium substrate. J Mater Sci: Mater Med 2003;14:797–801.
153. Sadeghian Z, Heinrich JG, Moztarzadeh F. Preparation of highly concentrated aqueous hydroxyapatite suspensions for slip casting. J Mater Sci 2005;40:4619–4623.
154. Kawasaki T, Niikura M, Kobayashi Y. Fundamental study of hydroxyapatite high-performance liquid chromatography: II. Experimental analysis on the basis of the general theory of gradient chromatography. J Chromatogr 1990;515:91–123.
155. Kandori A, Oda S, Fukusumi M, Morisada Y. Synthesis of positively charged calcium hydroxyapatite nano-crystals and their adsorption behavior of proteins. Colloids Surfaces B: Biointerfaces 2009;73:140–145.
156. Boghak S, Bose S, Bandyopadhyay A. Electro-Thermally Polarized Hydroxyapatite (HAp) Ceramics: Influence of MgO, SrO, and ZnO Dopants, Society for Biomaterials 2010 Annual Meeting & Exposition, Seattle, WA; 2010, presentation #474.
157. Cai Y, Yao J. Effect of proteins on the synthesis and assembly of calcium phosphate nanomaterials. Nanoscale 2010;2:1842–1848.
158. Shaw DJ. Introduction to Colloid and Surface Chemistry, Oxford, UK: Butterworth Heinemann; 1992.
159. Dorozhkin SV. Calcium orthophosphates in nature, biology and medicine, Materials 2009;2:399–498.
160. Giocondi JL, Nancollas GH, Chernov AA, Orme C. Does the Incorporation of Calcium or Phosphate Control the Rate of Brushite Mineralization? Presented at the Materials Research Society Spring Meeting, San Francisco, CA; 2009.
161. Leontidis E. Hofmeister anion effects on surfactant self-assembly and the formation of mesoporous solids. Curr Opin Colloid Interface Sci 2002;7:81–91.
162. Filankembo A, Giorgio S, Lisiecki I, Pileni MP. Is the anion the major parameter in the shape control of nanocrystals. J Phys Chem B 2003;107:7492–7500.
163. Orme CA, Giocondi JL. The Use of Scanning Probe Microscopy to Investigate Crystal-Fluid Interfaces, In: Skowronski M, DeYoreo JJ, Wang CA, editors. Perspectives on Inorganic, Organic, and Biological Crystal Growth: From Fundamentals to Applications. Berlin: Springer; 2007.
164. Riddick TM. Control of Colloid Stability through Zeta Potential and its Relationship to Cardiovascular Disease. Wynnewood, PA: Livingston Publishing; 1968.
165. Ngankam P, Lavalle Ph, Voegel JC, Szyk L, Decher G, Schaaf P, Cuisinier FJG. Influence of polyelectrolyte multilayer films on calcium phosphate nucleation. J Am Chem Soc 2000;122: 8998–9005.
166. Qiu SR, Orme CA. Dynamics of biomineral formation at the near-molecular level. Chem Review 2008;108:4784–4822.
167. Bengtsson A, Shchukarev A, Persson P, Sjoberg S. A solubility and surface complexation study of a non-stoichiometric hydroxyapatite. Geochim Cosmochim Acta 2009;73:257–267.
168. Lu X, Leng Y. Theoretical analysis of calcium phosphate precipitation in simulated body fluid. Biomaterials 2005;26: 1097–1108.
169. Harding JH, Duffy DM, Sushko ML, Rodger PM, Quigley D, Elliott JA. Computational techniques at the organic-inorganic interface in biomineralization. Chem Rev 2008;108:4823–4854.
170. Pan H, Tao J, Yu X, Fu L, Zhang J, Zeng X, Xu G, Tang R. Anisotropic demineralization and oriented assembly of hydroxyapatite crystals in enamel: smart structures of biominerals. J Physical Chem B 2008;112:7162–7165.
171. van Kemenade MJJM, de Bruyn PL. A kinetic study of precipitation from supersaturated calcium phosphate solutions. J Colloid Interface Sci 2001;118:564–585.
172. Szczes A, Holysz L, Chibowski E. Influence of magnetic field on the properties of freshly precipitated calcium phosphate: implication in adhesion to glass surface. J Adhes Sci Technol 2006;20:345–358.
173. Tai CY, Wu CK, Chang MC. Effects of magnetic field on the crystallization of $CaCO_3$ using permanent magnets. Chem Eng Sci 2008;63:5606–5612.
174. Tai CY, Chang MC, Shieh RJ, Chen TG. Magnetic effects on crystal growth rate of calcite in a constant-composition environment. J Crystal Growth 2008;310:3690–3697.
175. Gavira JA, Garca-Ruiz Jma. Effects of a magnetic field on lysozome crystal nucleation and growth in a diffusive environment. Crystal Growth Design 2009;9:2610–2615.
176. Sikirić MD, Furedi-Milhofer H. The influence of surface active molecules on the crystallization of biominerals in solution. Adv Colloid Interface Sci 2006;128–130:135–158.
177. Posner AS, Betts F, Blumenthal NC. Formation and structure of synthetic and bone hydroxyapatite. Prog Crystal Growth Character Mater 1980;3:49–64.
178. Brecević Lj, Hlady V, Furedi-Milhofer H. Influence of gelatin on the precipitation of amorphous calcium phosphate. Colloids Surf 1987;28:301–313.
179. Melikhov IV. Crystallization Behavior of Nanodisperse Phases. Inorg Mater 2000;36:278–286.
180. Lazić S. Microcrystalline hydroxyapatite formation from alkaline solutions. J Crystal Growth 1995;147:147–154.
181. Privman V, Goia DV, Park J, Matijević E. Mechanism of formation of monodispersed colloids by aggregation of nanosize precursors. J Colloid Interface Sci 1999;213:36–45.
182. Privman V. Growth of nanosize and colloid particles by controlled addition of singlets. Mater Res Soc Symp Proc 2002;703: 577–585.
183. Privman V. Mechanisms of diffusional nucleation of nanocrystals and their self-assembly into uniform colloids. Ann NY Acad Sci 2009;1161:508–526.
184. Matijević E. Nanosize precursors as building blocks for monodispersed colloids. Colloid J 2007;69:29–38.
185. Oh M, Mirkin CA. Chemically tailorable colloidal particles from infinite coordination polymers. Nature 2005;438:651–654.
186. Robb DT, Halaciuga I, Privman V, Goia DV. Computational model for the formation of uniform silver spheres by aggregation of nanosize precursors. J Chem Phys 2008;129:184705.
187. Cho K-S, Talapin DV, Gaschler W, Murray CB. Designing PbSe nanowires and nanorings through oriented attachment of nanoparticles. J Am Chem Soc 2005;127:7140–7147.
188. Alivisatos P. Chemical Transformations in Nanocrystals, Presented at the Materials Research Society Spring Meeting, San Francisco, CA; 2009.
189. Jokanović V, Nikčević I, Dačić B, Uskoković D. Synthesis of nanostructured carbonated calcium hydroxyapatite by ultrasonic spray pyrolysis. J Ceram Process Res 2004;5:157–162.
190. Chow LC, Sun L. Properties of nanostructured hydroxyapatite prepared by a spray drying technique. J Res Natl Inst Stand Techol 2004;109:543–551.
191. Liu C, Huang Y, Shen W, Cui J. Kinetics of hydroxyapatite precipitation at pH 10 to 11. Biomaterials 2001;22:301–306.
192. Lazić S, Katanić-Popović J, Zec S, Miljević N. Properties of hydroxyapatite crystallized from high temperature alkaline solutions. J Crystal Growth 1996;165:124–128.

193. Lazić S, Zec S, Miljević N, Milonjić S. The effect of temperature on the properties of hydroxyapatite precipitated from calcium hydroxide and phosphoric acid. Thermochim Acta 2001;374: 13–22.
194. Larsen MJ. Ion products and solubility of calcium phosphates. Denmark: Royal Dental College; 2001.
195. Kibalczyc W, Zielenkiewicz A, Zielenkiewicz W. Calorimetric investigations of calcium phosphate precipitation in relation to solution composition and temperature. Thermochim Acta 1988; 131:47–55.
196. Termine JD, Eanes ED. Comparative chemistry of amorphous and apatitic calcium phosphate preparation. Calcified Tissue Res 1972;10:171–197.
197. Meyer JL, Weatherall CC. Amorphous to crystalline calcium phosphate transformation at elevated pH. J Colloid Interface Sci 1982;89:257–267.
198. Marshall AF, Lawless KR. TEM study of the central dark line in enamel crystallites. J Dental Res 1981;60:1773–1782.
199. Fernandez ME, Reyes-Gasga J. A model for human tooth enamel central dark line its HRTEM images contrast transfer function analysis. Microsc Microanal 2003;9(Suppl 2):1290–1291.
200. Reyes-Gasga J, Alcantara-Rodriguez CM. Structural analysis of the human tooth enamel by transmission electron microscopy. In: Brown PW, Constantz B, editors. Hydroxyapatite and Related Materials. Boca Raton, FL: CRC Press; 1994. pp 295–304.
201. Brown WE, Mathew M, Chow LC. Roles of OCP in surface chemistry of apatites. In: Dwarika Misra N, editor. Adsorption on and Surface Chemistry of Apatites. Berlin: Springer; 1984.
202. Chaari K, Baklouti S, Bouaziz J, Bouzouita K. Optimizing the dispersion of a fluoroapatite suspension using penta sodium triphosphate. Ann Chimie Sci Materiaux 2004;29:1–13.
203. Yin G, Liu Z, Zhan J, Ding F, Yuan N. Impacts of the surface charge property on protein adsorption on hydroxyapatite. Chem Eng J 2002;87:181–186.
204. Smith IO, Baumann MJ, McCabe LR. Electrostatic interactions as a predictor for osteoblast attachment to biomaterials. J Biomed Mater Res A 2004;70:436–441.
205. Feenstra TP, de Bruyn PL. The Ostwald rule of stages in precipitation from highly supersaturated solutions: A model and its application to the formation of the nonstoichiometric amorphous calcium phosphate precursor phase. J Colloid Interface Sci 1981; 84:66–72.
206. Boskey AL, Posner AS. Conversion of amorphous calcium phosphate to microcrystalline hydroxyapatite. A pH-dependent, solution-mediated, solid-solid conversion. J Phys Chem 1973;77: 2313–2317.
207. Martin RI, Brown PW. Aqueous formation of hydroxyapatite. J Biomed Mater Res 1997;35:299–308.
208. Meier W. Nanostructure synthesis using surfactants and copolymers. Curr Opin Colloid Interface Sci 1999;4:6–14.
209. Greish YE, Brown PW. Phase evolution during the formation of stoichiometric hydroxyapatite at 37.4°C. J Biomed Mater Res B: Appl Biomater B 2003;67:632–637.
210. tenHuisen KS, Brown PW. Variations in solution chemistry during calcium-deficient and stoichiometric hydroxyapatite formation from $CaHPO_4 \times 2H_2O$ and $Ca_4(PO_4)_2O$. J Biomed Mater Res 1997;36:233–241.
211. Uskoković V, Drofenik M. Synthesis of nanocrystalline nickel-zinc ferrites via a microemulsion route. Mater Sci Forum 2004; 453–454:225–230.
212. Uskoković V, Drofenik M. A mechanism for the formation of nanostructured nizn ferrites via a microemulsion-assisted precipitation method. Colloids Surf A: Physicochem Eng Aspects 2005; 266:168–174.
213. Robbins H. The preparation of Mn-Zn ferrites by co-precipitation. In: Watanabe H, Iida S, Sugimoto M, editors. Proceedings of the 3rd International Conference on Ferrites. Tokyo: Reidel; 1982. pp 7–10.
214. Grier DG. When like-charges attract: Interactions and dynamics in charge-stabilized colloidal suspensions. J Phys Condens Matter 2000;12:A85–A94.
215. Grier DG. Colloids: A surprisingly attractive couple. Nature 1998; 393:621.
216. Kunz W, Lo Nostro P, Ninham BW. The present state of affairs with Hofmeister effects. Curr Opin Colloid Interface Sci 2004;9: 1–18.
217. Edwards SA, Williams DRM. Hofmeister effects in colloid science and biology explained by dispersion forces: Analytic results for the double layer interaction. Curr Opin Colloid Interface Sci 2004;9:139–144.
218. Ninham B. Self-Assembly—Some Thoughts, In: Robinson BH, editor. Self-Assembly. Amsterdam: IOS Press; 2003.
219. Cölfen H, Mann S. Higher-order organization by mesoscale self-assembly and transformation of hybrid nanostructures. Angew Chem Int Ed Engl 2003;42:2350–2365.
220. Uskoković V. Trends in Practical Colloid Science. Hauppauge, NY: Nova Science Publishers; 2009.
221. De Aza PN, Guitian F, Merlos A, Lora-Tamayo E, De Aza S. Bioceramics—Simulated body fluid interfaces: pH and its influence of hydroxypatite formation. J Mater Sci: Mater Med 1996;7:399–402.
222. Canham LT, Reeves CL, Loni A, Houlton MR, Newey JP, Simons AJ, Cox TI. Calcium phosphate nucleation on porous silicon: Factors influencing kinetics in acellular simulated body fluids. Thin Solid Films 1997;297:304–307.
223. Kokubo T, Takadama H. How useful is SBF in predicting in vivo bone bioactivity? Biomaterials 2006;27:2907–2915.
224. Melikhov IV, Lazić S, Vuković Ž. The effect of dissolved impurity on calcium phosphate nucleation in supersaturated medium. J Colloid Interface Sci 1989;127:317–327.
225. Budz JA, LoRe M, Nancollas GH. Hydroxyapatite and carbonated apatite as models for the dissolution behavior of human dental enamel. Adv Dental Res 1987;1:314–321.
226. Wang L, Guan X, Du C, Moradian-Oldak J, Nancollas GH. Amelogenin promotes the formation of elongated apatite microstructures in a controlled crystallization system, J Phys Chem C 2007; 111:6398–6404.
227. Tarasevich BJ, Howard CJ, Larson JL, Snead ML, Simmer JP, Paine M, Shaw WJ. The nucleation and growth of calcium phosphate by amelogenin. J Crystal Growth 2007;304:407–415.
228. Wu W, Nancollas GH. Kinetics of nucleation and crystal growth of hydroxyapatite and fluoroapatite on titanium oxide surfaces. Colloids Surf B: Biointerfaces 1997;10:87–94.
229. Koutsopoulos S, Dalas E. Hydroxyapatite crystallization in the presence of serine, tyrosine and hydroxyproline amino acids with polar side groups. J Crystal Growth 2000;216:443–449.
230. Wagner RS, Ellis WC. Vapor-liquid-solid mechanism of single crystal growth. Appl Phys Lett 1964;4:89–90.
231. Sivakov VA, Scholz R, Syrowatka F, Falk F, Gosele U, Christiansen SH. Silicon nanowire oxidation: The influence of sidewall structure and gold distribution. Nanotechnology 2009;20(40):5607.
232. Zhang JW, Nancollas GH. Mechanisms of growth and dissolution of sparingly soluble salts. In: Hochella MF, Jr., White AF, editors. Mineral-Water Interface Geochemistry, Reviews in Mineralogy, 1990; Vol.23, Washington D.C.: Mineralogical Society of America. pp 365–396.
233. Moradian-Oldak J. Amelogenins: Assembly, processing and control of crystal morphology. Matrix Biol 2001;20:293–305.
234. De Yoreo JJ, Vekilov PG. Principles of crystal nucleation and growth. Rev Mineral Geochem 2003;54:57–93.
235. Uskoković V. Isn't self-assembly a misnomer? Multi-disciplinary arguments in favor of co-assembly. Adv Colloid Interface Sci 2008;141:37–47.
236. Mutaftschiev B. The Atomistic Nature of Crystal Growth. Berlin: Springer; 2001.
237. A Saenz, Montero ML, Mondragon G, Rodriguez-Lugo V, Castano VM. Effect of pH on the precipitation of hydroxyapatite on silica gels. Mater Res Innovation 2003;7:68–73.
238. Hayakawa S, Li Y, Tsuru K, Osaka A, Fujii E, Kawabata K. Preparation of nanometer-scale rod array of hydroxyapatite crystal. Acta Biomater 2009;5:2152–2160.
239. Tomoda K, Ariizumi H, Nakaji T, Makino K. Hydroxyapatite particles as drug carriers for proteins. Colloids Surf B: Biointerfaces 2010;76:226–235.
240. Koutsopoulos S. Synthesis and characterization of hydroxyapatite crystals: A review study on the analytical methods. Int J Biomed Mater Res 2002;62:600–612.

241. Barth A, Zscherp C. What vibrations tell us about proteins. Quart Rev Biophys 2002;35:369–430.
242. Tsuda H, Arends J. Raman spectra of human dental calculus. J Dental Res 1993;72:1609–1613.
243. Tsuda H, Arends J. Raman spectroscopy in dental research: A short review of recent studies. Adv Dental Res 1997;11: 539–547.
244. Penel G, Leroy G, Rey C, Bres E. Micro Raman spectral study of the PO_4 and CO_3 vibrational modes in synthetic and biological apatites. Calcif Tissue Int 1998;63:475–481.
245. Awonusi A, Morris DM, Tecklenburg MJ. Carbonate assignment and calibration in the Raman spectrum of apatite. Calcif Tissue Int 2007;81:46–52.
246. Gibson IR, Bonfield W. Novel synthesis and characterization of an AB-type carbonate-substituted hydroxyapatite. J Biomed Mater Res 2002;59:697–708.
247. LeGeros RZ, Trautz OR, Klein E, LeGeros JP. Two types of carbonate substitution in the apatite structure. Experimentia 1969; 25:5–7.
248. Rey C, Renugopalakrishnan V, Collins B, Glimcher MV. Fourier transform infrared spectroscopic study of the carbonate ions in bone mineral during aging. Calcif Tissue Int 1991:49;251–258.
249. Wopenka B, Pasteris JD. A mineralogical perspective on the apatite in bone. Mater Sci Eng C 2005;25:131–143.
250. Schroder E, Jonsson T, Poole L. Hydroxyapatite chromatography: Altering the phosphate-dependent elution profile of protein as a function of pH. Anal Biochem 2003;313:176–178.
251. Giovannini R, Freitag R. Comparison of different types of ceramic hydroxyapatite for the chromatographic separation of plasmid DNA and a recombinant anti-rhesus D antibody. Bioseparation 2000;9:359–368.
252. Fujii S, Okada M, Furuzono T. Hydroxyapatite nanoparticles as stimulus-responsive particulate emulsifiers and building block for porous materials. J Colloid Interface Sci 2007;315: 287–296.
253. Phandugath C. Casein micelle structure: A concise review. Songklanakarin J Sci Technol 2005;27:201–212.
254. Sas L, Tang C, Rengel Z. Suitability of hydroxyapatite and iron phosphate as P sources for Lupinus albus grown in nutrient solution. Plant Soil 2001;235:159–166.
255. Reichert J, Binner JGP. An evaluation of hydroxyapatite-based filters for removal of heavy metal ions from aqueous solutions. J Mater Sci 2004;31:1231–1241.
256. Uskoković V. Nanotechnologies: What we do not know. Technol Soc 2007;29:43–61.
257. Yang L, Sheldon BW, Webber TJ. Nanophase ceramics for improved drug delivery. Am Ceram Soc Bull 2010;89:24–31.
258. Duncan R. Nanomedicine gets clinical. Materials Today 2005;8 (Suppl1):16–17.
259. Bawa R. Nanoparticles-based therapeutics in humans. Nanotechnol Law Business 2008;5:135–155.
260. Caruthers SD, Wickline SA, Lanza GM. Nanotechnological applications in medicine. Curr Opin Biotechnol 2007;18:26–30.
261. Zhang J-Y, Shen Z-G, Zhong J, Hu T-T, Chen J-F, Ma Z-Q, Yun J. Preparation of amorphous cefuroxime axetil nanoparticles by controlled nanoprecipitation method without surfactants. Int J Pharm 2006;323:153–160.
262. Branco MC, Schneider JP. Self-assembling materials for therapeutic delivery. Acta Biomater 2009;5:817–831.
263. Korenstein R. Targeted drug delivery by nanoparticles and theranostics, Presentation retrieved from www.tyndall.ie/n2l/SRPA%20on%20targeted%20drug%20delivery%20and%20 theranostics%20Cork%20Meeting; 2009.
264. Bisht S, Bhakta G, Mitra S, Maitra A. DNA loaded calcium phosphate nanoparticles: Highly efficient non-viral vector for gene delivery. Int J Pharm 2005;288:157–168.
265. Zhang M, Kataoka K. Nano-structured composites based on calcium phosphate for cellular delivery of therapeutic and diagnostic agents. Nano Today 2009;4:508–517.
266. Epple M, Ganesan K, Heumann R, Klesing J, Kovtun A, Neumann S, Sokolova V. Application of calcium phosphate nanoparticles in biomedicine. J Mater Chem 2010;20:18–23.
267. Wiethoff CM, Middaugh CR. Barriers to nonviral gene delivery. J Pharm Sci 2003;92:203–217.
268. Roszek B, de Jong WH, Geertsma RE. Nanotechnology in medical applications: State-of-the-art in materials and devices. RIVM Report 265001001; 2005.
269. Zhang Q, Zhao D, Zhang X-Z, Cheng S-X, Zhuo R-X. Calcium phosphate/DNA co-precipitates encapsulated fast-degrading polymer films for substrate-mediated gene delivery. Int J Biomed Mater Res Part B: Appl Biomater B 2009;91:172–180.
270. Watson A, Latchman D. Gene delivery into neuronal cells by calcium phosphate-mediated transfection. Methods 1996;10:289–291.
271. Chowdhury EH, Akaike T. Fibronectin-coated nano-precipitates of calcium-magnesium phosphate for integrin-targeted gene delivery. J Control Release 2006;116:e68–e69.
272. Okazaki M, Yoshida Y, Yamaguchi S, Kaneno M, Elliott JC. Affinity binding phenomena of DNA onto apatite crystals. Biomaterials 2001;22:2459–2464.
273. Olton D, Li J, Wilson ME, Rogers T, Close J, Huang L, Kumta PN, Sfeir C. Nanostructured calcium phosphates (NanoCaPs) for non-viral gene delivery: Influence of the synthesis parameters on transfection efficiency. Biomaterials 2007;28:1267–1279.
274. Faraji AH, Wipf P. Nanoparticles in cellular drug delivery. Bioorg Med Chem 2009;17:2950–2963.
275. Kester M, Heakal Y, Fox T, Sharma A, Robertson GP, Morgan TT, Altinoglu EI, Tabakovic A, Parette MR, Rouse SM, Ruiz-Velasco V, Adair JH. Calcium phosphate nanocomposite particles for in vitro imaging and encapsulated chemotherapeutic drug delivery to cancer cells. Nano Lett 2008;8:4116–4121.
276. Singh N, Manshian B, Jenkins GJS, Griffiths SM, Williams PM, Maffeis TGG, Wright CJ, Doak SH. NanoGenotoxicology: The DNA damaging potential of engineered nanomaterials. Biomaterials 2009;30:3891–3914.
277. Cölfen H, Mann S. Higher-order organization by mesoscale self-assembly and transformation of hybrid nanostructures. Angew Chemie Int Ed: Engl 2003;42:2350–2365.
278. Dorozhkin SV. A hierarchical structure for apatite crystals. J Mater Sci: Mater Med 2007;18:363–366.
279. Lim GK, Wang J, Ng SC, Gan LM. Processing of fine hydroxyapatite powders via an inverse microemulsion route. Mater Lett 1996;28:431–436.
280. Ball V, Planeix J-M, Flix O, Hemmerl J, Schaaf P, Hosseini MW, Voegel JC. Molecular tectonics: Abiotic control of hydroxyapatite crystals morphology. Crystal Growth Design 2002;2:489–492.
281. Jevtić M, Mitrić M, Škapin S, Jančar B, Ignjatović N, Uskoković D. Crystal structure of hydroxyapatite nano-rods synthesized by sonochemical homogenous precipitation. Crystal Growth Design 2008;8:2217–2222.
282. Fowler CE, Li M, Mann S, Margolis HC. Influence of surfactant assembly on the formation of calcium phosphate materials-A model for dental enamel formation. J Mater Chem 2005;15: 3317–3325.
283. Wang P, Li C, Gong H, Jiang X, Wang H, Li K. Effects of synthesis conditions on the morphology of hydroxyapatite nanoparticles produced by wet chemical process. Powder Technol 2010; 203:315–321.
284. Uskoković V. Insights into morphological nature of precipitation of cholesterol. Steroids 2008;73:356–369.
285. Fischer EK, Aleman BJ, Tao SL, Hugh Daniels R, Li EM, Bunger MD, Nagaraj G, Singh P, Zettl A, Desai TA. Biomimetic nanowire coatings for next generation adhesive drug delivery systems. Nano Lett 2009;9:716–720.
286. Ducheyne P, Radin S, King L. The effect of calcium phosphate ceramic composition and structure on in vitro behavior. I. Dissolution. J Biomed Mater Res 1993;27:25–34.
287. Yamada S, Heymann D, Bouler JM, Daculsi G. OSteoclastic resorption of calcium phosphate ceramic with different hydroxyapatite/β-tricalcium phosphate ratios. Biomaterials 1997;18: 1037–1041.
288. Melville AJ, Rodriguez-Lorenzo LM, Forsythe JS. Effects of calcination temperature on the drug delivery behaviour of ibuprofen from hydroxyapatite powders. J Mater Sci: Mater Med 2008;19: 1187–1195.
289. Raynaud S, Champion E, Bernache-Assollant D. Characterization of hydroxyapatite-tricalcium phosphate bioceramics issued from Ca-deficient hydroxyapatite powders: Influence of Ca/P ratio. Phosphorus Res Bull 1999;10:214–218.

290. Raynaud S, Champion E, Bernache-Assollant D, Thomas P. Calcium phosphate apatites with variable Ca/P atomic ratio I. Synthesis, characterisation and thermal stability of powders. Biomaterials 2002;23:1065–1072.
291. Gamble W. Atherosclerosis: The carbonic anhydrase, carbon dioxide, calcium concerted theory. J Theor Biol 2006;239: 16–21.
292. Uskoković V. Surface charge effects involved in the control of stability of sols comprising uniform cholesterol particles. Mater Manuf Process 2008;23:620–623.
293. Craven BM. Crystal structure of cholesterol monohydrate. Nature 1976;260:727–729.
294. Dorozhkin SV, Epple M. Biological and medical significance of calcium phosphates. Angew Chem Int Ed 2002;41:3130–3146.
295. Sumer B, Gao J. Theranostic nanomedicine for cancer. Nanomedicine 2008;3:137–140.
296. Boccaccini AR, Blaker JJ. Bioactive composite materials for tissue Engineering Scaffolds. Expert Rev Med Dev 2005;2: 303–317.
297. Wahl DA, Sachlos E, Liu C, Czernuszka JT. Controlling the processing of collagen-hydroxyapatite scaffolds for bone tissue engineering. J Mater Sci: Mater Med 2007;18:201–209.
298. Best S. Nanostructured Apatites: The Next Generation of Bioactive Materials, Presented at the 10th YUCOMAT Conference in Herceg-Novi, Montenegro (2008).
299. Yan W-Q, Nakamura T, Kobayashi M, Kim H-M, Miyaji F, Kokubo T. Bonding of chemically treated titanium implants to bone. J Biomed Mater Res A 1998;37:267–275.
300. Cui F-Z, Jiang T-F. Tissue-Engineered Bone. In: Wiley Encyclopedia of Biomedical Engineering. New York, NY: Wiley; 2009.
301. Best SM, Porter AE, Thian ES, Huang J. Bioceramics: Past, present and for the future. J Eur Ceram Soc 2008;28:1319–1327.
302. Ignjatović N, Liu C, Czernuszka J, Uskoković D. Micro and nano/injectable composite biomaterials containing calcium phosphate coated with poly(dl-lactide-*co*-glycolide). Acta Biomater 2007;3: 927–935.
303. Daculsi G, Uzel AP, Weiss P, Goyenvalle E, Aguado E. Developments in injectable multiphasic biomaterials. The performance of microporous biphasic calcium phosphate granules and hydrogels. J Mater Sci: Mater Med 2010;21:855–861.
304. Doty H, Haggard W, Courtney H, Bumgardner J. Effectiveness of a dual drug delivery calcium sulfate, chitosan-calcium phosphate bone scaffold, Society for Biomaterials 2010 Annual Meeting & Exposition, Seattle, WA; 2010, presentation #677.
305. Combes C, Rey C. Amorphous calcium phosphates: synthesis, properties and uses in biomaterials. Acta Biomater 2010;6: 3362–3378.
306. Huang J, Lin YW, Fu XW, Best SM, Brooks RA, Rushton N, Bonfield W. Development of nano-sized hydroxyapatite reinforced composites for tissue engineering scaffolds. J Mater Sci: Mater Med 2007;18:2151–2157.
307. Zheng X, Zhou S, Xiao Y, Yu X, Feng B. In situ preparation and characterization of a novel gelatin/poly(D, L-Lactide)/hydroxyapatite nanocomposite. J Biomed Mater Res Part B: Appl Biomater B 2009;91:181–190.
308. Ignjatović N, Tomić S, Dakić M, Miljković M, Plavšić M, Uskoković D. Synthesis and properties of hydroxyapatite/poly-L-lactide composite biomaterials. Biomaterials 1999;20:809–816.
309. Ignjatović N, Ninkov P, Kojić V, Bokurov M, Srdić V, Krnojelac D, Selaković S, Uskoković D. Cytotoxicity and fibroblast properties during in vitro test of biphasic calcium phosphate/poly-dl-lactide-*co*-glycolide biocomposites and different phosphate materials. Microsc Res Tech 2006;69:976–982.
310. Vukomanović M, Mitrić M, Šapin SD, Žagar E, Plavec J, Ignjatović N, Uskoković D. Influence of ultrasonic processing on the macromolecular properties of poly (D,L-lactide -*co*-glycolide) alone and in its biocomposite with hydroxyapatite. Ultrasonics Sono Chem 2010;17:902–908.
311. Stevanović M, Maksin T, Petković J, Filipič M, Uskoković D. An innovative, quick and convenient labeling method for the investigation of pharmacological behavior and the metabolism of poly(DL-lactide-*co*-glycolide) nanospheres. Nanotechnology 2009; 20:335102.
312. Uskoković V, Ignjatović N, Petranović N. Synthesis and characterization of hydroxyapatite-collagen biocomposite materials. Mater Sci Forum 2003;413:269–274.
313. Kretlow JD, Young S, Klouda L, Wong M, Mikos AG. Injectable biomaterials for regenerating complex craniofacial tissues. Adv Mater 2009;21:1–26.
314. Miyai T, Ito A, Tamazawa G, Matsuno T, Sogo Y, Nakamura C, Yamazaki A, Satoh T. Antibiotic-loaded poly-e-caprolactone and porous b-tricalcium phosphate composite for treating osteomyelitis. Biomaterials 2008;29:350–358.
315. Martins VCA, Goissis G, Ribeiro AC, Marcantonio E, Jr., Bet MR. The controlled release of antibiotic by hydroxyapatite: Anionic collagen composites. Artif Organs 1998;22: 215–221.
316. Rauchmann MA, Wichelhaus TA, Stirnal V, Dingeldein E, Zichner L, Schnettler R, Alt V. Nanocrystalline hydroxyapatite and calcium sulphate as biodegradable composite carrier material for local delivery of antibiotics in bone infections. Biomaterials 2005;26:2677–2684.
317. El-Kamel A, Baddour M. Gatifloxacin biodegradable implant for treatment of experimental osteomyelitis: In vitro and in vivo evaluation. Drug Deliv 2007;14:349–356.
318. Ignjatović NL, Ninkov P, Sabetrasekh R, Uskoković DP. A novel nano drug delivery system based on tigecycline-loaded calcium phosphate coated with poly-DL-lactide-*co*-glycolide. J Mater Sci: Mater Med 2010;21:231–239.
319. Hylands J. Tigecycline: A new antibiotic. Intensive Critic Care Nurs 2008;24:260–263.
320. Nandi SK, Kundu B, Ghosh SK, Mandal TK, Datta S, De DK, Basu D. Cefuroxime-impregnated calcium phosphates as an implantable delivery system in experimental osteomyelitis. Ceram Int 2009;35:1367–1376.
321. Xu QG, Czernuszka JI. Controlled release of amoxicillin from hydroxyapatite-coated poly(lactic-*co*-glycolic acid) microspheres. J Control Release 2008;127:146–153.
322. Xu QG, Tanaka Y, Czernuszka JT. Encapsulation and release of a hydrophobic drug from hydroxyapatite coated liposomes. Biomaterials 2007;28:2687–2694.
323. Victor SP, Kumar TSS. Tailoring calcium-deficient hydroxyapatite nanocarriers for enhanced release of antibiotics. J Biomed Nanotechnol 2008;4:203–209.
324. Stevanović M, Radulović A, Jordović B, Uskoković D. Poly(DL-lactide-*co*-glycolide) nanospheres for the sustained release of folic acid. J Biomed Nanotechnol 2008;4:349–358.
325. Stevanović MM, Jordović B, Uskoković DP. Preparation and characterization of poly(D,L-lactide-*co*-glycolide) microparticles containing ascorbic acid. J BioMed Biotechnol 2007:1–9. Article ID 84965;2007.
326. Stevanović M, Savić J, Jordović B, Uskoković D. Fabrication, in vitro degradation and the release behaviours of poly(DL-lactide-*co*-glycolide) nanospheres containing ascorbic acid. Colloids Surf B: Biointerfaces 2007;59:215–223.
327. Stevanović M, Uskoković D. Influence of different degradation medium on release of ascorbic acid from poly(D,L-lactide-*co*-glycolide) nano- and microspheres. Russian J Phys Chem A 2009; 83:1457–1460.
328. Nehilla BJ, Bergkvist M, Popat KC, Desai TA. Purified and surfactant-free coenzyme Q10-loaded biodegradable nanoparticles. Int J Pharm 2008;348:107–114.
329. Schmidt HT, Gray BL, Wingert PA, Ostafin AE. Assembly of aqueous-cored calcium phosphate nanoparticles for drug delivery. Chem Mater 16:4942–4947.
330. Ma MY, Zhu YJ, Li L, Cao SW. Nanostructured porous hollow ellipsoidal capsules of hydroxyapatite and calcium silicate: Preparation and aplication in drug delivery. J Mater Chem 2008;18: 2722–2727.
331. Akasha AA, Sotiriadou I, Doss MX, Halbach M, Winkler J, Baunach JJS, Katsen-Glob A, Zimmermann H, Chood Y, Hescheler J, Sachinidis A. Entrapment of embryonic stem cells-derived cardiomyocytes in macroporous biodegradable microspheres: Preparation and characterization. Cell Physiol Biochem 2008;22:665–672.
332. Tielens S, Declercq H, Gorski T, Lippens E, Schacht E, Cornelissen M. Gelatin-based microcarriers as embryonic stem cell

delivery system in bone tissue engineering: An in-vitro study. Biomacromolecules 2007;8:825–832.
333. Ashton RS, Banerjee A, Punyani S, Schaffer DV, Kane RS. Scaffolds based on degradable alginate hydrogels and poly(lactide-*co*-glycolide) microspheres for stem cell culture. Biomaterials 2007;28:5518–5525.
334. Liao S, Chan CK, Ramakrishna S. Stem cells and biomimetic materials strategies for tissue engineering. Mater Sci Eng C 2008;28:1189–1202.
335. Yanga Y, Rossib FMV, Putninsa EE. Ex vivo expansion of rat bone marrow mesenchymal stromal cells on microcarrier beads in spin culture. Biomaterials 2007;28:3110–3120.
336. Matsusaki M, Kadowaki K, Tateishi K, Higuchi C, Ando W, Hart DA, Tanaka Y, Take Y, Akashi M, Yoshikawa H, Nakamura N. Scaffold-free tissue-engineered construct-hydroxyapatite composites generated by an alternate soaking process: Potential for repair of bone defects. Tissue Eng A 2009;15:55–63.
337. Gonzales-McQuire R, Chane-Ching J-Y, Vignaud E, Lebugle A, Mann S. Synthesis and characterization of amino acid-functionalized hydroxyapatite nanorods. J Mater Chem 2004;14: 2277–2281.
338. Wormuth K. Superparamagnetic latex via inverse emulsion polymerization. J Colloid Interface Sci 2001;241:366–377.
339. El-Backly RM, Massoud AG, El-Badry AM, Sherif RA, Marei MK. Regeneration of dentine/pulp-like tissue using a dental pulp stem cell/poly(lactic-*co*-glycolic) acid scaffold construct in New Zealand white rabbits. Australian Endodontic J 2008;34: 52–67.
340. Chevalier J, Gremillard L. Ceramics for medical applications: A picture for the next 20 years. J Eur Ceram Soc 2009;29: 1245–1255.
341. Kokubo T, Matsushita T, Takadama H, Kizuki T. Development of bioactive materials based on surface chemistry. J Eur Ceram Soc 2009;29:1245–1255.
342. Teller M, Gopp U, Neumann HG, Kuhn KD. Release of gentamicin from bone regenerative materials: An in vitro study. J Biomed Mater Res Part B: Appl Biomater B 2007;81:23–29.
343. Grasset F, Labhsetwar N, Li D, Park DC, Saito N, Haneda H, Cador O, Roisnel T, Mornet S, Duguet E, Portier J, Etourneau J. Synthesis and magnetic characterization of zinc ferrite nanoparticles with different environments: Powder, colloidal solution, and zinc ferrite-silica core-shell nanoparticles. Langmuir 2002;18: 8209–8216.
344. Tago T, Hatsuta T, Miyajima K, Kishida M, Tashiro S, Wakabayashi K. Novel synthesis of silica-coated ferrite nanoparticles prepared using water-in-oil microemulsion. J Am Ceram Soc 2002; 85:2188–2194.
345. Arriagada FJ, Osseo-Asare K. Controlled hydrolysis of tetraethoxysilane in a nonionic water-in-oil microemulsion: A statistical model of silica nucleation. Colloids Surf A: Physicochem Eng Aspects 1999;154:311–326.
346. Uskoković V, Košak A, Drofenik M. Silica-coated lanthanum-strontium manganites for hyperthermia treatments. Mater Lett 2006;60:2620–2622.
347. V. Uskoković, Matijević E. Uniform particles of pure and silica coated cholesterol. J Colloid Interface Sci 2007;315:500–511.
348. Park K, Lee S, Kang E, Kim K, Choi K, Kwon IC. New generation of multifunctional nanoparticles for cancer imaging and therapy. Adv Funct Mater 2009;19:1–14.
349. Jongpaiboonkit L, Franklin-Ford T, Murphy WL. Mineral-coated polymer microspheres for controlled protein binding and release. Adv Mater 2009;21:1–4.
350. Vukomanović M, Škapin S, Jančar B, Maksin T, Ignjatović N, Uskoković V, Uskoković D. Poly(d,l-lactide-*co*-glycolide)/hydroxyapatite core-shell nanospheres. Part 1: A multifunctional system for controlled drug delivery. Colloids Surf B: Biointerfaces. Forthcoming.
351. Fischer S, Foerg C, Merkle HP, Gander B. Chitosan coated PLGA-microspheres—A modular system for targeted drug delivery. Euro Cells Mater 2004;7(Suppl 2):11–12.
352. Stevanović MM, Uskoković DP. Poly(lactide-*co*-glycolide)-based micro and nanoparticles for the controlled drug delivery of vitamins. Curr Nanosci 2009;5:1–14.
353. Ong HT, Loo JSC, F. Boey YC, Russell SJ, Ma J, Peng KW. Exploiting the high-affinity phosphonate-hydroxyapatite nanoparticle interaction for delivery of radiation and drugs. J Nanoparticle Res 2008;10:141–150.
354. Morgan TT, Muddana HS, Altinoglu EI, Rouse SM, Tabakovic A, Tabouillot T, Russin TJ, Shanmugavelandy SS, Butler PJ, Eklund PC, Yun JK, Kester M, Adair JH. Encapsulation of organic molecules in calcium phosphate nanocomposite particles for intracellular imaging and drug delivery. Nano Lett 2008;8:4108–4115.
355. Yang PP, Quan ZW, Li CX, Kang XJ, Lian HZ, Lin J. Bioactive, luminescent and mesoporous europium-doped hydroxyapatite as a drug carrier. Biomaterials 2008;29:4341–4347.
356. Graeve OA, Kanakala R, Madadi A, Williams BC, Glass KC. Luminescence variations in hydroxyapatites doped with Eu^{2+} and Eu^{3+} ions. Biomaterials 2010;31:4259–4267.
357. Mondejar SP, Kovtun A, Epple M. Lanthanide-doped calcium phosphate nanoparticles with high internal crystallinity and with a shell of DNA as fluorescent probes in cell experiments. J Mater Chem 2007;17:4153–4159.
358. Doat A, Fanjul M, Pelle F, Hollande E, Lebugle A. Europium-doped bioapatite: A new photostable biological probe, internalizable by human cells. Biomaterials 2003;24:3365–3371.
359. Kovtun A, Heumann R, Epple M. Calcium phosphate nanoparticles for the transfection of cells. J Biomed Eng Mater 2009;19: 241–247.
360. Nehilla BJ, Allen PG, Desai TA. Surfactant-free, drug-quantum-dot coloaded poly(lactide-*co*-glycolide) nanoparticles: Towards multifunctional nanoparticles. ACS Nano 2008;2:528–544.
361. Guo Y, Shi DL, Lian J, Dong ZY, Wang W, Cho HS, Liu GK, Wang LM, Ewing RC. Quantum dot conjugated hydroxylapatite nanoparticles for in vivo imaging. Nanotechnology 2008;19: 175102.
362. Sokolova V, Kovtun A, Heumann R, Epple M. Tracking the pathway of calcium phosphate/DNA nanoparticles during cell transfection by incorporation of red-fluorescing tetramethylrhodamine isothiocyanate-bovine serum albumin into these nanoparticles. J Biol Inorg Chem 2007;12:174–179.
363. LeGeros RZ. Biological and synthetic apatites. In: Brown PW, Constantz B, editors. Hydroxyapatite and Related Materials. Boca Raton, FL: CRC Press; 1994. pp 3–28.
364. Banerjee SS, Tarafder MS, Bandyaopadhyay A, Bose S. Tricalcium Phosphate Based Resorbable Ceramics: Influence of MgO and SrO Addition on Mechanical Properties and Biocompatibility, Society for Biomaterials 2010 Annual Meeting & Exposition, Seattle, WA; 2010, presentation #435.
365. Bohner M. Silicon-substituted calcium phosphates—A critical view. Biomaterials 2009;30:6403–6406.
366. Xynos ID, Edgar AJ, Buttery LDK, Hench LL, Polak JM. Gene-expression profiling of human osteoblasts following treatment with the ionic products of Bioglass (R) 45S5 dissolution. J Biomed Mater Res 2001;55:151–157.
367. Hench LL. Genetic design of bioactive glasses. J Eur Ceram Soc 2009;29:1257–1265.
368. Hench LL, Polak JM. Third-generation biomedical materials. Science 2002;295:1014–1017.
369. Veselinović Lj, Karanović Lj, Stojanović Z, Bračko I, Marković S, Ignjatović N, Uskoković D. Crystal structure of cobalt-substituted calcium hydroxyapatite nanopowders prepared by hydrothermal processing. J Appl Crystallogr 2010;43:320–327.
370. Stojanović Z, Veselinović Lj, Marković S, Ignjatović N, Uskoković D. Hydrothermal synthesis of nanosize pure and cobalt-exchanged hydroxyapatite. Mater Manuf Process 2009;24: 1096–1103.
371. Wu H-C, Wang T-W, Sun J-S, Wang W-H, Lin F-H. A novel biomagnetic nanoparticle based on hydroxyapatite. Nanotechnology 2007;18:165601–165610.
372. Low HR, Phonthammachai N, Maignan A, Stewart GA, Bastow TJ, Ma LL, White TJ. The crystal chemistry of ferric oxyhydroxyapatite. Inorg Chem 2008;47:11774–11782.
373. Liu X, Kaminski MD, Chen H, Torno M, Taylor L, Rosengart AJ. Synthesis and characterization of highly-magnetic biodegradable poly(D,L-lactide-*co*-glycolide) nanospheres. J Control Release 2007;119:52–58.

374. Tarafder MS, Bandyopadhyay A, Bose S. Osteoblast Interactions on Electrically Polarized Biphasic Calcium Phosphate, Society for Biomaterials 2010 Annual Meeting & Exposition, Seattle, WA; 2010, presentation #234.
375. Bock N, Riminucci A, Dionigi C, Russo A, Tampieri A, Landi E, Goranov VA. A novel route in bone tissue engineering: Magnetic biomimetic scaffolds. Acta Biomater 2010;6:786–796.
376. Misono M, Hall WK. Oxidation-reduction properties of copper- and nickel-substituted hydroxyapatites. J Phys Chem 1973;77: 791–800.
377. Wakamura M, Kandori K, Ishikawa T. Surface structure and composition of calcium hydroxyapatites substituted with Al(III), La(III) and Fe(III) ions. Colloids Surf A 2000;164:297–305.
378. Uskoković V, Košak A, Drofenik M. Preparation of silica-coated lanthanum-strontium manganite particles with designable curie point, for application in hyperthermia treatments. Int J Appl Ceram Technol 2006;3:134–143.
379. Hou C-H, Hou S-M, Hsueh Y-S, Lin J, Wu H-C, Lin F-H. The in vivo performance of biomagnetic hydroxyapatite nanoparticles in cancer hyperthermia therapy. Biomaterials 2009;30:3956–3960.
380. Uskoković V, Drofenik M, Ban I. The characterization of nanosized nickel-zinc ferrites synthesized within reverse micelles of CTAB/1-hexanol/water microemulsion. J Magn Magn Mater 2004;284:294–302.
381. Wu H-C, Wang T-W, Bohn MC, Lin F-H, Spector M. Novel magnetic hydroxyapatite nanoparticles as non-viral vectors for the glial cell line-derived neurotrophic factor gene. Adv Funct Mater 2010;20:67–77.
382. Chen H, Kaminski MD, Liu X, Mertz CJ, Xie Y, Torno MD, Rosengart AJ. A novel human detoxification system based on nanoscale bioengineering and magnetic separation techniques. Med Hypotheses 2007;68:1071–1079.
383. Silva GA. Nanotechnology approaches to crossing the blood-brain barrier and drug delivery to the CNS. BMC Neurosci 2008; 10(9)Suppl 3:S4:1–4.
384. Bawa R. NanoBiotech 2008: Exploring global advances in nanomedicine. Nanomedicine 2009;5:5–7.
385. Patel LN, Zaro JL, Shen WC. Cell penetrating peptides: Intracellular pathways and pharmaceutical perspectives. Pharm Res 2007; 24:1977–1992.
386. Gratton SE, Ropp PA, Pohlhaus PD, Luft JC, Madden VJ, Napier ME. The effect of particle design on cellular internalization pathways. Proc Nat Acad Sci USA 2008;105:11613–11618.
387. Chithrani BD, Chan WC. Elucidating the mechanism of cellular uptake and removal of protein-coated gold nanoparticles of different sizes and shapes. Nano Lett 2007;7:1542–1550.
388. Lubbe AS, Bergemann C, Brock J, McClure DG. Physiological aspects in magnetic drug-targeting. J Magn Magn Mater 1999: 194;149–155.
389. Pankhurst QA, Connolly J, Jones SK, Dobson J. Applications of magnetic nanoparticles in biomedicine. J Phys D 2003;36: R167–R181.
390. Mistry AS, Mikos AG. Tissue engineering strategies for bone regeneration. Adv Biochem Eng/Biotechnol 2005;94:1–22.
391. Harush-Frenkel O, Debotton N, Benita S, Altschuler Y. Targeting of nanoparticles to the clathrin-mediated endocytic pathway. Biochem Biophys Res Commun 2007;353:26–32.
392. Klesing J, Wiehe A, Gitter B, Grafe S, Epple M. Positively charged calcium phosphate/polymer nanoparticles fro photodynamic therapy. J Mater Sci: Mater Med 2010;21:887–892.
393. Mrksich M. Using self-assembled monolayers to model the extracellular matrix. Acta Biomater 2009;5:832–841.
394. Tang S, Jin A, Wang Y. Preparation of plastic nano-hydroxyapatite/poly (3-hydroyybutyrate-hydroxyvalerate)-polyethy lene glycol gentamicin drug delivery system. Zhongguo Xiu Fu Chong Jian Wai Ke Za Zhi 2006;20:758–761.
395. Ho ML, Fu YC, Wang GJ, Chen HT, Chang JK, Tsai TH, Wang CK. Controlled release carrier of BSA made by W/O/W emulsion method containing PLGA and hydroxyapatite. J Control Release 2008;128:142–148.
396. Wilson OC, Jr, Hull JR. Surface modification of nanophase hydroxyapatite with chitosan. Mater Sci Eng C 2008;28:434–437.
397. Zhou G, Li Y, Zhang L, Zuo Y, Jansen JA. Preparation and characterization of nano-hydroxyapatite/chitosan/konjac glucomannan composite. J Biomed Mater Res Part A 2007;83:931–939.
398. Tan ML, Choong PF, Dass CR. DNAzyme delivery systems: getting past first base. Expert Opin Drug Deliv 2009;6:127–138.
399. Dass CR, Choong PFM. The use of chitosan formulations in cancer therapy. J Microencapsul 2003;25:275–279.
400. Reves BT, Bumgardner JD, Cole JA, Yang Y, Haggard WO. Lyophilization to improve drug delivery for chitosan-calcium phosphate bone scaffold construct: A preliminary investigation. J Biomed Mater Res B 2009;90:1–10.
401. Adair J. Nano Delivery of Cancer Therapeutics & siRNA, Presentation retrieved from nanotechinstitute.org/wp-content/cornwall_-keystone-nano-10-25.ppt; 2009.
402. Mukesh U, Kulkarni V, Tushar R, Murthy RSR. Methotrexate loaded self stabilized calcium phosphate nanoparticles: A novel inorganic carrier for intracellular drug delivery. J Biomed Nanotechnol 2009;5:99–105.
403. Cheng X, Kuhn L. Chemotherapy drug delivery from calcium phosphate nanoparticles. Int J Nanomed 2007;2:667–674.
404. Oh J-M, Choi S-J, Lee G-E, Han S-H, Choy J-H. Inorganic drug-delivery nanovehicle conjugated with cancer-cell-specific ligand. Adv Funct Mater 2009;19:1–8.
405. Baba K, Pudavar HE, Roy I, Ohulchanskyy TY, Chen Y, Pandey RK, Prasad PN. New method for delivering a hydrophobic drug for photodynamic therapy using pure nanocrystal form of the drug. Mol Pharm 2007;4:289–297.
406. Koh AL, Shachaf CM, Elchuri S, Nolan GP, Sinclair R. Electron microscopy localization and characterization of functionalized composite organic-inorganic SERS nanoparticles on leukemia cells. Ultramicroscopy 2008;109:111–121.
407. Cheng S-H, Lee C-H, Yang C-S, Tseng F-G, Mou C-Y, Lo L-W. Mesoporous silica nanoparticles functionalized with an oxygen-sensing probe for cell photodynamic therapy: Potential cancer theranostics. J Mater Chem 2009;19:1252–1257.
408. Sokolova VV, Radtke I, Heumann R, Epple M. Effective transfection of cells with multi-shell calcium phosphate-DNA nanoparticles. Biomaterials 2006;27:3147–3153.
409. Mazin AL. Hydroxyapatite thin-layer chromatography of nucleic acid. Mol Biol 1977;11:477–498.
410. Gagnon P. Improved antibody aggregate removal by hydroxyapatite chromatography in the presence of polyethylene glycol. J Immunol Methods 2008;336:222–228.
411. Fargues C, Bailly M, Grevillot G. Adsorption of BSA and hemoglobin on hydroxyapatite support: Equilibria and multicomponent dynamic adsorption. Adsorption—J Int Adsorption Soc 1998;4:5–16.
412. Sokolova V, Epple M. Inorganic nanoparticles as carriers of nucleic acids into cells. Angew Chem Int Ed 2008;47:1382–1395.
413. Nguyen DN, Green JJ, Chan JM, Langer R, Anderson DG. Polymeric materials for gene delivery and DNA vaccination. Adv Mater 2009;21:847–867.
414. Graham FL, van der Eb AJ. A new technique for the assay of infectivity of human adenovirus 5 DNA. Virology 1973;63:456–467.
415. Dass CR, Choong PFM. The use of chitosan formulations in cancer therapy. J Microencapsul 2008;25:275–279.
416. Zhu S, Zhou K, Huang B, Huang S, Liu F, Li Y, Xue Z, Long Z. Hydroxyapatite nanoparticles: A novel material of gene carrier. Sheng Wu Yi Xue Gong Cheng Xue Za Zhi 2005;22:980–984.
417. Sokolova V, Prymak O, Meyer-Zaika W, Cölfen H, Rehage H, Shukla A, Epple M. Synthesis and characterization of DNA-functionalized calcium phosphate nanoparticles. Mat Werkstofftech 2006;37:441–445.
418. Schwiertz J, Meyer-Zaika W, Ruiz-Gonzalez L, Gonzalez-Calbet JM, Vallet-Regi M, Epple M. Calcium phosphate nanoparticles as templates for nanocapsules prepared by the layer-by-layer technique. J Mater Chem 2008;18:152.
419. Bai X, More K, Rouleau CM, Rabiei A. Functionally graded hydroxyapatite coatings doped with antibacterial components. Acta Biomater 2010;6:2264–2273.
420. Gopalakrishnan B, Wolff J. siRNA and DNA transfer to cultured cells. Methods Mol Biol 2009;480:31–52.

421. Zhang M, Ishii A, Nishiyama N, Matsumoto S, Ishii T, Yamasaki Y, Kataoka K. PEGylated Calcium Phosphate Nanocomposites as Smart Environment-Sensitive Carriers for siRNA Delivery. Adv Mater 2009;21:1–6.
422. Seferos DS, Prigodich AE, Giljohann DA, Patel PC, Mirkin CA. Polyvalent DNA nanoparticle conjugates stabilize nucleic acids. Nano Lett 2009;9:308–311.
423. Ren J, Zhao P, Ren T, Gu S, Pan K. Poly (D,L-lactide)/nano-hydroxyapatite composite scaffolds for bone tissue engineering and biocompatibility evaluation. J Mater Sci: Mater Med 2008; 19:1075–1082.
424. Wang M, Li Y, Wu J, Xu F, Zuo Y, Jansen JA. In vitro and in vivo study to the biocompatibility and biodegradation of hydroxyapatite/poly(vinyl alcohol)/gelatin composite. J Biomed Mater Part A 2008;85:418–426.
425. Najman S, Savić V, Djordjević Lj, Ignjatović N, Uskoković D. Biological evaluation of hydroxyapatite/poly-L-lactide (HAp/PLLA) composite biomaterials with poly-L-lactide of different molecular weights intraperitoneally implanted into mice. Biomed Mater Eng 2004;14:61–70.
426. Ignjatović N, Savić V, Najman S, Plavšić M, Uskoković D. Study of HAp/PLLA composite as a substitute for bone powder, using FT-IR spectroscopy. Biomaterials 2001;22:571–575.
427. Service RF. Nanomaterials show signs of toxicity. Science 2003; 300:243.
428. Oberdörster G, Oberdörster E, Oberdörster J. Nanotoxicology: An emerging discipline evolving from studies of ultrafine particles. Environ Health Perspect 2005;113:823–839.
429. Stellacci F. On the Role of Interfacial Energy in Bio-interfaces, Presentation at the Materials Research Society Conference, San Francisco, CA, April 2010.
430. Shi D, Cho HS, Chen Y, Xu H, Gu H, Lian J, Wang W, Liu H, Huth C, Wang L, Ewing RC, Budko S, Pauletti GM, Dong Z. Fluorescent polystyrene-Fe_3O_4 composite nanospheres for in vivo imaging and hyperthermia. Adv Mater 2009;21:1–4.
431. Lee J-H, Lee K, Moon SH, Lee Y, Park TG, Cheon J. All-in-one target-cell-specific magnetic nanoparticles for simultaneous molecular imaging and siRNA delivery. Angew Chem Int Ed: Engl 2009;48:4174–4179.
432. Ashokan A, Menon D, Nair S, Koyakutty M. A molecular receptor targeted, hydroxyapatite nanocrystal based multi-modal contrast agent. Biomaterials 2010;31:2606–1616.
433. Kim J, Park S, Lee JE, Jin SM, Lee JH, Lee IS, Yang I, Kim JS, Kim SK, Cho MH, Hyeon T. Designed fabrication of multifunctional magnetic gold nanoshells and their application to magnetic resonance imaging and photothermal therapy. Angew Chem Int Ed 2006;45:7754–7758.